Charles University
Faculty of Science

Study programme: Biology
Branch of study: Genetics, Molecular Biology and Virology – Molecular Biology and Genetics of Eukaryots

Bc. Petra Kremserová

Role of PML in ribosomal stress

Role PML v ribozomálním stresu

Diploma Thesis

Supervisor: Ing. Pavla Vašicová, Ph.D.

Prague, 2019

Prohlášení:

Prohlašuji, že jsem závěrečnou práci zpracovala samostatně a že jsem uvedla všechny použité informační zdroje a literaturu. Tato práce ani její podstatná část nebyla předložena k získání jiného nebo stejného akademického titulu.

V Praze, 12. 8. 2019

Podpis

Ráda bych zde poděkovala své školitelce Ing. Pavle Vašicové, Ph.D. za trpělivost při vedení mé diplomové práce a za to, že bylo kdykoli možné požádat o radu či pomoc. Velice také děkuji Mudr. Zdeňku Hodnému,Ph.D., že mi umožnil vypracovat diplomovou práci na Oddělení genomové integrity. Dále bych ráda poděkovala Mgr. Magdaléně Opravilové za pomoc v závěrečných fázích experimentální části. V neposlední řadě patří velký dík celému kolektivu Oddělení genomové integrity, mé rodině a kamarádům.

Práce byla finančně podpořena z projektu GAČR 17-02080S.

Abstract

PML is involved in many cellular processes. It organizes nuclear structures PML nuclear bodies (PML NBs) and it associates with nucleolus in response to ribosomal stress to form PML nucleolar associations (PNAs). The function of PNAs is unclear. To elucidate this question, one can attempt to identify proteins interacting with PML at nucleolus. The common method is co-immunoprecipitation, however, this approach cannot be used for PML due to its low solubility. To defeat this, an alternative way of proximity-dependent biotin labelling could be used.

The goal of this work was to explore a suitability of biotin labelling for identification of PML nucleolar partners. For this purpose I prepared constructs of wild type or mutated PML with GFP and biotin ligase for transient and stable expression and analysed their propensity to form PML NBs and doxorubicin-induced PNAs, and biotinylate their vicinity.

In transient expression, both fusion proteins formed PML NBs and only wild type but not mutated PML IV formed PNAs after doxorubicin treatment with preserved biotinylation capability.

In stable expression of fusion proteins in cells with PML knockout the number and composition of PML NBs was aberrant and no PNAs were observed. However, this system was utilized for optimization of solubilisation of biotinylated proteins using detergents.

My findings indicate that after a modification the biotin proximity labelling might be used for identification of PML partners.

Key words: PML protein, PML-nucleolar association, ribosomal stress, protein-protein interaction, biotin ligase, proximity-dependent biotin identification – BioID2

Abstrakt

PML je zapojen do řady buněčných procesů. Je organizátorem subjaderných struktur zvaných jaderná tělíska PML a asociuje s jadérkem při odpovědi na ribozomální stres tvorbou jadérkových struktur PML (PNAs). Funkce těchto struktur je nejasná a jednou z možností jejího objasnění je identifikace proteinů interagujících s PML v jadérku. Běžně používanou metodou je koimunoprecipitace, bohužel tento přístup nelze u PML použít pro jeho nízkou rozpustnost. Jednou z alternativ pro překonání této překážky je metoda značení interakčních partnerů biotinem.

Cílem této práce bylo ověření využitelnosti metody značení biotinem pro identifikaci interakčních partnerů PML v jadérku. Za tímto účelem jsem vytvořila konstrukty kódující PML IV či její mutovanou formu fúzované s GFP a biotin ligázou pro tranzientní a stabilní expresi, a analyzovala jsem jejich schopnost tvořit PML NBs, doxorubicinem indukované PNAs a schopnost biotinylace.

Oba tranzientně exprimované fúzní proteiny tvořily PML NBs a jen divoká forma PML IV tvořila PNAs po ovlivnění doxorubicinem. Schopnost biotinylovat byla zachována.

V buňkách s deletovaným genem pro PML stabilně exprimujících fúzní proteiny bylo detekováno aberantní množství a kompozice PML NBs a nebyly pozorovány PNAs. Nicméně tento systém byl využit pro optimalizaci solubilizace biotinylovaných protienů za použití detergentů.

Má zjištění ukazují, že po modifikaci může být na proximitě závislé značení biotinem použito pro identifikaci partnerů PML.

Klíčová slova: protein PML, jadérkové asociace PML, ribozomální stress, protein-proteinové interakce, na proximitě závislá identifikace biotinem – BioID2

List of abbreviations

53BP1 – p53 binding protein 1

ARF – alternate reading frame

ATM – ataxia telangiectasia mutated

ATR – ataxia telangiectasia and Rad3 related

ATRX – ATP-dependent helicase ATRX

B23 – nucleophosmin

BB – B-box domain

BCA – bicinchoninic acid

BioID2 – proximity-dependent biotin identification method

BSA – bovine serum albumin

CC – coiled-coil domain

Chk2 – checkpoint kinase 2

CK2 – casein kinase 2

DAPI – 4,6-diamidine-2-phenylidole

DAXX – death-associated protein 6

dATP – deoxyadenosine triphosphate

dCTP – deoxycytidine triphosphate

dGTP – deoxyguanosine triphosphate

dTTP – deoxythymidine triphosphate

ddH_2O – double distilled water

DFC – dense fibrillar component

DMEM – Dulbecco's Modified Eagle's medium

DNA – deoxyribonucleoc acid

dNTP – doxyribonucleotide triphosphate

ECL – enhanced chemiluminiscence

FBS – fetal bovine serum

FC – fibrillar centre

FLASH – FLICE-associated huge protein

FRAP – fluorescence recovery after photobleaching

GC – granular component

GFP – green fluorescence protein

HIRA – histone cell cycle regulator

HRP – horseradish peroxidase

HP1 – heterochromatin protein 1

hTERT – human telomerase

ICP0 – infected cell polypeptide 0

IFN – interferon

INF β – interferon β

JAK – Janus kinase

LB medium – lysogeny broth medium

lenti- PML-BioID-GFP - PML IV-$(GGGGS)_{3x}$-BioID2-GFP in lentiviral vector

lenti- PML MUT-BioID-GFP – PML IV Δ560-633-$(GGGGS)_{3x}$-BioID2-GFP in lentiviral vector

MageA2 – melanoma antigen gene A2

Mdm2 – mouse double minute 2

MRE11 – meiotic recombination 11

NAD – nicotinamide adenine dinucleotide

NES – nucleolar export signal

NLS – nuclear localization signal

NOR – nucleolus organizer region

ORF23 – open reading frame 23

PBS – phosphate saline buffer

PCR – polymerase reaction

PEG – polyethylene glycol

PML – promyelocytic leukemia protein

PML NBs – PML nuclear bodies

PML-BioID-GFP – PML IV-$(GGGGS)_{3x}$-BioID2-GFP fusion protein

PML MUT-BioID-GFP – PML IV Δ560-633-$(GGGGS)_{3x}$-BioID2-GFP fusion protein

pPML-BioID-GFP – PML IV-$(GGGGS)_{3x}$-BioID2-GFP plasmid DNA

pPML MUT-BioID-GFP – PML IV Δ560-633-$(GGGGS)_{3x}$ -BioID2-GFP plasmid DNA

PNAs – PML-nucleolar associations

PNK – T4 polynucleotide kinase

pRB – retinoblastoma protein

RARα – retinoic acid receptor α

Ras – rat sarcoma

rDNA – ribosomal DNA

RING – really interesting new gene

RNF168 – E3 ubiquitin-protein ligase ring finger protein 68

RNPs – ribonucleoprotein complexes

RPA – replication protein A

RPE1 – retinal pigment epithelial 1

RPE1 PML KO – retinal pigment epithelial 1 PML knockout

RPL11 – ribosomal protein L11

RPL5 – ribosomal protein 5

rRNA – ribosomal ribonucleic acid

SARA – Smad anchor for receptor activation

SDS – sodium dodecylsulphate

SDS-PAGE – SDS-polyacrylamide gel electrophoresis

SIM – SUMO-interacting motif

Sirt 1 – sirtuin 1 deacetylase

Smad – “small” worm phenotype/”Mothers Against Decapentaplegic”

snoRNA – small nucleolar RNA

snoRNA – small nucleolar RNA

SP100 – speckled 100 kDa nuclear autoantigen

sRNP – small ribonucleoprotein

SUMO – small ubiquitin-like modifier

TAE buffer – Tris-acetate-EDTA

TGF β – transforming growth factor β

UBC9 – ubiquitin carrier protein 9

UBF – upstream binding factor

Content

1. Introduction

PML is a multifunctional protein expressed in mammalian cells. It participates in several cellular processes. It is most often described as a tumour suppressor as well as protein assigned with important role in antiviral defence or cellular metabolism.

The PML is a main organizer of PML nuclear bodies. Distinct nuclear domains with many diverse functions provided by the ability of the scaffold PML to recruit other protein partners and, based on specific association, fulfil the specific function. Recruitment of interacting partners into the PML NBs is mainly mediated by SUMO-SIM interactions. The PML provides and important post-translational modification site in the cell nucleus.

According to several studies and recent unpublished data, two out of seven known isoforms of the PML associate with nucleolus in several types of distinct structures (PNAs). These associations are generated under conditions of ribosomal stress manifesting itself by impaired ribosomal biogenesis or function. The highest number of PML-nucleolar associations has been detected in cells subjected to treatment with agents inhibiting RNA polymerase I and topoisomerases. What is not known are, firstly, the interaction partners of PML and the protein network proximal to PML protein during its association with nucleolus, and secondly, what is the purpose of PML-nucleolar associations and how it is connected to the conditions under which it happens. We believe that identification of specific interaction partners will help to explain the purpose of PML-nucleolar associations and dynamic of this process.

This thesis is a part of an on-going research in the Laboratory of Genome Integrity, Institute of Molecular Genetics, AS CR dedicated to the functions of the PML. Experimental part of the thesis attempted to adapt the proximity-dependent biotin identification method for identification of PML interaction partners during its association with nucleolus. The proximity labelling was chosen as the PML can multimerise and form high molecular weight structures that are not soluble in buffers used for co-immunoprecipitation and therefore this commonly used technique cannot be used in this case. The experimental approach was designed to compare specifically biotinylated proteins using BioID2 method isolated form cells expressing either wild type PML IV or its truncated form lacking domains responsible for the PML-nucleolar association after identification by mass spectrometry.

2. Literature Review

2.1. Promyelocytic leukemia protein

The PML is nuclear matrix-associated multifunctional protein first described as part of fusion protein PML-RARα in patients diagnosed with acute promyelocytic leukemia as a result of t(15;17) chromosomal translocation *(de Thé, H. et al., 1991)*. This protein is strictly mammalian and in humans coded by approximately 53 kilobases (kb) long *PML* gene located on chromosome 15q24.

2.2. PML isoforms

PML consists of nine exons. Exons 5-9 undergo alternative splicing which results in various PML protein isoforms *(Condemine, 2006, Jensen et al., 2001)*. Alternative splicing produces seven isoforms (Figure 1) majority of which is mainly nuclear with the exception of isoform VIIB being strictly cytoplasmic and PML I isoform containing nuclear localization signal (NLS) as well as nuclear export signal (NES) as part of exon 9, thus being cytoplasmic as well as nuclear *(Nisole, 2013; Condemine, 2006)*.

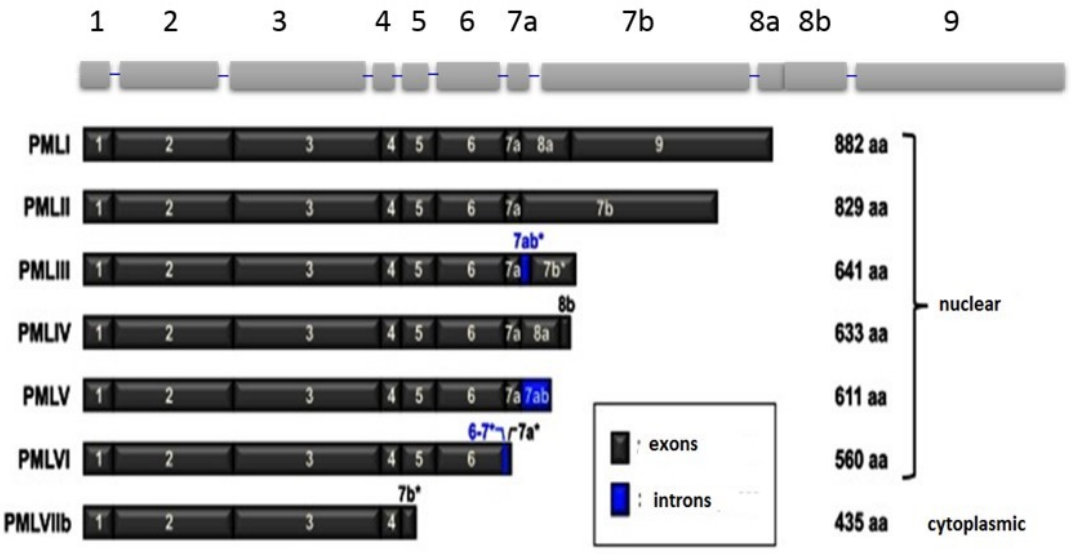

Figure 1: PML isoforms generated by alternative splicing. *Schematic representation of PML isoforms. Isoforms I – VI are mainly nuclear whilst isoform VIIB is strictly cytoplasmic. Adapted and modified from Nisole et al., 2013*

2.3. N-terminal PML domains

2.3.1.Tripartite motif

The PML belongs to the tripartite motif family which is characteristic for conserved N-terminal TRIM/RBCC consisting of RING finger, two B-boxes and α-helical coiled coil domain (CC) (Figure 2). C-terminal region is variable in all PML isoforms *(Reymond et al., 2001)*. In general, proteins containing TRIM motif are able to homomultimerise and form high molecular weight structures that constitute the basis for cellular subcompartments with distinct functions *(Zhog et al., 2000).* CC domain is crucial for the process of homomultimerisation. However, without Ring domain or B-box domains, CC domain forms different subcompartments (*Reymond et al., 2001)*. Known ability of TRIM-containing proteins, for which mainly CC domain is important, is the formation of scaffold for either cytoplasmic or nuclear subcompartments with ability to recruit other protein partners leading to execution of distinct function to which is the subcompartment dedicated. In addition to PML, an organizer of nuclear structures called PML nuclear bodies (PML NBs), TRIM5α protein trimerises and serves as an anti-retroviral restriction factor providing an antiviral activity against human immunodeficiency virus (HIV-1) *(Javanbakht 2006, et al).*

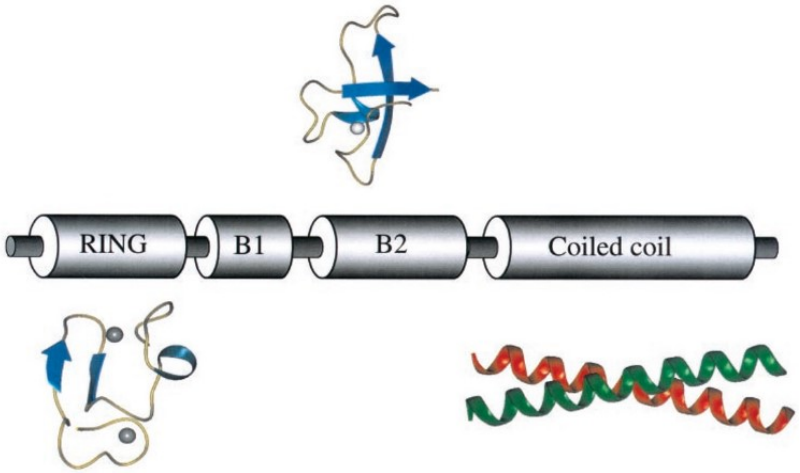

Figure 2: Schematic of the TRIM motif. *Schematic representation of TRIM motif and 3D representation of each domain (Borden et al., 1995). Zinc atoms are represented by grey spheres, β-strands correspond to blue arrows and α-helices are ribbons. Adapted from Jensen et al., 2001 and Borden et al, 1995*

TRIM motif, encoded by exons 1, 2 and 3 in the *PML* gene, has also been connected with E3 ubiquitin ligase activity for other proteins of TRIM motif family *(Urano, 2002; Meroni, Diez-Roux, 2005)*.

2.4. Post-translational modifications of the PML

Post-translational modifications are highly important for the PML. It represents a tool through which specific functions of the PML and its association partners are performed.

2.4.1.Phosphorylation

Phosphorylation of the PML occurs on tyrosine or serine residues. Phosphorylation plays an important role in PML function as a tumour suppressor and in DNA damage response. Upon DNA damage signalling the PML is subjected to phosphorylation by ATR kinase (ataxia telangiectasia mutated and Rad3-related), one of the main DNA damage sensors activated by DNA single strand break, and Chk2 kinase (checkpoint kinase 2), which is involved in regulation of cell division and DNA double strand break repair. Casein kinase 2 (CK2), Ser-Thr kinase characterised as proto-oncogene, has been shown to phosphorylate the PML to direct it to ubiquitin-proteasome pathway *(Scaglioni et al., 2006)*.

2.4.2.Sumoylation

Sumoylation is one of the most common post-translational modifications and is considered to be in competition with ubiquitination. Small ubiquitin-like modifier (SUMO) proteins are conjugated to specific protein lysine residues. The conjugation is reversible and dynamic and this particular modification has been linked with subcellular localization, protein-protein interaction, DNA-protein interaction and DNA repair, transcription regulation and genome organization *(Gluo et al., 2014, Hickey et al., 2012)*.

The PML can be modified by all three known members of SUMO family including SUMO-1, SUMO-2 and SUMO-3 *(Ayaydin et al., 2004.; Kamitani et al., 1998)*. Last two members being referred to as SUMO-2/3 because of their almost identical amino acid sequences. The PML has three specific sumoylation sites represented by lysines K65, K160 and K490 located in Ring domain and B-box domain of TRIM/RBCC motif and in NLS of the PML *(Duprez et al., 1999)*. Through these sumoylation sites the PML directly binds the SUMO and SUMO-conjugating enzyme UBC9 *(Sahin et al., 2014)*.

The PML also possesses SUMO-interacting motif (SIM) which allows its association with other sumoylated proteins including itself *(Sternsdorf, et al., 1997)*.

The SUMO allows the sumoylated protein to be dynamically conjugated with SIM of target proteins and very efficiently modulates their stability, activity or solubility and also enables specific recruitment of other proteins through SUMO-SIM interactions *(Sahin et al., 2014)*.

2.4.3.Ubiquitination

Ubiquitination is a type of post-translational modification active not only in protein degradation. It targets proteins to proteasome by adding ubiquitin to the protein sequence.

PML ubiquitination at lysine 401 results in its proteasomal degradation *(Hakli et al., 2004).* The PML is often ubiquitinated by viral E3 ubiquitin ligases such as ICP0 that targets PML ubiquitination-mediated degradation in sumoylation-dependent manner *(Boutell et al., 2003).*

2.4.4.Acetylation

PML acetylation influences the level of its sumoylation. Specifically PML acetylation on lysines 487 and 515 promotes its acetylation *(Hayakawa et al., 2008)*. On the other hand, it was reported, that the PML is more abundant and the level of sumoylation increases upon overexpression of Sirt 1 deacetylase *(Campagna et al., 2001).* The complex relationship between sumoylation and acetylation of the PML is also supported by a study revealing that the SUMO itself can be acetylated. Acetylation of the SUMO appears to have an inhibitory effect on assembly of PML NBs by preventing the interaction between SUMO moiety of the PML and SIMs of the PML NBs components *(Ullman et al, 2012).*

2.5. PML nuclear bodies

The PML is a main organizer and scaffold protein of the PML NBs *(Ishov et al., 1999)*. Nucleus usually contains 10 – 30 PML NBs of 0.2 – 1.2 μm in diameter *(Nisole et al., 2013)*, but the number varies depending on cell type, phase of a cell cycle and cell metabolic state *(Brand, 2010)*.

These subnuclear structures are a representation of relatively newly proposed concept characterized as biomolecular condensates. These are described as nonmembranous discrete cellular subcompartments participating in cellular processes, whose composition is highly

dynamic. Typically their formation is based on liquid-liquid phase separation using weak multivalent interaction between molecules. Formation of such a structure demands a presence of scaffold molecules that are crucial for its existence. Other resident molecules of the condensate are not necessary for their formation, but contribute to specific function of the sub-compartment *(Ditlev et al., 2018; Wheeler et al., 2017; Uversky et al, 2017)*.

The PML nuclear body formation is based on several separate mechanisms. First, the oxidation that induces the homomultimerisation of the PML through the TRIM/RBCC motif occurrs *(Reymond et al., 2001, Sahin 2014)*. Second step depends on sumoylation of three lysine residues (K65, K160 and K490) of PML and interaction of the SUMO with the SIM of other molecule of the PML *(Shen et al., 2006, Sahin 2014)* (Figure 3). Sumoylation is important for proper PML NB formation (*Seeler et al., 2001)*. The PML forms a shell-like structure that is able to recruit other proteins through SUMO-SIM interaction.

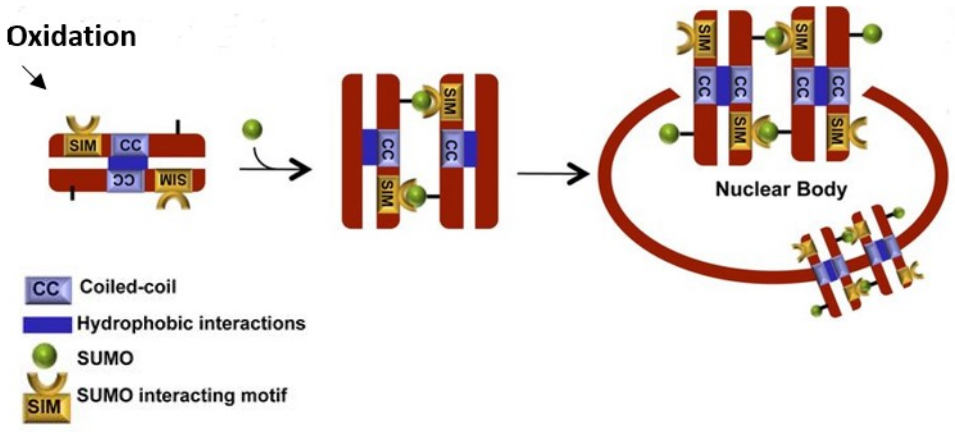

Figure 3: Assembly of PML nuclear body. *Schematic representation how PML NBs assembly is based on SUMO-SIM interaction and interactions between coiled coil domains of PML molecules. Adapted and modified from Sahin et al., 2014*

The PML is sumoylated during cell cycle interphase, which supports formation of PML NBs complex structure and simultaneously is able to recruit other partners such as death domain-associated protein (DAXX) or nuclear autoantigen Sp100 (SP100). On the other hand, the PML is de-sumoylated in mitotic cells and therefore many stable components of PML NBs dissociate during this cell cycle phase. However the PML still remains aggregated due to the TRIM/RBCC motif and able to homomultimerize *(Bernardi, Pandolfi, 2007)*.

2.6. Functions of the PML

2.6.1.PML isoform-specific functions

Different structures of C-terminal region of the PML determine specific interactions with its partners and consequently specific functions of each isoform *(Nisole, 2013; Li et al., 2017)*. Western blotting analysis performed by Condemine and colleagues proved the isoforms PML I and PML II to be the most abundant in cells endogenously expressing the PML followed by the rest of isoforms being approximately ten times less abundant *(Condemine, 2006)*.

Each PML isoform has been linked with a specific function in cell and it is believed that endogenously expressed PML is a well-tuned mixture of the PML isoforms ensuring the variety of functions of the protein.

It was reported that the PML I is specifically involved in myeloid lineage differentiation by interaction with acute myeloid leukemia 1 protein (AML) *(Nguyen et al., 2005)* and is degraded in SUMO-independent manner by the ICP0 produced by HSV-1 virus *(Boutell et al., 2011)*.

Similarly, the PML II isoform is known to interact with adenovirus type 5 E4 Orf3 protein. It was described that this interaction promotes a disruption of the PML NBs *(Leppard et al., 2009)*. The PML II also positively modulates viral transcription by cooperation with Ad5 E1A-13S *(Berscheminski et al., 2013)*.

It was suggested that the PML III isoform has a role in centrosome stability by influencing the checkpoint involved in centrosome duplication. It directly interacts with Aurora A kinase followed by targeting to the centrosome *(Xu et al., 2001)*.

The PML IV isoform is specifically involved in anti-viral defence by sequestration of certain viral proteins, thus disabling successful viral propagation *(Maroui et al., 2011)*. In addition, the PML IV is responsible for growth-suppression effect of the PML. It recruits the tumour suppressor p53 to the PML NBs and enhances p53 activation in a promoter specific manner by promoting its acetylation and phosphorylation and doing so enhances apoptosis or senescence *(Fogal et al., 2000; Bischof et al., 2002; Nisole et al., 2013)*. Other reported function of the PML IV isoform is destabilization c-Myc, which specifically supports differentiation of hematopoetic precursor cells. c-Myc protein family contains important regulatory genes and proto-oncogenes involved in cellular proliferation by coding important

transcription factors and also negatively regulates differentiation process *(Bushbeck et al., 2007)*. This identifies the PML IV as important senescence inducer. The PML IV also represses transcription of various genes through interaction with histone deacetylase *(Wu et al., 2001)*.

Using FRAP (fluorescence recovery after photobleaching) experiments showed that the PML V isoform have the longest retention time out of all PML isoforms in PML NBs suggesting that this particular isoform may be the scaffold subunit of the PML NBs *(Weidtkamp-Peters et al., 2008; Geng et al., 2012)*.

Patients with acute promyelocytic leukemia carrying PML-RARα fusion protein usually have disrupted pattern of the PML NBs. Treatment with As_2O_3 proved to be efficient for these patients. According to the study published by Maroui and colleagues, the PML VI does not contain SIM, therefore it lost the ability to be polyubiquitinated and recruited to the proteasome. This results in resistance to the As_2O_3-mediated PML pattern normalization used in treatment of patients suffering from acute promyelocytic leukemia *(Maroui et al., 2012)*.

Lastly, the PML isoform VIIb lacking nuclear localization signal (NLS) is present in cytoplasm. It was proposed that cytoplasmic PML isoform is important for signalling of transforming growth factor β (TGF β) by interacting with Smad 2/3 and Smad anchor for receptor activation (SARA) *(Lin et at., 2004)*.

2.6.2.The role of PML in specific cellular processes

2.6.2.1. Transcriptional regulation

The PML participates in regulation of transcription. Its main role seems to be the recruitment of transcription factors *(Zhong et al., 2000)*. For example, recent study reported an important role of specifically the PML II isoform in assembly of transcriptional complex on gene promoters mediating the induction of interferon β (INFβ) and several interferon-stimulated genes *(Chen et al, 2015)*.

Other information working in favour of PML role in transcriptional regulation is frequent PML NBs localization near highly acetylated, hence transcriptionally active chromatin, or nascent RNA often detected in close proximity to the PML NBs *(Kiesslich et al., 2002).* The PML can regulate transcription positively or negatively. This is demonstrated by the fact, that the PML associates with important heterochromatin-maintaining proteins such

as heterochromatin protein 1 (HP1), or its interaction with transcriptional corepressors *(Seeler at al.; 1998)*.

2.6.2.1. DNA damage response

The DNA damage response is an envelope term for elaborate and complex set of pathways designed to fight against genome instability caused by constant presence of various mutagenic agents, therefore continuous occurrence of new mutations in genome *(Jackson, Bartek, 2009)*.

The PML is subjected to phosphorylation by ATR and Chk2 kinases as a part of cellular DNA damage response to genotoxic stress. Upon phosphorylation, pattern of the PML NBs is changed and their size and number increases *(Dellaire et al., 2006)*. Considerable number of proteins involved in DNA damage (e.g. ATR, MRE11, BLM, Chk2) translocate to or from PML NBs in response to DNA damage signalling. These proteins *(Bazett-Jones, Dellaire, 2004)*. The PML is involved in homologous recombination-mediated DNA damage repair *(Boichuk et al., 2011)*. Most recently published study reports a recruitment of the PML NBs to DNA damage sites in RNF168- and 53BP1-dependent manner and proposes a role of the PML in homologous recombination-mediated DNA damage repair *(Vancurova et al., 2019)*.

2.6.2.2. Role of PML in cancer

The PML is mainly characterized as a tumour suppressor, this is supported by findings that followed PML discovery reporting that when the *PML* gene is inactivated, cells proliferate in an accelerated manner and are suspected to be prone to tumorigenesis *(Mu et al., 1994; Wang et al., 1998)*. It is known the PML expression is down-regulated in majority of tumours. The PML tumour-suppressive function was confirmed by several studies working with populations of mice with deficient PML expression that were prone to tumorigenesis *(Scaglioni et al., 2006)*.

The PML is known to interact with the p53. The PML IV isoform appears to be important for recruitment of p53 to the PML NBs. The PML is also important for regulation of p53 stability by sequestration of ubiquitin-ligase Mdm2, which suppresses p53 activity, to nucleolus *(Bernardi et al, 2004)*.

Changes in the PML resulting in complete or partial PML loss of function in cancerous cells usually occur on post-translational level. Ubiquitination and subsequent proteasomal degradation of the PML is one of often used mechanisms how cancerous cell regulates the

PML expression *(Guerrieri et al., 2004)*. Proteasomal degradation of the PML is preceded by other forms of post-translational modifications that contribute to the final targeting of the PML by proteasome. First example is PML phosphorylation by casein kinase 2 that promotes its proteasomal degradation in lung cancer *(Scaglioni et al., 2006)*. Second example discusses sumoylation and acetylation. MageA2 (melanoma antigen gene A2) interacts with the PML IV isoform and this interaction results in attenuation of sumoylation and acetylation of the PML. *(Peche et al., 2012)*. Repair of the aberrant PML degradation in various cancers by targeting the degradation pathways may have therapeutic benefits.

2.6.2.3. Role of PML in cellular senescence

Cellular senescence is primarily characterized by irreversible cell cycle arrest caused by elevated expression levels of cyclin-dependent kinase inhibitors.

The PML is often upregulated in senescent cells especially upon treatment by genotoxic stress-inducing drugs, such as distamycin A, camptothecin, etoposide and others. This elevation of PML expression in cellular senescence is mediated by p53 *(Bischof et al., 2002; Rufini et al., 2013)* or by JAK/STAT signalling pathways *(Hubackova et al., 2010)*. The PML IV isoform leads to rapid cell growth arrest within several days of ectopic expression *(Bischof et al., 2002*). This is consistent with PML-pRB (retinoblastoma) protein association. pRB has a major role in senescence, because it specifically targets E2F transcription factors involved in expression of several DNA replication and cell-cycle progression-related genes *(Talluri et al., 2014)*. Role of the PML in senescence is also supported by ability of the PML IV to recruit the p53. Specific regulator of the p53, ARF protein (alternate reading frame protein), interacts with the PML IV and UBC9 SUMO-conjugating enzyme *(Ivanschitz et al., 2015)*.

Another way of involvement of the PML in cellular senescence is the ability of the PML NBs to regulate a formation of senescence-associated heterochromatin. Histone chaperone HIRA, important for senescence-associated heterochromatin formation, translocates to the PML NBs before the cell shows any other senescence markers. It is believed that the senescence-associated heterochromatin represses activity of growth-promoting genes *(Zhang et al., 2005)*.

2.6.2.4. Role of PML in regulation of apoptosis

Apoptosis is a programmed cell death designed to eliminate chosen cell or set of cells without any damaging effect on nearby surroundings.

It was reported that the PML regulates apoptosis in the p53-dependent manner. As mentioned above, the p53 is recruited to the PML NBs by the PML IV isoform and the PML subsequently promotes its acetylation and phosphorylation. Another way of p53 regulation by the PML is sequestration of p53 ubiquitin ligase Mdm2, which usually negatively regulates the p53, to the nucleolus *(Bernardi et al., 2004; Takahashi et al., 2004; Olausson et al., 2012)*.

Apoptosis can also be, perhaps rather indirectly, mediated by the PML in the p53-independent manner (*Bernardi et al., 2004; Takahashi et al., 2004; Olausson et al., 2012)*. First possibility is Chk2 expression being promoted by the PML. On the other hand, Chk2 dissociates from the PML NBs in response to the DNA damage *(Yang et al., 2006)*. Other options are related to the extrinsic pathway of apoptosis. They include the DAXX. The DAXX is active in Fas-induced apoptosis and acts as a transcriptional repressor. This role of DAXX correlates with its sumoylation and subsequent localization to the PML NBs (*Zhong et al 2000*; *Takahashi et al., 2004*). Functionally, DAXX localization to the PML NBs and its sequestration may facilitate the activation of certain pro-apoptotic genes usually repressed by the DAXX *(Li et al., 2000)*. However, *DAXX* gene knock-out in mice was accompanied with extensive apoptosis during embyogenesis and downregulation of the DAXX also suggests its anti-apoptotic function *(Bernardi et al., 2003; Takahashi et al., 2004)*. Another discussed protein in relation to the PML contributing to the p53-independed apoptosis is FLASH protein (FLICE-associated huge protein) that is commonly associated with the PML NBs, but upon activation of Fas receptor it is released from the PML NBs and localizes to mitochondria where it activates initiator caspase 8 *(Milovic-Holm et al., 2007)*.

The PML is also involved in induction of apoptosis executed in caspase-independent manner. It was reported that overexpressed PML recruits cell death effector BAX and inhibitor of cyklin-dependent kinases $p27^{KIP1}$ to the PML NBs. No caspase activity was detected in this process. In addition, no apoptosis-related changes requiring caspase 3 activity, such as chromatin condensation and nuclear fragmentation, were observed *(Quignon et al., 1998)*.

2.6.2.5. Role of PML in antiviral defence

Many types of viral infections have been known to target and modify the PML and therefore PML NBs dynamics and function. Similarly to many other functions of the PML NBs, their involvement in cellular response to viral infection is rather complex. Although many studies suggest the role of PML in anti-viral defence, there is some evidence that specific viruses can evade this defence.

An example of antiviral defence mediated by the PML NBs has been described for herpes virus infection. Within the intrinsic immunity pathways, virus is targeted to the PML NBs shortly after it enters the cell and its genome is silenced. Several components of the PML NBs, including PML, DAXX, Sp100, and ATRX, function as a cellular restriction factors. Another way to prevent progression of viral infection is the ability of the PML to associate with a specific viral capsid protein ORF23 (open reading frame 23) and prevent nuclear egress, hence viral capsid assembly. The PML NBs undergo rapid relocalization to cytoplasm upon viral infection *(Tavalai et al., 2008)*.

Innate immunity is also connected with the PML and PML NBs influencing the induction of interferon-induced anti-viral response. Importantly, interferons are responsible for upregulation of some PML NBs components such as PML or SP100 *(Regad et al., 2001)*.

Some viruses are also able to evade the anti-viral defence the PML participates in. For example, adenoviral transactivator protein E1A-13S, which is essential for activation of viral transcription, thus is one of the first viral proteins expressed upon adenoviral infection, targets the PML NBs and specifically interacts with the PML II isoform. This interaction results in enhanced E1A-mediated transcriptional activation *(Berscheminski et al., 2013)*.

2.7. Nucleolus

Nucleolus is one of the earliest identified and most prominent nuclear structures discovered by Wagner in 1835 and Valentin in 1836. Ultrastructure of the nucleolus is defined by three structural components called fibrillar centre (FC), dense fibrillar component (DFC) and granular component (GC). Generation and localization of nucleolus in nucleus of human cell depends on localization of acrocentric chromosomes 13, 14, 15, 21 and 22 that on their shorter arm contains arrays of ribosomal DNA (rDNA). Upon activation of pre-rRNA transcription rDNA loci serve as nucleolar organization regions (NORs) *(McClintock, 1934)*. One of typical features of nucleolus is its dynamic nature not only during interphase, but in

mitosis as well, when it disassembles at the beginning of mitosis and subsequently reassembles at its end *(D'amours et al, 2004; Torres-Rosell, 2004)*.

Perhaps the best known function of nucleolus is ribosome biogenesis tightly connected with cell growth and proliferation. rDNA is transcribed into 47S pre-ribosomal RNA followed by cleavage resulting in several rRNA (23S and 16S in prokaryotes and 28S, 18S and 5.8S in eukaryotes). Ribosomal RNA associates with approximately 80 ribosomal proteins and 5S rRNA, transcribed by RNA polymerase III eventually forming ribosomal subunits *(Scheer et al., 1999)*.

Nucleolar compartments have specific role in the process of ribosome biogenesis. Nascent 47S rRNA transcripts accumulate in DFC *(Hozák et al, 1994; Cmarko et al., 2000)*. Pre-ribosomal RNA undergoes maturation in a process controlled by approximately 150 small nucleolar RNAs (snoRNAs) and several ribonucleoprotein complexes (RNPs). RNPs responsible for small and large pre-ribosomal subunit assembly accumulates in small subunit (SSU) processome and large subunits (LSU) processome respectively *(Fromont-Racine et al., 2003).* This maturation continues during migration of the transcript in nucleolus towards GC, where the final assembly of ribosomal subunits takes place *(Gautier et al, 1994; Cmarko et al, 2000)*.

Since Pederson's hypothesis from 1998 that nucleolus could be a multifunctional cellular subcompartment *(Pederson, 1998)*, further research discovered nucleolar association of up to 4500 proteins *(Ahmad et al., 2008)*. The 70% majority of these proteins are active in various cellular processes other than ribosome biogenesis including DNA damage response and cellular stress response, cell cycle progression, proliferation, gene expression, mRNA export and protein folding and degradation *(Carmo-Fornesca et al., 2000; Andersen et al., 2005, Ahmad et al., 2008)*.

2.8. Ribosomal stress

Ribosomal or in other words nucleolar stress occurs when ribosome biogenesis is disrupted or functionality of ribosomes is altered. Process of ribosome biogenesis can be blocked, for example, either by inhibition of RNA polymerase I, which is experimentally achieved, for instance, by using low doses of actinomycin D, or by interfering rRNA processing/transport. This manifests itself by reorganization of nucleolar components and segregation of nucleolus *(Junéra et al., 1995; Sirri et al., 2008)*.

Several studies published over the past decade have been focused on the relationship between ribosome biogenesis and cell cycle progression. Results suggest that the p53 is involved in nucleolar stress response. Ribosomal proteins L11 (RPL11) and L5 (RPL5) participate in activation of cellular stress response pathways, specifically by binding Mdm2, thus promoting stabilization of the p53. This can result in the p53-mediated cell cycle arrest or apoptosis *(Fumagalli et al., 2012; James et al., 2014)*. In addition to the p53, which is frequently mutated or not present in tumour cells, it was reported that tumour suppressor ARF, which can respond to the increased mitogenic activity of c-Myc or Ras proteins, is also active in cellular response to nucleolar stress as well as other nucleolar protein NPM (nucleophosmin; B23) *(Donati et al., 2012)*.

Disrupted nucleolar function and increased ribosome biogenesis due to altered proto-oncogene and tumour suppressor gene expression, is a typical feature of cancerous cells both in many types of solid tumours and leukemia. Extensive studies showed that the expression of ribosomal proteins in these cells is either significantly increased or lowered. This suggest that some of the ribosomal proteins might be of tumour-suppressive nature *(Montanaro et al; 2008)*.

Another topic related to ribosomal stress is rDNA topology and a role of topoisomerases. These enzymes participate in DNA transcription by maintaining its topology. Their activity is based on ability to break the DNA phosphate backbone and reseal it while passing one DNA strand through another. There are two known types of topoisomerases. Type I topoisomerases generate single strand breaks on DNA, thus allowing it to rotate around other strand and then be resealed. Type II topoisomerases generate double strand breaks on DNA and allow to one strand of DNA pass through another and then be resealed preserving the new topology. These processes mitigate stress from DNA being supercoiled or uncoiled during transcription or replication. In contrast to type II topoisomerases, type I topoisomerases do not require ATP for their function *(Osheroff et al., 1989; Froelich-Ammon et al., 1995; Meyer et a.l, 1997).*

Results support the notion that both types of topoisomerases participate in rDNA transcription assuring correct folding into functional topological organization of rDNA genes in mammalian cells. Detection of type I topoisomerases in nucleolus supports the connection of these enzymes with rDNA transcription, such as regulation of the cleavage site in rRNA

flanking regions or phosphorylation-dependent activation of rRNA splicing factors *(Bonven et al., 1985; Rossi et al., 1996)*. In case of type II topoisomerases, the highly probable conclusion is that topoisomerase IIα localizes in nucleolus and is important for rDNA transcription, on the other hand topoisomerase IIβ is completely excluded from nucleolus *(Meyer 1997)*.

The hypothesis says that ribosomal stress, defined as disruption of ribosome biogenesis or altered functionality of ribosome, is strongly influenced by topological properties of rDNA and later rRNA. When a cell faces a certain level of topological stress resulting from incorrectly functioning or non-functional topoisomerases usually active in nucleolus, whole rDNA/rRNA metabolism can be damaged. This is likely to have a significant impact on ribosome biogenesis, therefore supporting ribosomal stress progression.

2.9. Association of PML with nucleolus

One of the first information about connection between the PML and the nucleolus was reported in cells with inhibited proteasome degradation. Under these conditions it is possible to observe an accumulation of the PML and other resident protein of PML NBs in nucleolus *(Mattsson at al., 2001)*. The accumulation of the PML in nucleolus was also observed after the DNA damage that was caused by doxorubicin treatment *(Bernardi et al., 2004)*. Similar PML localization was later detected in replicatively senescent human mesenchymal stem and when these cells were treated with low doses of actinomycin D that inhibits rRNA synthesis *(Janderová-Rossmeislová et al., 2007)*. Findings of Condemine and colleagues revealed the crucial role of the PML I and PML IV in PML-nucleolar association *(Condemine at al., 2007).* Recent data from our laboratory show that PML-nucleolar associations (PNAs) are most common when the PML IV is ectopically expressed compared to other PML isoforms and that this association is dependent on its C-terminus.

2.10. Proximity-dependent biotin identification

The proximity-dependent biotin identification method (BioID) is used for detection of direct, indirect and even transient protein-protein interactions *(Roux et al., 2012)*. It also allows to study cellular environment inproximity to studied association of interest, because it does not need two proteins to be in the direct contact to detect the interaction (Figure 4). Protein of interest is fused to mutant form of bacterial biotin ligase (BioID) from *Escherichia*

coli (Choi-Rhee, 2004; Cronan; 2005, Roux, 2012). BioID contrary to wild type biotin ligase (Bir2) does random biotinylation in its proximity by binding of biotin to lysine residues. Biotin ligase biotinylates proteins present in 10 nm biotinylation radius. Biotinylated proteins are then isolated using methods based on strong affinity between biotin and streptavidin. Isolation is followed by identification of proteins using mass spectrometry analysis *(Roux et al., 2012)*. Considering the relatively easy application of BioID method and exploitation for proteins insoluble in buffers used for routine methods studying protein-protein interactions such as co-immunoprecipitation as well as weak or transient protein-protein interactions, over 100 studies to date employed this method. BioID method was used in studies dealing with centrosome structure *(Firat-Karalar et al., 2015; Gheiratmand et al., 2019),* identifying proteins associating with nuclear envelope *(Kim, Jensen, Roux, 2016)*, lamin *(Methus et al., 2016)* or mitotic spindle *(Gu et al., 2017)*. Other than structural analysis, this method was used, for example, to identify interactors of GTPase *(Gillingham et al., 2019)* or methyltransferase NSD2 *(Huang et al., 2019)*

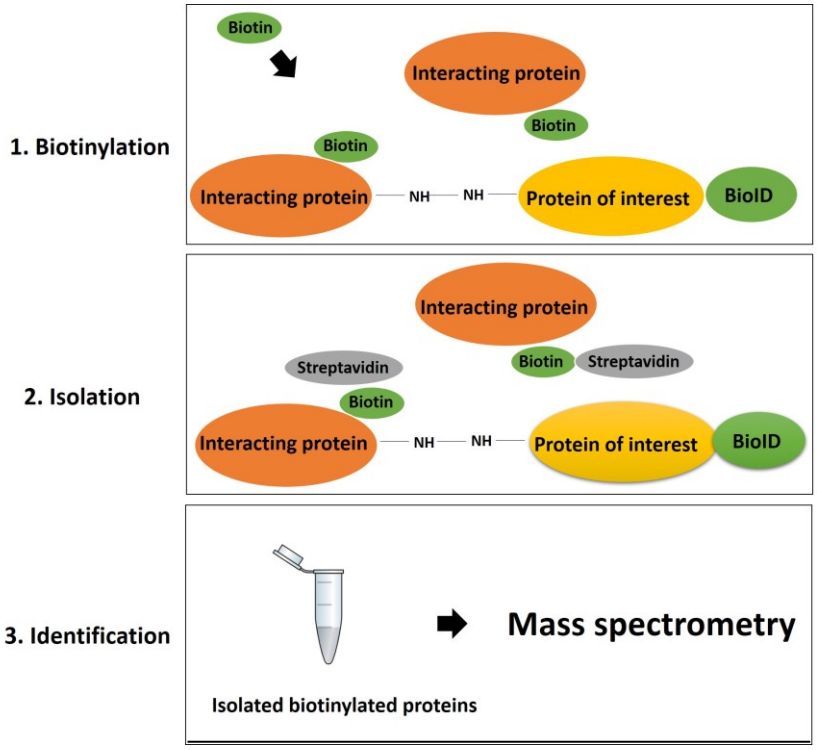

Figure 4: Detection of protein-protein interactions using BioID method. *Schematic representation of the process leading to identification of proteins interacting with the protein of interest.*

Bacterial biotin ligase BirA belongs to a family of enzymes also characterized as holocarboxylasesynthetases as they attach biotin, serving as a cofactor, to carboxylases/decarboxylases active in metabolic functions and catalyse transfer of CO_2 between respective metabolites. The reaction of biotinylation is first started by biotin ligase-catalysed attack of α-phosphate in ATP molecule by oxygen atom from biotin-carboxylate forming biotinoyl-5-AMP. Biotinylated protein has a biotinylation site represented by lysine with nucleophilic εNH_2 group that attacks biotinoyl-adenylate and forms amid bond with biotin. AMP is other product of the reaction *(Chapman-Smith and Cronan, 1999)*.

BioID method was developed as an alternative and improvement to other methods dedicated to investigation of protein-protein interactions, such as co-immunoprecipitation requiring appropriate solubility of studied proteins.

Biotin ligase used in BioID method is a 36 kDa protein consisting of catalytic domain, ATP binding domain and DNA binding domain *(Roux et al, 2012; Chapman-Smith and Cronan, 1999)*. It has been known that in some cases cellular localization of fusion protein is not very precise. To provide a solution to this problem Kim and colleagues developed an improved smaller biotin ligase BioID2. Unlike biotin ligase BioID, BioID2 does not possess DNA binding domain, hence is smaller and reportedly more precise in cellular localization and biotinylation than BioID (Figure 5) *(Kim et al., 2016)*.

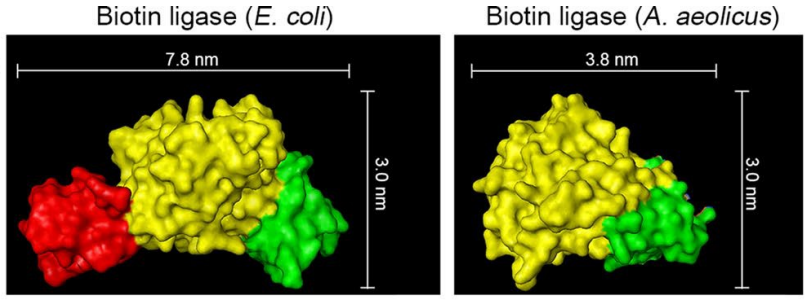

Figure 5: Biotin ligase BioID versus biotin ligase BioID2. *Schematic structure of biotin ligases BioID and BioID2. BioID2 does not possess DNA binding domain, which means that it is smaller than BioID.*

3. Aims of the thesis

Main aim of the thesis

- To test a suitability of proximity-dependent biotin identification 2 method (BioID2) for identification of the PML interaction partners during PML association with nucleolus

Specific aims of the thesis

- To construct expression vectors containing either fusion of wild type or mutant form of PML protein with BioID2:

PML IV-$(GGGGS)_{3x}$-BioID2-GFP (PML-BioID-GFP)

PML IV Δ560-633-$(GGGGS)_{3x}$ BioID2-GFP (PML MUT-BioID-GFP)

- To analyse both fusion proteins using transient transfection. The ability to form PML NBs, associate with nucleolus and the level of biotinylation after biotin addition was tested.

- To construct lentiviral vectors containing the either fusion of wild type or mutant form of PML protein with BioID2

lenti PML-BioID-GFP

lenti PML MUT-BioID-GFP

- To generate stable cell lines expressing either one of the DNA constructs.
- To analyse obtained stable cell lines
- To isolate biotinylated proteins for mass spectroscopy analyses.

4. Materials and methods

4.1. Mammalian cell lines

Retinal pigmented epithelial cell line immortalized by human telomerase with wild type of *PML* gene (hTERT RPE1) and with *PML* ablated by CRISPR technology (hTERT RPE1 PML KO) and human embryonic kidney cell line 293 (HEK 293T) were cultured in Dulbecco's modified Eagle's medium (DMEM) with high concentration of glucose (4.5 g/L) supplemented with 10% foetal bovine serum and 1% penicillin/streptomycin.

4.1.1.Treatments

Two different treatments were used in diploma thesis. First one was performed by genotoxic agent doxorubicin. Doxorubicin was used in concentration 0.75 μM and treatment lasted for 24 or 48 hours. Secondly, cells were cultivated with addition of 50 μM biotin for 4, 6 or 24 hours.

4.2. Bacterial strains

DNA constructs were amplified using either *Escherichia coli (E. coli)* derived XL10 Gold strain (endA1 glnV44 recA1 thi-1 gyrA96 relA1 lac Hte Δ(mcrA)183 Δ(mcrCB-hsdSMR-mrr)173 tet^R F'[proAB $lacI^qZ\Delta M15$ Tn10(Tet^R Amy Cm^R) obtained from *Stratagene* (USA) or Sbtl2 strain (F^- *mcr*A Δ(*mcr*BC-*hsd*RMS-*mrr*) *rec*A1 *end*A1 *lon gyr*A96 *thi sup*E44 *rel*A1 λ^- Δ(*lac-pro*AB)) obtained from *Thermofisher Scientific (USA)*. Both strains were cultivated in LB media (Luria-Bertani media: Tryptone, 10 g; NaCl, 10 g; Yeast extract, 5 g; 950 mL H_2O) or SOC (Tryptone, 20 g; NaCl, 0.5 g; Yeast extract, 5 g; 950 mL H_2O).

4.3. Vectors

DNA vectors used in diploma thesis are listed in a table below (Table 1)

Table 1: DNA vectors used in this thesis

name	description	source	citation
MCS-BioID2-HA	Vector suitable for C-terminal fusion of BioID2 with the protein of interest	Addgene plasmid # 74224	*Kim DI, Jensen SC, MolCelBiol 2016*
pCDH-CMV-MCS-EF1-Neo	Cloning and expression lentivector with strong CMV promoter and neomycin resistance marker	*System Biosciences, USA*	
EGFP-N1-PML IV (hereinafter pPML-GFP)	Mammalian expression vector with CMV promoter coding C-terminal fusion of PML isoform IV with EGFP	Genome Integrity/IMG	Jan Kosla
EGFP-N1-PML IV Δ560-633 (hereinafter pPML MUT-GFP)	Mammalian expression vector coding C-terminal fusion of PML isoform IV with EGFP, the amino acids 560-633 of PML IV were deleted	Genome Integrity/IMG	PavlaVasicova
PML IV-L-BioID2-GFP (hereinafter pPML-BioID2-GFP)	Mammalian expression vector coding C-terminal fusion of PML isoform IV with three GGGGS linkers, BioID2 and EGFP	This work	
PML IV Δ560-633-L-BioID2-GFP (hereinafter PML pMUT-BioID-GFP)	Mammalian expression vector coding C-terminal fusion of truncated form of PML isoform IV Δ560-633 with three GGGGS linkers, BioID2 and EGFP	This work	
pCDH-CMV-PML IV-L-BioID2-GFP-EF1-Neo (hereinafter lenti-PML-BioID2-GFP)	Cloning and expression lentivector with strong CMV promoter and neomycin resistance marker coding for C-terminal fusion of PML isoform IV with three GGGGS linkers, BioID2 and EGFP	This work	
pCDH-CMV-PML IV Δ560-633-L-BioID2-GFP-EF1-Neo (hereinafter lenti-PML MUT-BioID-GFP)	Cloning and expression lentivector with strong CMV promoter and neomycin resistance marker coding C-terminal fusion of truncated form of PML isoform IV Δ560-633 with three GGGGS linkers, BioID2 and EGFP	This work	

4.4. DNA cloning

4.4.1.DNA isolation

GeneJET Plasmid Miniprep Kit *(Thermofisher Scientific, USA)* was used for plasmid DNA isolation according to the manufacturer`s protocol. This isolation kit was used for isolation of up to 20 µg of plasmid DNA for cloning purposes and sequencing.

QIAGEN Plasmid Midi/Maxi Kit *(Qiagen, Germany)* was used form plasmid DNA isolation according to the manufacturer's protocol. This isolation kit was used for production of plasmid DNA utilized in lentiviral production.

Concentration of isolated DNA was measured by NanoDrop.

4.4.2.PCR reaction

For all PCR reactions the Phusion polymerase was used and the reaction mix was prepared according to the Table 2. Conditions of respective PCR reaction are described individually in each experiment. Information about primers are listed in Table 3

Table 2: PCR reaction mix

	Final concentration
DNA	15 – 20 ng
Forward and reverse primer (10 µM)	0.5 µM
dNTP (2 mM)	20 µM
5 x GC buffer	1 x
Phusion DNA polymerase	1U/50 µL
ddH_2O	to 20 uL

Table 3: List of all primers use in this work

Primer	Sequence	Purpose
GGGGS-1-base-shift_F	ggtggcggtggctcg ggcggtggtgggtcg ggtggcggcggatc gg	5' oligo for assembling of $(GGGGS)_{3x}$ linker in front of BioID2 (ligation into *Bmt*I *Bam*HI)
GGGGS-1-base-shift_R	gatcccgatccgccg ccacccgacccacca ccgcccgagccacc gccaccctag	3' oligo for assembling of $(GGGGS)_{3x}$ linker in front of BioID2 (ligation into BmtI BamHI)
PML IV-GS-BioID-Fra-F	tctaatttggggtggc ggtggct	Gibson Assembly, insertion of $(GGGGS)_{3x}$-BioID2 into PML WT - GFP
PML IV-GS-BioID-Fra-R	ccggtggatcgcttct tctcaggctgaa	Gibson Assembly, insertion of $(GGGGS)_{3x}$-BioID2 into PML WT - GFP
PML IV-d560-633-GS-BioID-Fra-F	ggtgatctggggtgg cggtggct	Gibson Assembly, insertion of $(GGGGS)_{3x}$- BioID2 into PML MUT - GFP
PML IV-d560-633-GS-BioID-Fra-R	ccggtggatcgcttct tctcaggctgaactc g	Gibson Assembly, insertion of $(GGGGS)_{3x}$-BioID2 into PML MUT - GFP
PML IV-GS-BioID-vec-F	gagaagaagcgatc caccggtcgccac	Gibson Assembly, insertion of $(GGGGS)_{3x}$-BioID2 into PML WT - GFP
PML IV-GS-BioID-vec-R	caccgccaccccaaa ttagaaaggggtgg ggg	Gibson Assembly, insertion of $(GGGGS)_{3x}$ -BioID2 into PML WT - GFP
PML IV-d560-633-GS-BioID - vec-F	gagaagaagcgatc caccggtcgccac	Gibson Assembly, insertion of $(GGGGS)_{3x}$-BioID2 into PML MUT - GFP
PML IV-d560-633-GS-BioID-vec-R	caccgccaccccag atcaccacaacgc	Gibson Assembly, insertion of $(GGGGS)_{3x}$ -BioID2 into PML MUT - GFP
CMV_F	cgcaaatgggcggta ggcgtg	Sequencing

4.4.3.DNA digestion

For cloning purposes, between 1 – 1.5 µg of DNA was digested. Subsequently, 300 ng was digested for verification of vectors after cloning. Choice of the used restriction enzymes listed in Table 30, will be specified in each individual experiment. As the fast digest restriction enzymes provided from *ThermoFisher Scientific* were used in all reactions unless otherwise specified, all the reactions were done according to the Tables 4 and 5. All digestion was performed in 37°C for 20 minutes.

Table 4: Restriction reaction of DNA for cloning purposes

DNA	1 – 1.5 µg
10 × FD buffer	6 µL
Restriction enzyme	2 – 3 µL
ddH_2O	to 60 µL

Table 5: Restriction reaction of DNA for control purposes

DNA	300 ng
10 × FD buffer	2 µL
Restriction enzyme	1 µL
ddH_2O	to 20 µL

4.4.4.Isolation of DNA fragments

DNA fragments were isolated from agarose gel using QIAquick Gel Extraction Kit *(Qiagen, Germany)* according to the manufacturer's protocol. DNA was isolated from the agarose gel for purposes of construction of vectors coding desired fusion proteins containing PML IV or its truncated version, biotin ligase BoID2 and GFP.

4.4.5.Dephosphorylation/phosphorylation

Digested DNA of vectors, into which desired fragment was cloned, was defosforylated by adding 1 µL of Shrimp Alcaline Phosphatase (SAP, 0.05 U SAP/1 pmol DNA) and incubating in 37°C for 1 hour.

The assembled DNA of linker $(GGGGS)_{3\times}$ was phophorylated by T4 polynucleotide kinase (PNK) according to Table 6. The reaction mix was incubating at 37°C for 20 minutes followed by deactivation at 75°C for 10 minutes.

Table 6: Phosphorylation reaction

dsDNA (linker)	20 pmol
10 × buffer A for PNK	2 µL
ATP (10 mM)	2 µL
PNK (10 U/µL)	1 µL
ddH_2O	to 20 µL

4.4.6.DNA ligation

DNA was ligated by adding 1 µL of T4 DNA ligase and incubating in 22°C for 30 minutes (Table 7).

Table 7: Ligation reaction

DNA	10 – 20 ng
5 x rapid ligation buffer	2 µL
T4 DNA ligase	1 µL
ddH_2O	Replenished to 10 µL

4.4.7.Gibson assembly

The 1.3 × reaction mixture (Table 8) and 5 × isobuffer (Table 9) were prepared according to the protocol of Samuel Miller (*Miller, S., http://miller-lab.net/MillerLab/protocols/molecular-biology-and-cloning/gibson-assembly/, accessed 5. Aug. 2019*). We used previously completed aliquot of reaction mix and DNA fragments were added according to the following rules. The amount of DNA was estimated, usually by comparing the intensity of DNA fragment and DNA marker. Equimolar amount of vector and fragment was determined (0.03 – 0.5 pmol total for each) and mixed with 15 µL of 5 × reaction mixture and incubated at 50°C for 1 hour. After that 5 µL was used for transformation of competent cells.

Table 8: Composition of Gibson assembly reaction mixture for 4 reactions

Component	**Mix for 4 reactions**
5 × isobuffer	16 µL
T5 exonuclease 2U/µL	0.32µL
Phusion polymerase 2U/µl	1 µL
T4 DNA Ligase 40U/µL	8 µL
ddH_2O	1200 µL

Table 9: Composition of 5 × isobuffer used for Gibson assembly

5x Isobuffer		
Component	**Volume**	**Final concentration**
1M Tris-HCl, pH 7.5	3 mL	500 mM
2M $MgCl_2$	150 µL	1 mM
100 mM dGTP	600 µL	1 mM
100 mM dATP	600 µL	1 mM
100 mM dCTP	600 µL	1 mM
100 mM dTTP	600 µL	1 mM
1M DTT	300 µL	50 mM
100 mM NAD	300 µL	5 mM
PEG	1.5 mL	25%
ddH_2O	to 6 mL	-

4.4.8.DNA electrophoresis

The accuracy of all DNA isolations, restrictions and PCR reactions was checked by electrophoresis. Standard protocols were employed to perform electrophoresis and 0.7 – 1.2% agarose gel was used. Electrophoresis was run in 1 × TAE buffer (Table 10) for 1 hour at 95 V. DNA was visualized using RedSafe™ Nucleic Acid Staining Solution.

Table 10: Composition of 1 × TAE buffer

Tris base	40 mM
Acetic acid	20 mM
EDTA	1 mM

4.4.9.Bacterial transformation

E. coli competent cells were left on ice for 10 minutes. DNA was added to the 50 µL of competent cells and mixture was incubated on ice for 30 minutes. After incubation the heat shock reaction was performed by incubating cells with DNA at 42°C for 90 seconds and quickly transferring them on ice for 2 minutes. In the next step 350 µL of SOC media was added and the mixture was incubated on Eppendorf Thermomixer (750 rpm) at 37°C for 45 minutes. After incubation the mixture was transferred onto agar plate with appropriate selection antibiotics and spread evenly on the agar plate using sterile glass beads. Transformed cells were cultivated overnight at 37°C.

4.4.10. Construction of pPML-BioID-GFP and pPML MUT-BioID-GFP vectors

4.4.10.1. Insertion of the linker $(GGGGS)_{3\times}$ in front of BioID2

A flexible linker $(GGGGS)_{3\times}$ was inserted in front of BioID2 to extend the biotinylation radius of biotin ligase. Firstly, primers GGGGS-1-base-shift-F and GGGGS-1-base-shift-R were annealed by incubating the annealing mixture (Table 11 and 12) in the beaker with ddH_2O heated to 100°C and left to cool down naturally to approximately 30°C. Linker was then phosphorylated using PNK (Chapter 4.4.5). Note the primers were designed in the way that after annealing the cohesive ends compatible with restriction sites for *Bam*HI and *Bsp*OI were present.

Table 11: The composition of the annealing mixture

GGGGS-1-base-shift-F(100 µM)	11.25 µL
GGGGS-1 base shift-R (100 µM)	11.25 µL
0.5 × annealing buffer	2,5 µL
Total volume	**25 µL**

Table 12: 0.5x annealing buffer

Tris-HCl, pH 7.4	5 mM
NaCl	50 mM

Vector MCS-BioID2-HA was digested using restriction enzymes *BamH1* and *BspO1* (Chapter 4.4.3). Digested vector was dephosphorylated using SAP (Chapter 4.4.5). Obtained DNA of digested vector was isolated from agarose gel using QIAquick Gel Extraction Kit.

The efficiency of restriction/dephosphorylation reactions was tested by religation followed by transformation of competent cells. As the number of bacterial colonies after transformation was low, the prepared linker was ligated with vector (Chapter 4.4.6). Finally, the competent cells (*E. coli* XL10 Gold) were transformed with ligation mixture and plated on agar plates (LB medium; ampicillin) (Chapter 4.4.9). The obtained clones were analysed by *Bam*HI and *Hind*III digestion (Chapter 4.4.3) and by sequencing. Final vector $(GGGGS)_{3x}$-BioID2-HA was used for further cloning.

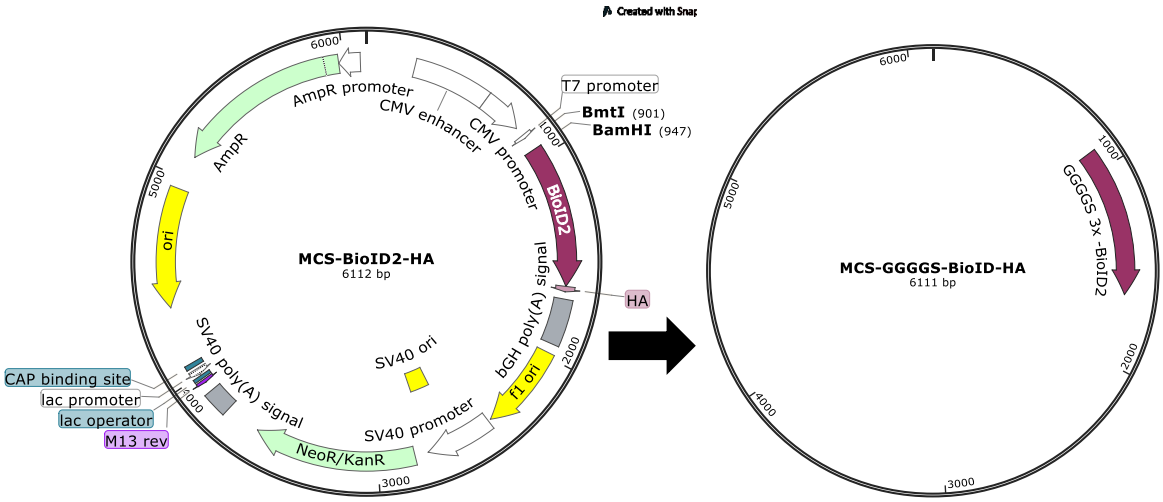

Figure 6: Insertion of the $(GGGGS)_{3x}$ linker in front of BioID2

4.4.10.2. Insertion of the DNA-fragment bearing $(GGGGS)_{3x}$-BioID2 in between PML and EGFP using Gibson assembly

As between PML and EGFP were not suitable restriction sites to clone $(GGGGS)_{3x}$-BioID2 there, we applied Gibson assembly method enabling joining of several DNA fragments without using restriction enzymes (Chapter 4.4.7). First, the DNA fragments bearing $(GGGGS)_{3x}$-BioID were prepared by PCR. Note, for amplification of $(GGGGS)_{3x}$-BioID two different set of primers were used. One for assembling the obtained product with pPML-GFP, for this PCR reaction PML IV-GS-BioID2-Fra_F/R primers (details in Table 3) were used. The second set of primes PMLIV Δ560-633-BioID2-Fra_F/R (details in Table 3) was used for assembling the obtained product with vector pPML MUT-GFP. Both vectors, pPML-GFP or pPML MUT-GFP, were linearized also by PCR using PML IV-GS-BioID-vec_F/R or PMLIV Δ560-633-BioID2-Vec_F/R, respectively (see Table 3 for details). The obtained PCR reaction was digested by *Dpn*I which targets methylated DNA, therefore the DNA template used for PCR, by adding 1 µL into the obtained PCR reaction. Finally, the PCR product was purified by isolation from the gel (Chapter 4.4.4). The conditions for all PCR reactions are in Tables 13 and 14. The fragments were joined by Gibson assembly (Chapter 4.4.7). Resulting product was used for transformation of competent cells. DNA from obtained colonies was analysed by restriction analysis using *Bam*HI restriction enzyme (Chapter 4.4.3)

and sequencing. Verified vectors were used for experiments (transient transfection) and as a source of DNA for cloning into lentivectors.

Table 13: Conditions of the PCR reaction used for linearization of vectors PML-GFP/PML MUT-GFP

Step	*Temperature (°C)*	*Time*
1	*98*	*30 s*
2	*98*	*20 s*
3	*65/67*	*20 s*
4	*72*	*4 min*
Steps 2 – 4 were 35 x repeated		
5	*72*	*10 min*

Table 14: Conditions of the PCR reaction used for amplification of fragment $(GGGGS)_{3x}$-BioID2

Step	Temperature (°C)	Time
1	98	30 s
2	98	20 s
3	65	20 s
4	72	1 min
Steps 2 – 4 were 35 x repeated		
5	72	10 min

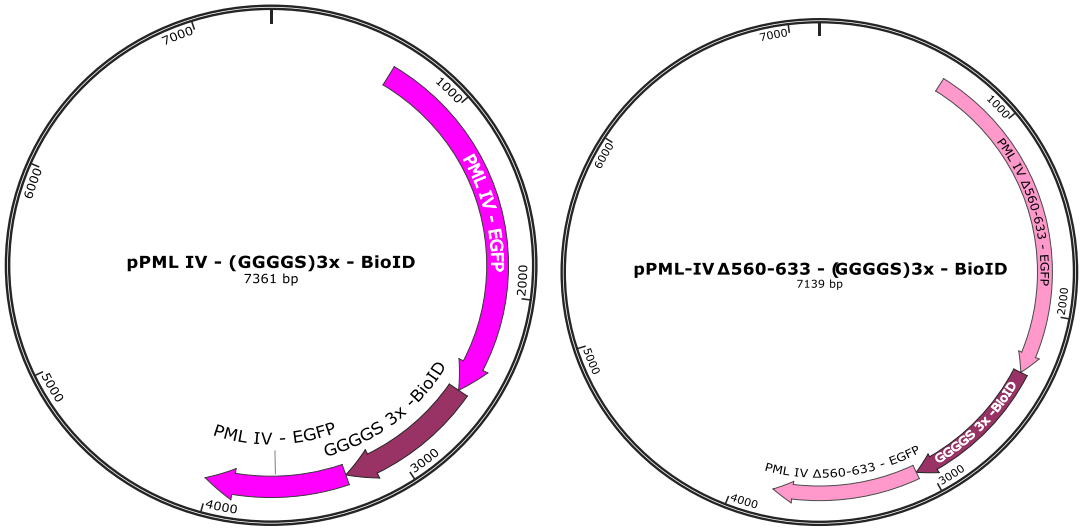

Figure 7: PML-BioID2-GFP and PML MUT-BioID2-GFP constructs

4.4.10.3. Inserting the PML-BioID-GFP and PML MUT-BioID-GFP into the lentiviral vector

To obtain tool for preparation of cell line stably expressing desired fusion proteins PML-BioID-GFP or PML MUT-BioID-GFP, we cloned the DNA fragments coding these fusion proteins from expression vectors pPML-BioID-GFP and pPML MUT-BioID-GFP into pCDH-CMV-MCS-EF1α-Neo lentiviral vector. For cloning, we digested pPML-BioID-GFP and pPML MUT-BioID-GFP with *Bmt*I and *Not*I (Chapter 4.4.3). Fragments bearing coding sequence of PML fusion protein were isolated from the gel and the concentration of DNA was estimated. Lentivector pCDH-CMV-MCS-EF1α-Neo was also digested with *Bmt*I and *Not*I (Chapter 4.4.3) and SAP was used for dephosphorylation, see (Chapter 4.4.5). The efficiency of digestion/dephosphorylation was tested by religation (Chapter 4.4.6) and transformation of competent cells (Chapter 4.4.9). As low number of colonies was present after this test, the vector and fragment were ligated (Chapter 4.4.6) and the ligation mixture was used for transformation of competent cells Sltb2. The DNA from obtained clones was analysed by restriction with *Kpn*I and sequencing. Digestion by *Kpn*I enzyme was performed according to the protocol described in Chapter 4.4.3, but as this enzyme requires buffer *Kpn*I+, we used it instead of usual FD buffer and the incubation at 37°C lasted 1 hour instead 20 minutes. The final products, pCDH-CMV-PML IV-BioID2-EGFP-EF1α-Neo (hereinafter lenti-PML-BioID-GFP) and pCDH-CMV-PML IV Δ560-633-BioID2-EGFP-EF1α-Neo (hereinafter lenti-PML MUT-BioID-GFP) were used for transduction.

4.5. Transient transfection

For that hTERT RPE1 PML KO cells were transfected with desired DNA using FuGENE 6 as transfection medium. Cells were seeded at the density of 25 000 cells/cm^2 on plastic TTP plate where the glass coverslips were placed. After 24 hours the glass coverslips were transferred to the 24-well plate with 500 μL of fresh media. Transfection volume of 50 μL contained plasmid DNA (c = 150 ng/μL) and FuGene 6 reagent in ratio 3 : 1 replenished with D-MEM medium with no FBS. Mixture was incubated for 15 minutes in room temperature and then added to the appropriate well. The efficiency of transfection was checked after 24 hours using inverted fluorescence microscope.

4.6. Transduction by lentiviruses

4.6.1.Transfection of HEK 293T cells

Cells HEK293T were seeded at the density of 50 000 cells/cm^2 on TPP plate (60 cm^2) one day before transfection. Medium was exchanged 2 hours before transfection. First Mix 1 and Mix 2 (mix of vectors) were prepared according Tables 15 and 16 and cultivated for 5 minutes at RT. Note, both mixtures were prepared in the way that final ration between DNA (total amount of all three vectors [µg]) and PEI [µg] was 1 : 4.

Table 15: Mix 1 for transfection of 293T

Component	amount
Opti-MEM	250 µL
lentivectors	9 µg
pMD2.G (VSV-G envelope proteins)	4 µg
psPax (packaging)	7 µg

Table 16: Mix 2 for transfection of 293T

Component	amount
Opti-MEM	250 µL
PEI (mg/mL)	80 µL

The final transfection mix was prepared by combining of Mix 1 and Mix 2 and incubation for 15 minutes. After this incubation, mixture was added to the plate with HEK293T cells. At this point the experiment was treated as infectious. Therefore, we used extra protection and worked in laminar flow box especially dedicated to work with viruses.

4.6.2.Collecting viral particles

Two days after transfection viral particles were collected. Necessary plastic was prepared along with inactivation reagents chloramine and 1% SDS in 70% ethanol for inactivation of used plastic in laminar flow box. Medium was harvested and collected into the 15 mL falcon tubes. The tubes were sealed and centrifuged at 1200 × g for 15 minutes at 4°C. Supernatant was collected into a new 15 mL falcon tube and to precipitate the viral particles PEGIT (20% PEG, 1.5M NaCl, filter sterilized) was added to 1/5 of final volume. Falcon tubes were sealed and incubated overnight at 4°C on rotator. The next day falcon tubes with precipitated viral particles were centrifuged at 1500 × g, at 4°C for 25 minutes. Supernatant and used plastic was inactivated in inactivating reagents. Pellet was centrifuged at 1200 g for

3 minutes. Supernatant was discarded and inactivated. Pellet was resuspended in 500 µL of PBS and stored in 100 µL aliquots in freezer at -80 °C.

4.6.3.Transduction

hTERT RPE1 PML KO cells were seeded one day before planned transduction on 24 well plate at the density of 50 000 cells/cm^2. Inactivating reagents were prepared in the laminar flow box. Viral particles (100 µL/well) were defrosted and added to the well with cells. Used plastic was inactivated.

4.6.4.Passages for selection

Before sorting transduced cells were extended 5 times according to scheme in the Figure 7. Medium was aspirated, cells were washed with 1 × PBS 3 times. Cells were trypsinized using appropriate amount of T/E (Trypsin-EDTA solution, 0.25 % trypsin, 0.2 g/l EDTA). Cells were harvested into appropriate amount of DMEM and transferred to the new cell culture plate. The G418 (final concentration 1.18 mg/mL) was always added for selection of positive clones. As control for selection condition of G418 the non-transducted hTERT RPE1 PML KO cells were used. During all passages every piece of used plastic was inactivated in chloramine and 1% SDS in 70% ethanol.

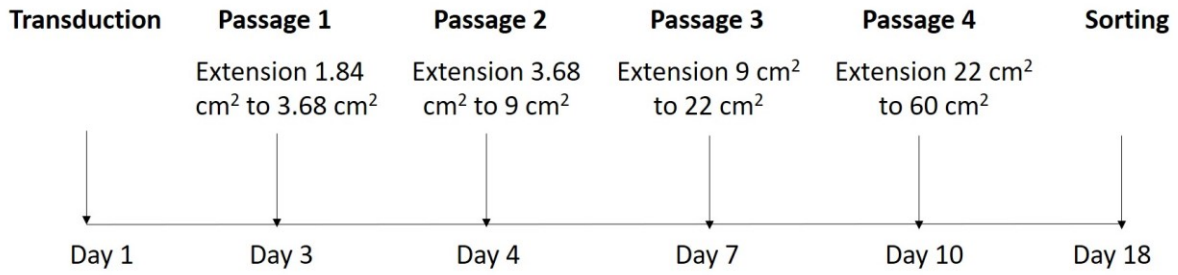

Figure 7: Extension and selection of transduced cells

4.6.5.Cell sorting

Medium was aspirated. Cells were washed with PBS 3 times and trypsinized using appropriate amount of T/E. Cells were counted and resuspended in an appropriate amount of DMEM without FBS and antibiotics in a density of 6 × 10^6/mL and transferred into a 15 mL falcon tube. Firstly cells were sorted into populations according low, medium and high GFP signal in cooperation with the Microscopy centre, Department of Light Microscopy and

Cytometry, Institute of Molecular Genetics, ASCR. Sorted cells were harvested into 1 mL of FBS. Secondly, the single cell sorting of GFP positive cells into 200 µL of conditioned media that was placed in 96 well plate was done. This sorting was done in cooperation with the same facility as mentioned above.

After sorting the cell populations and single cell colonies were microscopically analysed and expanded for further analyses.

4.7. Fluorescence microscopy

4.7.1. Fixation

After treatment cells were fixed in established time points 48 hours for doxorubicin treatment and 4, 6 or 24 hours for biotin treatment using 4% formaldehyde (FA). Cells we rinsed with 500 µL of 1 × PBS and added 300 µL of 4% formaldehyde for 15 minutes. After fixation the cells were three times washed with 500 µL of 1x PBS and then stored in PBS with 0.1% sodium azide at 4°C.

4.7.2. Detection of the proteins fused to GFP

Fixed cells on a cover slip were washed 3 times 5 minutes with 1 × PBS. Subsequently permeabilization was performed using 0.2% Triton X-100 in PBS for 10 minutes. The previous washing steps were repeated. Cover slips were transferred on Parafilm®. DAPI was diluted with ddH_2O to final concentration of 1 µg/mL. Cover slips were quickly rinsed in ddH_2O and DAPI was applied. Coverslips with applied DAPI were incubated for 3 minutes in the dark box. Cover slips were allowed to dry and mounted on a microscopic slide using ProLong™ Gold Antifade reagent. Cells were analysed using fluorescent microscope Leica DM6000.

4.7.3. Detection of biotinylated proteins

Fixed cells were washed 3 times 5 minutes with 1 × PBS. Subsequently permeabilization was performed using 0.2% Triton X-100 in 1x PBS for 10 minutes. The previous washing steps were repeated. Cover slips were transferred on Parafilm®. In the next step Streptavidin-R-Phycoerythrin fluorescent conjugate (Table 17) was diluted in 1 × PBS and 40 µL was pipetted on cover slip with treated cells and incubated for 1 hour. After incubation the washing steps were repeated. DAPI was diluted with ddH_2O to final concentration of 1 µg/mL. Cover slips were quickly rinsed in ddH_2O and DAPI was applied.

Coverslips with applied DAPI were incubated for 3 minutes in the dark box. Cover slips were allowed to dry and mounted on a microscopic slide using ProLong™ Gold Antifade reagent. Cells were analysed using fluorescent microscope Leica DM6000.

Table 17: Fluorescence conjungate fordetection of biotin

	Substrate	Purchased from, Cat. No.	Dilution
eBioscience ™ Streptavidin PE conjungate	Biotin	Invitrogen, USA, 12-4317-87	1 : 1000

4.7.4.Indirect immunofluorescence

Fixed cells on a cover slip were washed 3 times 5 minutes with 1 × PBS. Subsequently permeabilization was performed using 0.2% Triton X-100 in 1x PBS for 10 minutes. The previous washing steps were repeated. Cover slips were transferred on Parafilm®. In the next step primary antibody (Table 18) was diluted in 1 × PBS and 40 µL was pipetted on cover slip with treated cells and incubated for 1 hour. After incubation the washing steps were repeated. Secondary antibody (Table 19) was diluted in PBS and applied on a cover slip. Cover slips with applied secondary antibody were incubated for 1 hour in the dark box. After that the cells were washed twice with 500 µL of 1x PBS (5 min.). Subsequently DAPI was diluted 1000 × in ddH_2O. Cover slips were quickly rinsed in ddH_2O and DAPI was applied. Coverslips with applied DAPI were incubated for 3 minutes in the dark box. Cover slips were allowed to dry and mounted on a microscopic slide using ProLong ™ Gold Antifade reagent. Cells were analysed using fluorescent microscope Leica DM6000.

Table 18: Primary Antibodies

	Host	Purchased from, Cat. No.	Dilution
Anti-PML Ab	rabbit	Santa Cruz,USA, SC5621	1 : 200
Anti-PML Ab	mouse	Santa Cruz, USA, SC966	1 : 100
Anti-Sumo 1 Ab	rabbit	Abcam, Great Britain, AB32058	1 : 300
Anti-Sumo2/3 Ab	rabbit	Abcam, Great Britain, AB3742	1 : 100
Anti - DAXX 003 Ab	mouse	Gifted from Dr. Andera	1 : 100

Table 19: Secondary Antibodies

	Host	Purchased from, Cat. No.	Dilution
Alexa Fluor 568 anti Rabbit	Goat	Invitrogen, USA, A11036	1 : 1000
Alexa Fluor 568 anti Mouse	Goat	Invitrogen, USA, A11031	1 : 1000
Alexa Fluor 488 anti Rabbit	Goat	Invitrogen, USA, A11034	1 : 1000
Alexa Fluor 488 anti Mouse	Goat	Invitrogen, USA, A11029	1 : 1000

4.8. Whole cell lysates

Whole cell lysates were prepared from confluent cells incubated on 22 cm^2 untreated/treated with 50 µM biotin by aspirating medium, washing with 1 × PBS three times and adding 100 µL of 1 × sample buffer (95°C) diluted from the 4 × sample buffer stock (250 mM Tris-HCl, pH 6.8; 40% glycerol, 8% SDS). Lysate was harvested using a clean cell scraper and transferred into a 1.5 mL microtube. Samples were sonicated (15 seconds ON/10 seconds OFF, amplitude 2 microns, 3 cycles).

4.9. Estimation of protein concentration by BCA assay

Concentration of proteins in the samples was measured by BCA assay using Pierce BCA protein assay kit *(Thermofisher Scientific, USA)*. First, calibration was prepared from a bovine serum albumin (BSA) stock according to the manufacturer's protocol. Concentration of the samples was estimated based on the surface area and density of the original cell culture. BSA assay was performed according to the Table 20.

Reaction mix was prepared by combining appropriate amount of reagent 1 and 2 on 1 : 50 ratio. Subsequently 150 µL of reaction mic was added into each well and reaction was incubated in 37°C for 30 minutes and then the absorbance was measured. Concentration of each sample was calculated according to the standard curve (Microsoft Excel, linear regression).

Table 20: Mixture for BCA assay. X = Variable volume of sample.

	Volume	Background	Replicates	Reaction mix A+B
Standard	10 µL	X µL 1 × SB	2	150 µL
Sample	X µL	10 µL ddH_2O	3	150 µL

4.10. SDS-PAGE Electrophoresis

Stacking and separating gel was prepared according to Tables 21 – 23.

Table 21: Separating gel for SDS - PAGE

	8% gel, 1.5 mm
ddH_2O	3.6 mL
AA (30%)	2 mL
Buffer 1, pH 8.8	1.9 mL
APS (10%)	50 µL
TEMED	12.5 µL

Table 22: Stacking gel for SDS-PAGE

	1 × stacking gel, 1.5 mm
ddH_2O	1.8 mL
AA (30%)	0.45 mL
Buffer 2, pH 6.8	0.75 mL
APS (10%)	24 µL
TEMED	6 µL

Table 23: Composition of Buffer 1 and Buffer 2

Buffer 1, pH 8.8	
Tris base	1.5 M
SDS	0.4%
Buffer 2, pH 6.8	
Tris base	0.5 M
SDS	0.4%

Polyacrylamide gel was secured in the electrophoresis apparatus and the apparatus was filled with 1 × TGS running buffer (Table 24) diluted with ddH2O from 10 × TGS buffer (*Bio-Rad, USA)*. Each sample was loaded onto a polyacryalmide gel in 30 µL volume containing 30 µg of sample, 3 µL of DTT (1 mM) with bromphenol blue and replenished with 1 × SB. The electrophoresis was run at constant current of 25 mA per gel for approximately 1.5 hour.

Table 24: Composition of 1 × TGS running buffer

Tris base	25 mM
Glycine	192 mM
SDS	0.1%

4.11. Western blotting

The proteins from PAA gels were transferred on nitrocellulose membrane *(Amersham Protran 0.45 µm NC wester blotting membrane, GE Healthcare Life Sciences, USA)* by assembling the transfer sandwich using Whatman Filter Paper *(Sigma-Aldrich, USA)* (sponge-Whatman paper-PAA gel-membrane-Whatman paper-sponge, all soaked in transfer buffer) and the cassette with transfer sandwich was placed into a transfer tank with an ice block. The tank was filled with 1 × blotting TG buffer (Table 25) diluted with ddH_2O from 10 × TG buffer *(Bio-Rad, USA)* with added methanol to the final concentration 10%. Transfer was done in a cold room (4°C) at constant current of 400 mA for 1.5 hour.

Table 25: of 1x TG blotting

	1 × TGS blotting buffer
Tris base	25 mM
Glycine	192 mM
methanol	10%

T

The efficiency of the protein transfer was checked by staining the membrane with Ponceau S (0.1% Ponceau S, 5% acetic acid) washed 3 times in PBS-T (1 × PBS, 0.1% TWEEN-20) for 10 minutes and incubated in 5% non-fat milk for 1 hour. The membrane was washed 3 times in PBS-T. To detect biotinylated proteins, membrane was incubated in IRDye 800cw Strepavidin (Table 26) for 1 hour in RT. Subsequently the membrane was washed 3 times in PBS-T for 10 minutes and 1 time in 1 × PBS. Membrane was analysed using Odyssey imaging system.

To detect PML protein fused to GFP, the membrane was incubated in 1000 × diluted primary antibody (Table 26) overnight in 4°C. The membrane wash washed three times in PBS-T and membrane was incubated in and appropriate secondary antibody fused to HRP (Horseradish peroxidase) (Table 26) for 1 hour. After incubation in the secondary antibody the membrane was washed three times in PBS-T and ECL chemiluminescent substrate

(Amersham ECL Prime Western Blotting Detection Reagent, GE Healthcare Life Sciences, USA) was prepared and applied on the membrane and incubated for 1 minute. The chemiluminescent signal was captured on the film.

4.12. Membrane stripping

Membrane was stripped after detection of PML protein using anti-PML antibody in order to re-probe the membrane with anti-GFP antibody to detect GFP signal.

Membrane was 3 × washed with PBS-T and incubated in stripping buffer (*Restore^{TM} Western Blot Stripping Buffer, Thermofisher Scientific)* for 15 minutes. Subsequently membrane was blocked and incubated in another primary antibody.

4.13. Dot blotting

Samples for dot blotting were incubated in 95°C. Nitrocellulose membrane and two layers of filter paper were soaked in ddH_2O for 5 minutes and laid on the dot blotting apparatus. The upper part of dot blotting apparatus was secured on top of the lower part. Samples were applied in the volume of 100 µL containing 20 µg of sample and replenish with 1 × PBS and vacuum was used to embed the samples into the membrane. Membrane was incubated in Ponceau S (0.1% Ponceau S, 5% acetic acid) for 10 minutes and scanned. Subsequently it was blocked in 5% non-fat milk for 1 hour. In the next step the membrane was incubated in IRDye 800cw Strepavidin (Table 26) for 1 hour. After incubation in IRDye 800 cw Strepavidin the membrane was 3 times washed in PBS-T and 1 × in PBS for 10 minutes and analysed by Oddysey imaging system

Table 26: Antibodies and infrared dye for Western blotting and dot blotting

Antibodies and infrared dye Western blotting and Dot blotting			
Name	**Host**	**Purchased from, Cat. No.**	**Dilution**
Anti-PML Ab	rabbit	Santa Cruz, SC5621	1:1000
Anti GFP – HRP Ab	mouse	Termofisher Scientific, MA5-15256-HRP	1:1000
Secondary antibodies			
Goat anti rabbit IgG:HRP	Goat	Bio-Rad, 5196-2504	1:10000
Infrared Dye			
IRDye 800cw Strepavidin	-	LI-COR, 926-32230	1:1000

4.14. Nuclear fractionation

Cells harvested from 60 cm^2 were washed 3 times with 1 × PBS and trypsinized. Cells were collected into a 15 mL falcon tube and centrifuged for 5 minutes at 300 × g and 4°C. Pellet was washed twice in ice cold 1 × PBS. Volume of pellet (VP) was estimated and resuspended in 5 VP volumes of Hypo buffer (Table 27). The cells were incubated for 5 minutes on ice and then Nonidet P-40 (NP-40) was added to a final concentration 0.5%. Subsequently cells were incubated for 4 – 6 minutes to disrupt the cytoplasmic membrane and centrifuged for 5 minutes at 300 × g and 4°C. After centrifugation supernatant was stored as fraction 1 (S1). Pellet was washed twice with 500 µL of Hypo buffer (Table 27) and the washes were stored as W1 and W2. Pellet was resuspended in 2 VP volumes of ice cold Buffer B (Table 28) with 0.4% NP-40 and either 0.4% or 1% SDS. The samples were then sonicated (2 seconds ON/4 seconds OFF, amplitude 2 microns, 20 cycles) and centrifuged (16 000 × g, 20 min, 4°C). Supernatant was stored as fraction S2-0.4% SDS or S2-1% SDS. Pellet was resuspended in 1 × sample buffer in which 0.4% NP-40 and 0.4%/1% SDS was added and stored as fraction P. Concentration of the samples was measured by BCA assay.

Table 27: Composition of Hypo buffer

HEPES, pH 7.9	10 mM
$MgCl_2$	1.5 mM
KCl	10 mM
PI (protease inhibitors)	1 mM
DTT	1 mM

Table 28: Composition of Buffer B

HEPES, pH 7.4	50 mM
KCl	130 mM
PI (protease inhibitors)	1 mM
DTT	1 mM

4.15. Isolation of biotinylated proteins using Dynabeads™ My One™Strepavidin C1 magnetic beads

Soluble fraction of nuclear proteins in Buffer B (Table 28) with 1% NP-40 and 0.4% SDS was subjected to the isolation of biotinylated proteins. Firstly 50 µL of Dynabeads™My

One^{TM} Strepavidin C1 magnetic beads *(Invitrogen, USA)* was washed four times in equal volume of PBS. Beads were separated using magnetic holder between washes.

Soluble nuclear fraction (200 µL, 0.5 mg/mL) was incubated with 50 µL of magnetic beads for 1 hour. Before incubation, 22 µL of the sample was left as "input". The beads with isolated biotinylated proteins were separated using magnetic holder for 3 minutes and 22 µL of the samples was left as "output''. The beads were washed three times in 200 µL of Buffer B (Table 28), incubated in 4°C for 5 minutes and separated. Supernatant was stored as W1. The beads were further resuspended in 200 µL of Tris-HCl buffer, pH 7.4 containing 1% NP-40 and 0.4% SDS, incubated at 4°C for 5 minutes and placed into a magnetic holder for separation. Supernatant was stored as W2. Two more washes of beads followed using Buffer B and storing the supernatant as W3 and W4. In the next step 50 µL of 4 × sample buffer was added to the beads and they were incubated in 95°C for 5 minutes to release the isolated biotinylated proteins from the magnetic beads. After separation in magnetic holder for 3 minutes sample was stored as IP.

4.16. Laboratory instruments, enzymes and chemicals

All laboratory instruments used in experiments in this thesis are listed in a Table 29. All enzymes and chemicals used in experiments in this thesis are listed in Table 30.

Table 29: Laboratory instruments

Laboratory instruments	Company	Country
Thermomixer comfort	Eppendorf	USA
NanoDrop ND-1000 spectrophotometer	Thermofisher Scientific	USA
Axygen® horizontal gel box	Corning	USA
MJ Mini Personal Thermal Cycler	Bio-Rad	USA
Fluorescence microscope Eclipse TE300	Nikon	Japan
Centrifuge NF-40m	Nüve	Turkey
Rotator RM-5	Ingonieurbüro CAT	Germany
Haraeus Megafuge 16R	Termofisher Scientific	USA
Sonicator Soniprep 150	Shoeller Instruments	Czech Republic
Electrophoresis apparatus Mini-PROTEAN Tetra Cell	Bio-Rad	USA
Western blotting transfer tank	Bio-Rad	USA
Amersham Protran 0.45 µm NC western blotting membrane	GE Healthcare Life Sciences	USA
Odyssey 9120	LI-COR	USA
Optimax 2010	Protec	Germany
Centrifuge 5810 R	Eppendorf	USA
Dot/Slot System	Schleicher&Schuell	USA
Leica DM6000	Leica Microsystems	Germany
ProBlot™ Rocker 25	Labnet	USA
Centrifuge 5424	Eppendorf	USA
Centrifuge 5424 R	Eppdendorf	USA
Forma 3121 Water Jacketed CO Incubator, IR230	Thermofisher Scientific	USA
Microbiological Safety Cabinet Bio II A	Telstar, USA	Japan
Water Bath BM 402	Nüve	Turkey
Eclipse TS100	Nikon	Japan
Multiskan EX	Thermofisher Scientific	USA
TPP plastic	Thermofisher Scientific	USA

Table 30: Chemicals

Chemical/enzyme	Company, State, Cat. No.
FastDigest *Bam*HI	ThermoFisher Scientific, USA, FD0054
FastDigest *Bsp*OI	ThermoFisher Scientific, USA, FD2044
FastDigest *Hind*III	ThermoFisher Scientific, USA, FD0504
FastDigest *Not*I	ThermoFisher Scientific, USA, FD0594
10x FD buffer	ThermoFisher Scientific, USA
*Kpn*I	Fermentas, USA, ER0521
10x Buffer *Kpn*I+	Fermentas, USA
*Dpn*I	Fermentas, USA, ER1702
Phusion High-Fidelity DNA polymerase	New England Biolabs, USA, M0530L
5x GC Phusion reaction buffer	New England Biolabs, USA, B05119S
dNTP	ThermoFisher Scientific, USA
dGTP 100 mM	ThermoFisher Scientific, USA, R0161
dATP 100 mM	ThermoFisher Scientific, USA, R0141
dCTP 100 mM	ThermoFisher Scientific, USA, R0151
dTTP 100 mM	ThermoFisher Scientific, USAR0171
T4 Polynucleotide kinase (PNK)	ThermoFisher Scientific, USA, EK0031
Buffer A for PNK	Fermentas, USA
ATP	Fermentas, USA, R0481
Shrimp Alcaline Phosphatase	Fermentas, USA, EF0511
T4 DNA ligase	ThermoFisher Scientific, USA, EL0111
5x Rapid ligation buffer	ThermoFisher Scientific, USA, K1422
$MgCl_2$	ThermoFisher Scientific, USA
Dithiotreitol (DTT)	Sigma-Aldrich, USA
Nicotinamide adenine dinucleotide (NAD)	Sigma-Aldrich, USA, B9007S
Polyethylenglycol	LOBA, India
Fetal bovine serum	Gibco, USA
Penicillin/Streptomycin	Invitrogen
Dulbecco's modified Eagle's medium	Gibbco, Ireland
RedSafe™ Nucleic Acid Staining Solution	iNtRON Biotechnologies, South Korea 21141
Polyethylenimine	Sigma-Aldrich, USA, 408727
optiMEM	Gibco, Ireland, 51985
SDS	Serva, Germany, 20765
DAPI	Sigma-Aldrich, USA, 10236276001
ProLong ™ Gold Antifade Reagent	Invitrogen, USA, P36930
4% Formaldehyde	VWR-Chemicals, USA, 1.00496.8350
Sodium azide	Sigma-Aldrich, USA, 26628-22-8
TRITON™ X-100, 10%	Sigma-Aldrich, Usa, 9002-93-1
Acrylamine	Serva, Germany, 10-687
APS	Sigma-Aldrich, USA, A3679-25G
TEMED	Sigma-Aldrich, USA, T9281
Bromphenol Blue	Lachema
PonceauS	Sigma-Aldrich, USA, 81460-25G
TWEEN 20	Serva, Germany, 37470
Methanol	Lach-ner, Czech Republic, 67-56-1
Protease inhibitors	Roche, Switzerland,
FuGENE 6	Promega, USA, E2691

5. Results

5.1. Generation of DNA constructs containing biotin ligase (BioID2) and green fluorescent protein (GFP) fused to PML IV or its truncated form PML IV Δ560-633

The PML IV isoform associates with boundary of segregated nucleolus in reaction to ribosomal stress in this case caused by doxorubicin treatment. PML function in this interaction has not been clarified yet. Identification of protein in proximity to PML during its association with nucleolus could help to better understand the state of nucleolus in contact with the PML and may elucidate the role of the PML in this interaction.

For this experiment we chose wild type and mutated (Δ560-633) form of PML IV isoform (Figure 8). It is known, that PML IV interacts with nucleolus in response to doxorubicin treatment but portion of PML still localizes to PML NBs. The truncated form of PML IV does not associated with nucleolus after this treatment and accumulates only in PML NBs. The comparison of obtained biotinylated protein might help to find the proteins that are specific form nucleolar association, so the mutated form represents negative control for mass spectrometry analysis.

To enable the identification of PML interaction partners we fused human PML IV and its truncated form PML IV Δ560-633 to biotin ligase BioID2. We decided to insert the BioID2 behind the C-terminus of PML as C-terminal fusion of EGFP with PML for characterization of PML domains involved in its interactions with nucleolus was functional and we assumed that this will be no different. I inserted a flexible linker $(GGGGS)_{3x}$ between the PML and BioID2 to expand the biotinylation radius of BioID2. In addition both PML IV and its truncated form were previously fused to EGFP ensure comfortable detection by fluorescent microscopy. EGFP fusion mainly brings advantage during preparation of stable cell lines expressing fusion protein as the cells can be sorted according to the intensity of GFP that should mirror expression level of PML protein. Schematic representation of final fusion proteins and how they differ from original PML-GFP and PML MUT-GFP can be seen in Figure 9.

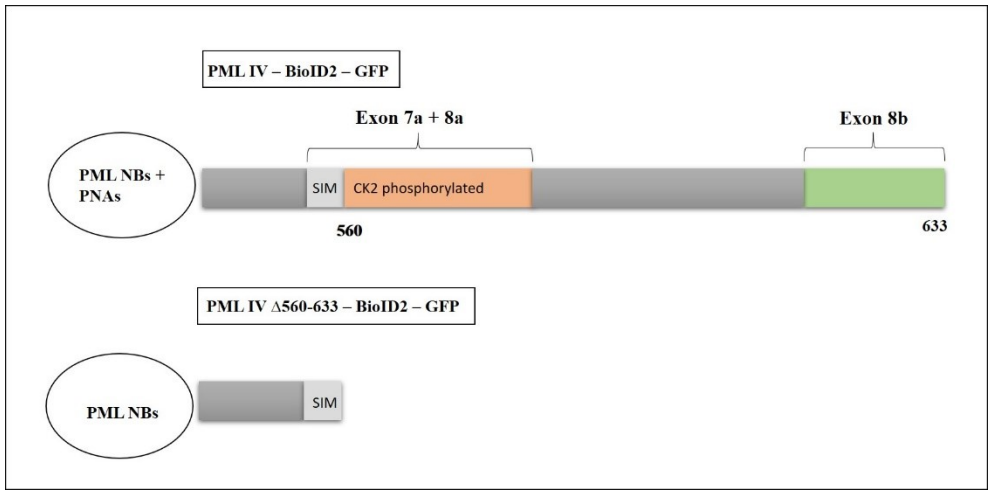

Figure 8: Truncated form of PML IV lacking amino acids 560-633 containing domains arguably responsible for association with nucleolus should not be able to do so in response to ribosomal stress. Scheme of wild type *PML IV and its mutant form lacking C-terminal domains arguably responsible for its association with nucleolus, thus unable to associate with nucleolus under conditions of stress.*

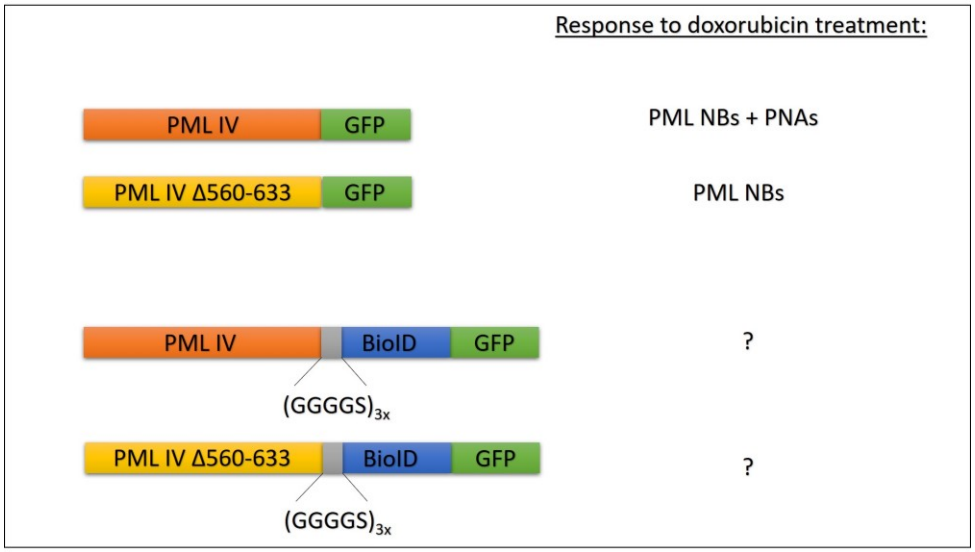

Figure 9: Scheme of constructed PML fusion proteins and their comparison with already existing PML constructs is shown. *PML IV – isoform of PML protein; PML IV Δ560-633 – deletion mutant of PML IV isoform lacking amino acids 560–633; BioID2 – biotin ligase; $(GGGGS)_{3x}$ – flexible linker comprising from three stretches of four glycines and serine; GFP – green fluorescent protein.*

I generated two types of expression vectors. First one allowed treansient expression in mammalian systems and is based on pEGFP-N1 expression vectors. Final vectors for transient expression were named pPML-BioID-GFP and pPML MUT-BioID-GFP. Second set of expression vectors enabled generation of cell lines stably expressing desired fusion protein. Final vectors for stable expression were named lenti-PML-BioID-GFP and lenti-PML MUT-BioID-GFP. Expression of both systems is driven from CMV promotor. This constitutive

CMV promoter was chosen based on previous positive experience with preparation of cell line stably expressing PML IV-EGFP and PML I-EGFP.

All fusion proteins were analysed in hTERT PML KO as presence of endogenous PML protein could camouflage the properties of PML MUT, because this mutant can associate with nucleolus in the presence of other endogenous PML isoforms.

5.2. Characterization of fusion proteins PML-BioID-GFP and PML MUT-BioID-GFP expressed in RPE1 PML KO cells after transient transfection

Both DNA constructs verified by sequencing (pPML-BioID-GFP and pPML MUT-BioID-GFP) needed to be tested for expression of PML fusion proteins. My aim was to verify the ability of wild type PML and its truncated form both fused to BioID-GFP to form PML NBs when transiently expressed in hTERT RPE1 PML KO cells. Next, I needed to evaluate PNAs formation after doxorubicin treatment and confirm the activity of biotin ligase in these fusion proteins. Finally, I analysed presence of some canonical interactors of PML in PML NBs formed by these fusion proteins.

5.2.1. PML-BioID-GFP and PML MUT-BioID-GFP can form PML NBs in RPE1 PML KO cells

To test the ability of both new fusion proteins to form PML NBs in hTERT RPE1 PML KO cells I transiently transfected these cells with plasmids expressing both these proteins and with plasmids expressing original fusion proteins PML-GFP and PML MUT-GFP. One day after transfection the cells were harvested and GFP pattern was analysed by wide field microscopy. According to the results of immunofluorescence analysis I assessed that cells expressing either PML-BioID-GFP or PML MUT-BioID-GFP successfully form PML NBs and that the pattern of these PML NBs was comparable with the pattern of PML NBs observed in positive controls represented by cells transfected with vectors pPML-GFP or pPML MUT-GFP (see Figures 10 and 11).

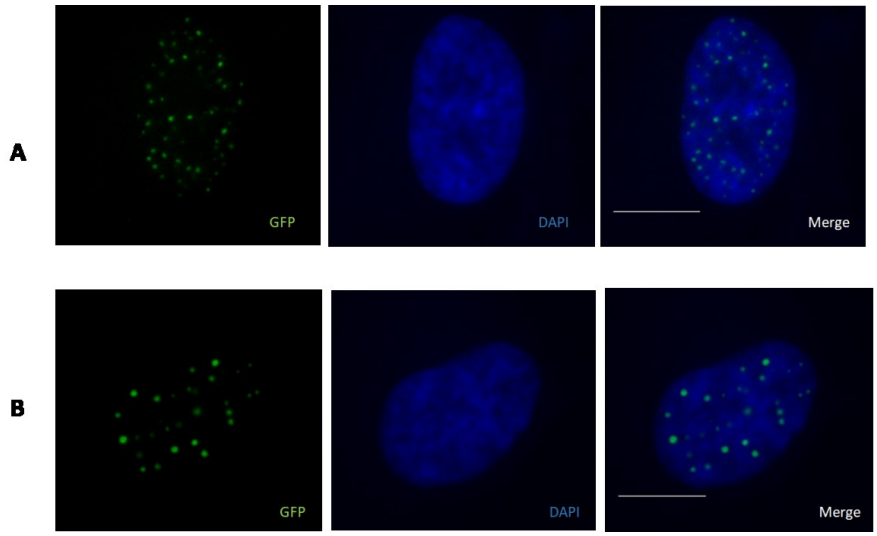

Figure 10: **PML-BioID-GFP forms PML NBs that are comparable with PML NBs formed by PML-GFP.** *Pattern of PML NBs (green) formed in hTERT RPE1 PML KO cells transfected with PML-GFP (A) and transfected with PML-BioID-GFP (B). The nuclei were stained by DAPI (blue). Scale bar, 10 µm*.

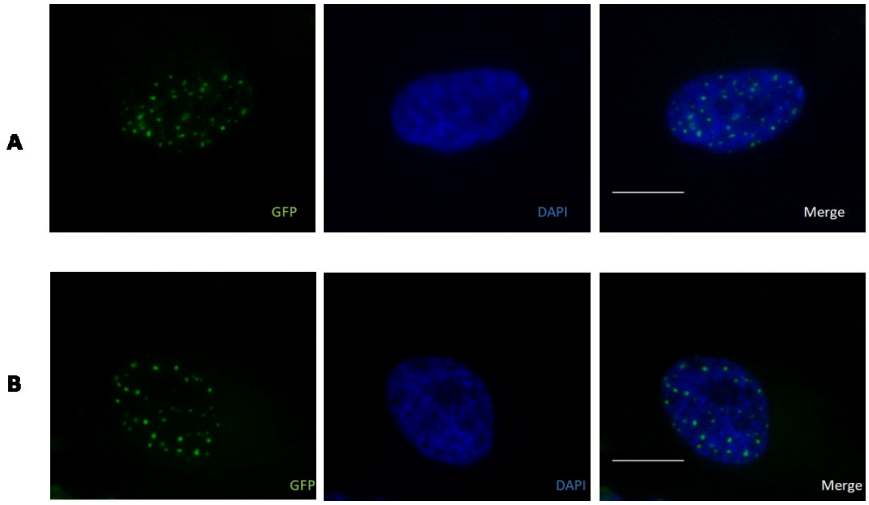

Figure 11: PML MUT-BioID-GFP forms PML NBs that are comparable with PML NBs formed by PML MUT-GFP. *Pattern of PML NBs (green) formed in hTERT RPE1 PML KO cells transfected with PML MUT-GFP (A) and transfected with PML MUT-BioID-GFP (B). The nuclei were stained by DAPI (blue). Scale bar, 10 µm.*

5.2.2.PML-BioID-GFP but no PML MUT-BioID-GFP can associate with nucleolus after doxorubicin treatment

Based on on-going research it is clear, that the PML IV isoform associates with nucleolus after doxorubicin treatment, whereas its mutant form of PML IV Δ560-633 isoform lacks this ability and after such treatment does not associate with nucleolus. To test whether the additional fusion of PML-GFP and PML MUT-GFP with BioID moiety did not change this characteristic, I transiently transformed hTERT RPE1 PML KO cells with plasmids expressing all four fusion proteins and 24 hours after transfection treated these cells for another 48 hours with 0.75 μM doxorubicin. Then the cells were harvested and analysed by wide field microscopy.

As is shown in Figure 12, 13 and Graph 1, PML-GFP and new fusion protein PML-BioID-GFP associated with nucleolus and showed similar response to doxorubicin treatment. I observed nucleolar associations in 24% of treated cells expressing PML-BioID-GFP, which roughly corresponds with 27% of cells expressing PML-GFP established as a positive control. In case of cells expressing PML MUT-BioID-GFP and PML MUT-GFP, this experiment revealed that these PML truncations did not associated with nucleolus at all (Figure 14).

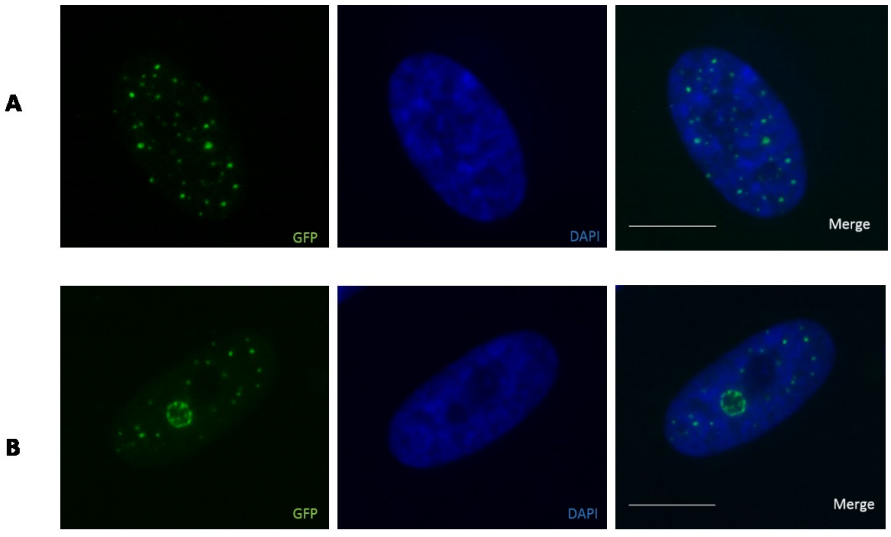

Figure 12: **PML-GFP forms PML nucleolar associations after doxorubicin treatment.** *hTERT RPE1 PML KO cells after transient transfection with pPML-GFP (green) and after 0.75 μM doxorubicin treatment (48 h) contain cells with only PML NBs (A) and cells with PNAs and PML-NBs (B). The nuclei were stained by DAPI (blue). Scale bar, 10 μm.*

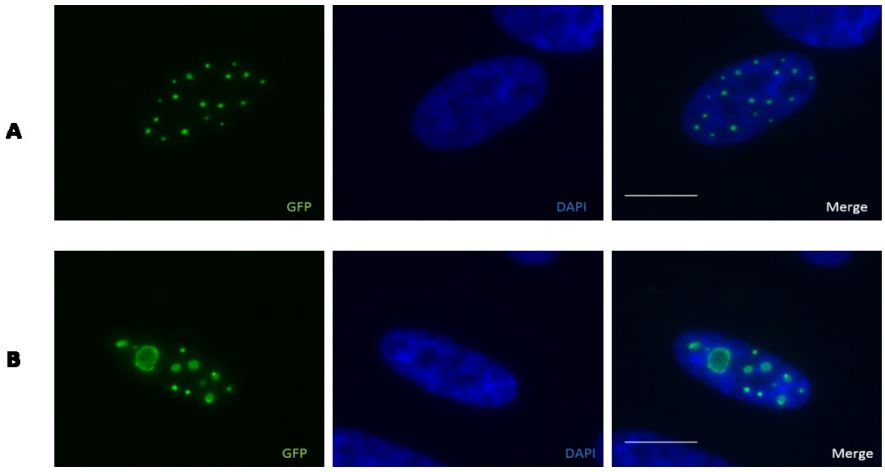

Figure 13: **PML-BioID-GFP forms PML nucleolar associations after doxorubicin treatment.** *hTERT RPE1 PML KO cells after transient transfection with pPML-BioID-GFP (green) and after 0.75 µM doxorubicin treatment (48 h) contained cells with only PML NBs (A) and cells with PNAs and PML NBs (B). The nuclei were stained with DAPI (blue). Scale bar, 10 µm.*

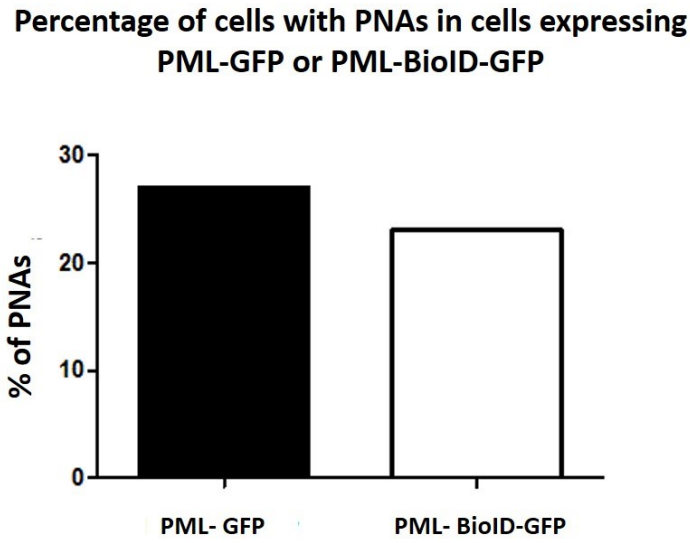

Graph 1: The portion of cells with PML nucleolar associations (PNAs) formed after doxorubicin treatment either by pPML-GFP or PML-BioID-GFP is comparable. *hTERT RPE-1 PML KO cells were transfected with pPML-GFP or PML-BioID-GFP and treated with 0.75 µM doxorubicin. After two days the number of cells with PNAs was counted and the portion of cells with PNAs [%] was plotted. Over 100 cells were analyzed. The results of one experiment are shown.*

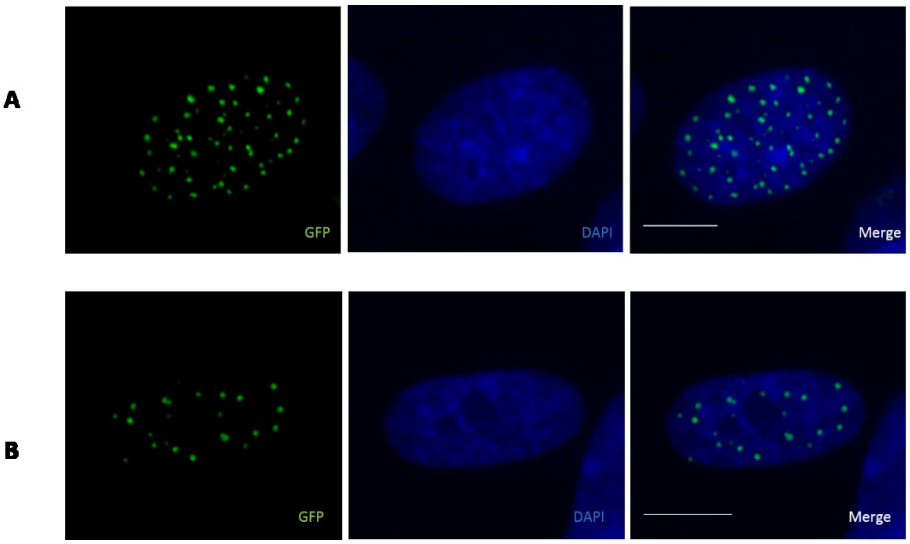

Figure 14: **PML MUT-GFP and PML MUT-BioID-GFP did not form nucleolar associations after doxorubicin treatment.** *Pattern of PML MUT-GFP (green); (A) and PML MUT-BioID-GFP (Green); (B) expressed in hTERT RPE1 PML KO cells after transfection. These cells were treated two days with 0.75 µM doxorubicin for 48 hours. The nuclei were stained with DAPI (blue). Scale bar, 10 µm.*

5.2.3.PML-BioID-GFP and PML MUT-BioID-GFP can accumulate biotinylated proteins in PML NBs

Next, I was interested in overall functionality of biotin ligase BioID2, level of biotinylation and also whether biotin background generated by endogenous biotin and biotin in cell culture media will or will not be an issue in further experiments.

Therefore, I again transfected RPE1 PML KO cells with vector expressing either PML-BioID-GFP or PML MUT-BioID-GFP. Note, for experiments aimed to test biotinylation both PML protein fused only to GFP (PML-GFP and PML MUT-GFP) were used as negative controls. One day after transfection the cells were further cultivated with/without addition of 50 µM biotin. Treatment was terminated after 4 or 24 hours. Then the cells were harvested and stained with streptavidin-phycoerythrin and analysed by wide field microscopy.

These experiments revealed that all PML NBs formed by PML-BioID-GFP or PML MUT-BioID-GFP were positive for biotinylated proteins (Figure 15 and 16) contrary to PML NBs formed by cells expressing PML-GFP or PML MUT-GFP (Figure 17). Notably, the weak biotinylation of PML NBs was detected also in cells expression PML fused to BioID2 but cultivated without biotin addition (Figure 15A and C, Figure 16A and C). This indicates that

endogenous level of biotin is sufficient to promote the addition of biotin to proteins that are in proximity of PML.

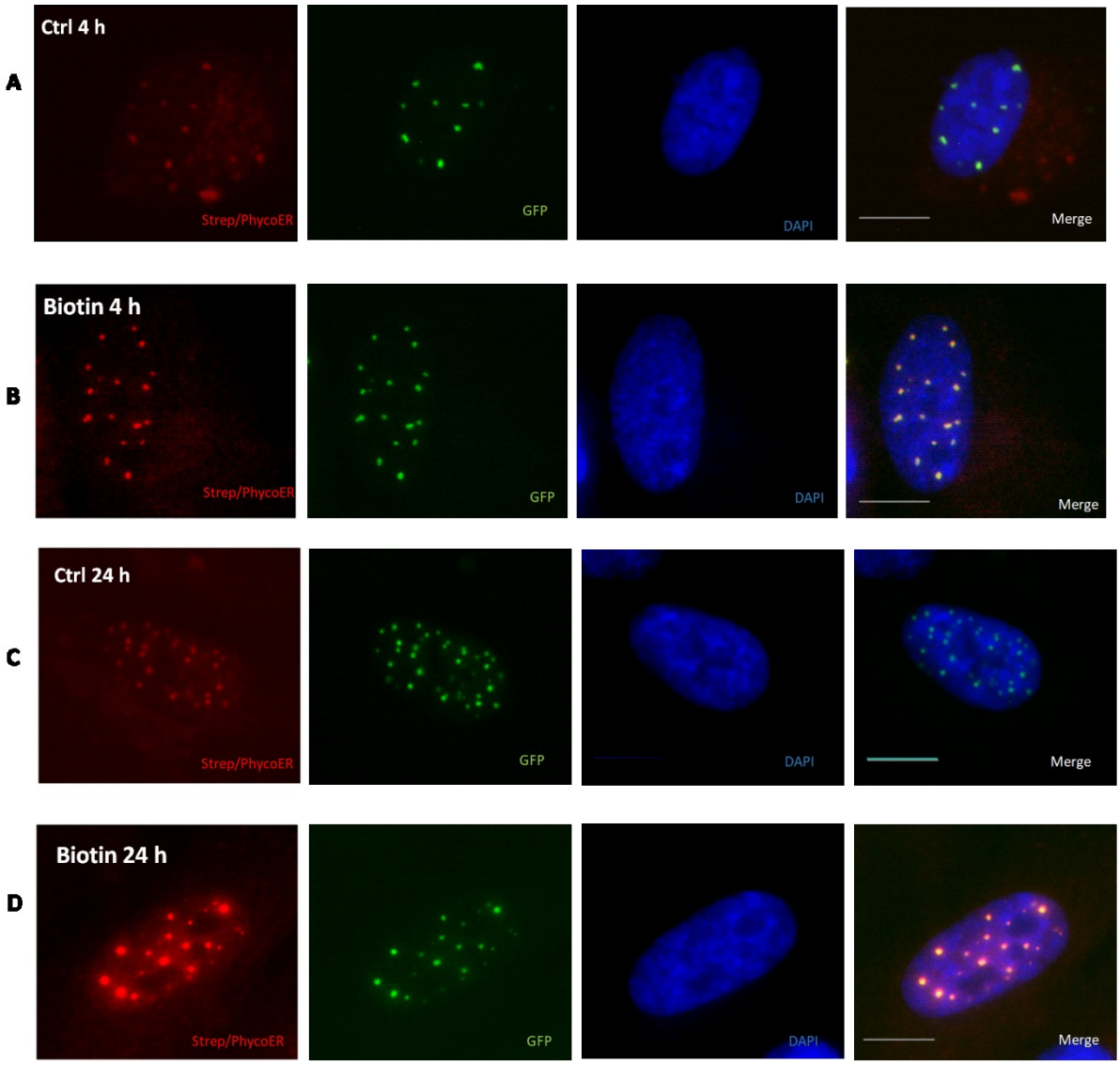

Figure 15: The expression of PML-BioID-GFP generated the accumulation of biotinylated proteins in PML NBs. *The RPE1 PML KO cells were transfected with vector coding PML-BioID-GFP (green). One day after transfection the fresh medium without added biotin (A and C) or with 50 μM biotin (B and D) was added. The cells were harvested after 4 hours (A and B) or after 24 hours (C and D) and stained with streptavidin-phycoerythrin (red) to detect biotinylated proteins. The nuclei were stained with DAPI (blue). Scale bar, 10 μm.*

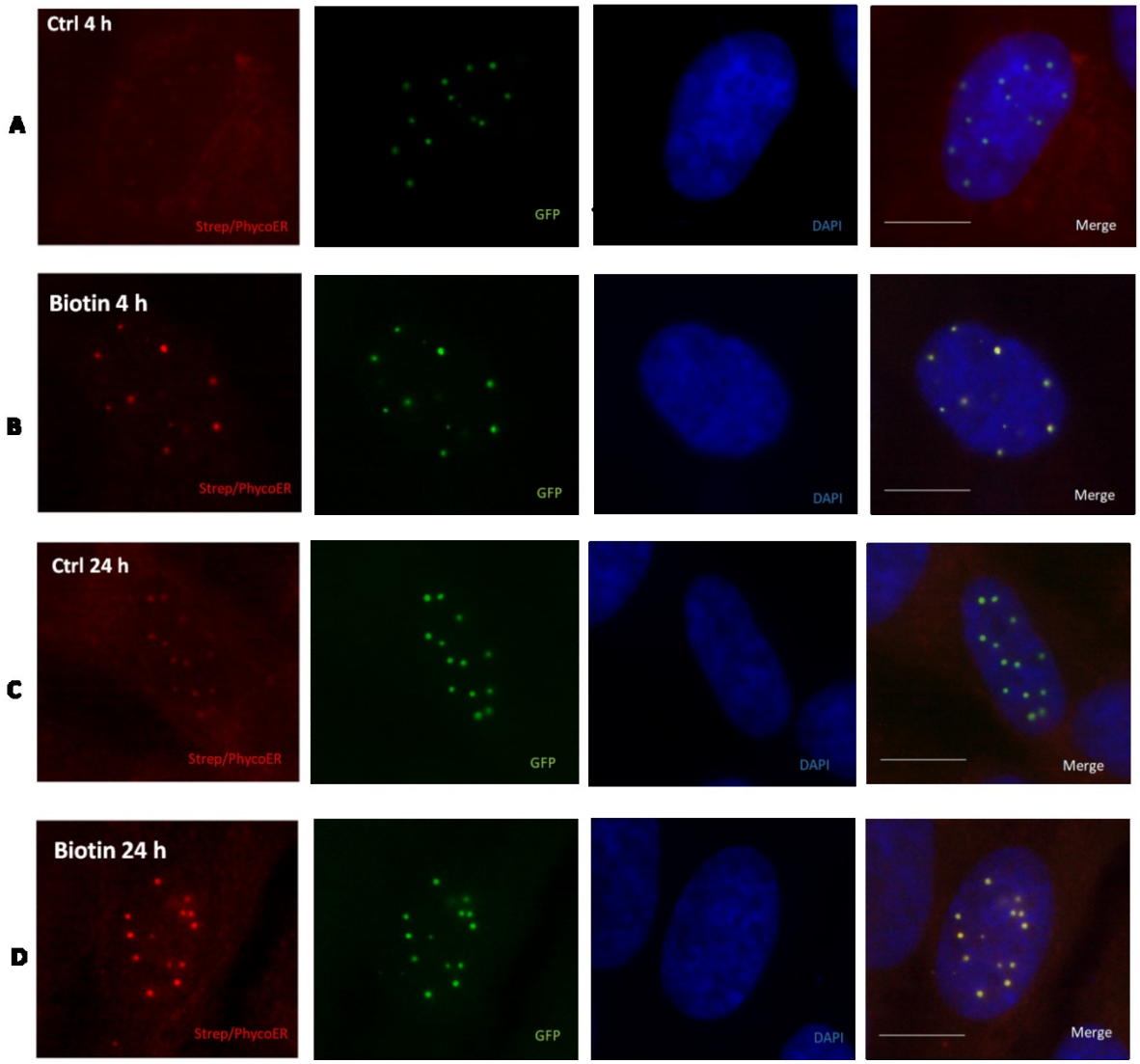

Figure 16: The expression of PML MUT-BioID-GFP generated the accumulation of biotinylated proteins in PML NBs. *The RPE1 PML KO cells were transfected with vector coding PML MUT-BioID-GF (green). One day after transfection the fresh medium without added biotin (A and C) or with 50 μM biotin (B and D) was added. The cells were harvested after 4 hours (A and B) or after 24 hours (C and D) and stained with streptavidin-phycoerythrin (red) to detect biotinylated proteins. The nuclei were stained with DAPI (blue). Scale bar, 10 μm.*

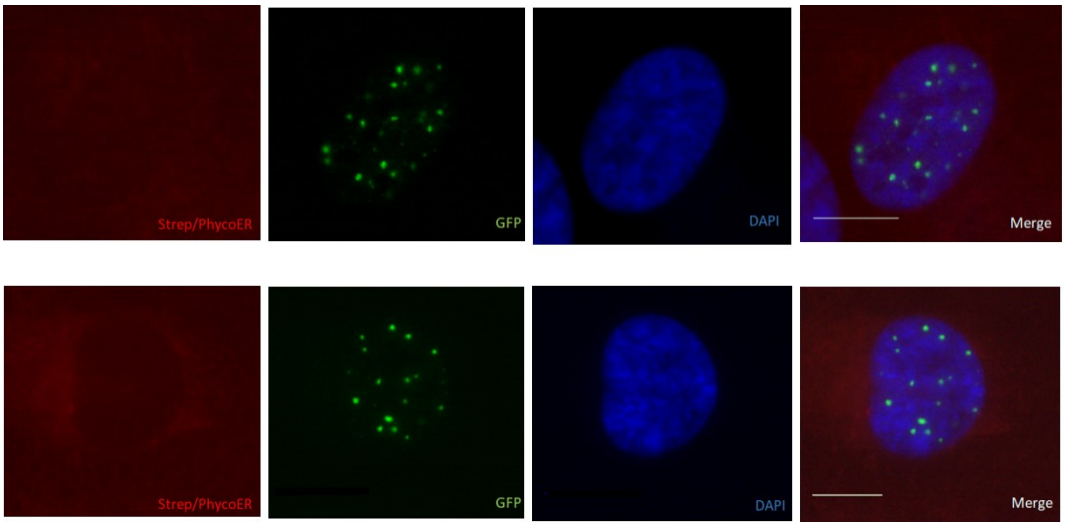

Figure 17: PML NBs formed by either PML-GFP or PML MUT-GFP did not contain biotinylated proteins after incubation with biotin. *RPE1 PML KO cells expressing PML-GFP (green);(A)) or PML MUT-GFP (green; (B)) were incubated with 50 µM biotin for 24 h. After that biotinylated proteins were detected using streptavidin-phycoeryhrin (red). The nuclei were stained with DAPI (blue). Scale bar, 10 µm.*

Lastly, the biotinylation of PML NBs and PNAs after doxorubicin treatment was tested. PML NBs formed by both PML-BioID-GFP or PML MUT-BioID-GFP were biotinylated (Figure 18, Figure 19) Our results indicate that the addition of biotin does not have any detectable effect on PNAs formation by PML-GFP and PML-BioID-GFP (Figure 18). Importantly, the PNAs formed by PML-BioID-GFP after doxorubicin treatment and addition of biotin were biotinylated (Figure 18B). Obtained results also confirmed that the biotinylation of PML NBs and PNAs under tested condition is BioID2-dependent as both type of structures were streptavidin-phycoerythrin negative when PML-GFP and PML-MUT-GFP fusions were expressed and incubated with doxorubicin and biotin (Figure 18A and 19A).

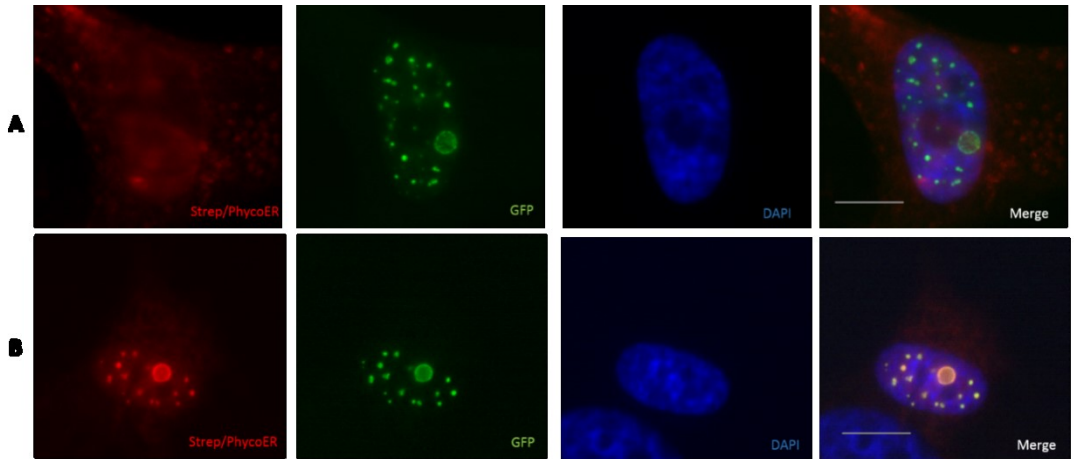

Figure 18: PNAs formation is not affected by incubation with biotin and the biotinylation of PNAs is dependent on presence of BioID2. *hTERT RPE1 PML KO cells expressing PML-GFP (green; (A)) and PML-BioID-GFP (green; (B)) were treated with 0.75 µM doxorubicin for 48 h and with 50 µM biotin for 24 hours. The biotinylated proteins were detected using streptavidin-phycoerythrin (red).The nuclei were stained with DAPI (blue). Scale bar, 10 µm.*

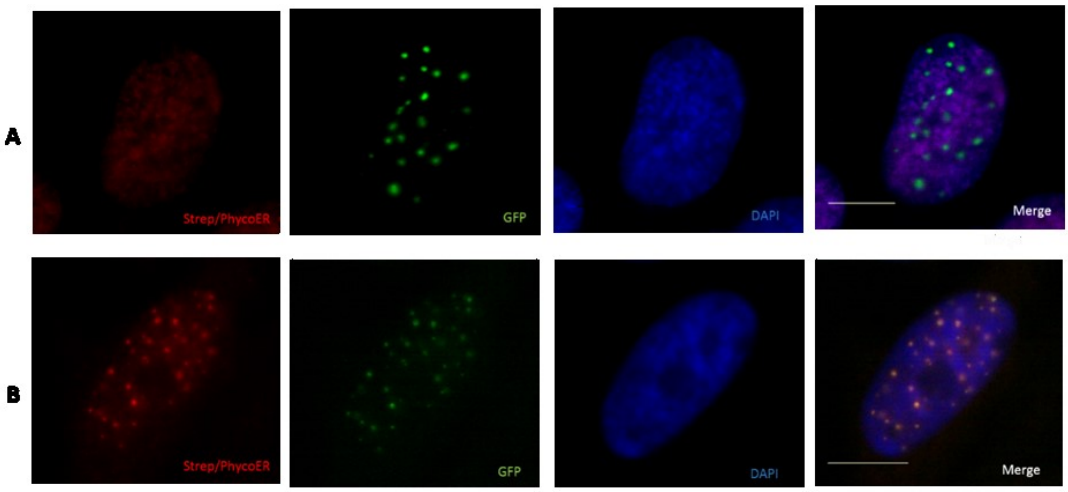

Figure 19: PML MUT-GFP and PML MUT-BioID-GFP did not form PNAs after doxorubicin and biotin treatment. *hTERT RPE-1 PML KO cells expressing PML MUT-GFP (green; (A)) and PML MUT-BioID-GFP (green; (B)) were treated with 0.75 µM doxorubicin for 48 h and with 50 µM biotin for 24 hours. The biotinylated proteins were detected using streptavidin-phycoerythrin (red). The nuclei were stained with DAPI (blue). Scale bar, 10 µm.*

5.2.4.PML NBs formed by PML-BioID-GFP and PML MUT-BioID-GFP are positive for DAXX, SUMO-1 and SUMO-2/3

To further confirm that PML-BioID-GFP and PML MUT-BioID-GFP form PML NBs with characteristic composition, the RPE-1 PML-KO cells transiently expressing above mentioned fusion proteins were analysed by wide field microscopy. After harvesting I detected the PML, SUMO-1, SUMO-2/3 and DAXX using indirect immunofluorescence staining. As is shown in Figure 20 and 21, these experiments revealed that PML NBs formed by both tested fusion proteins were recognized by PML antibody. In addition, such PML NBs were positive for SUMO-1, SUMO-2/3 and DAXX proteins.

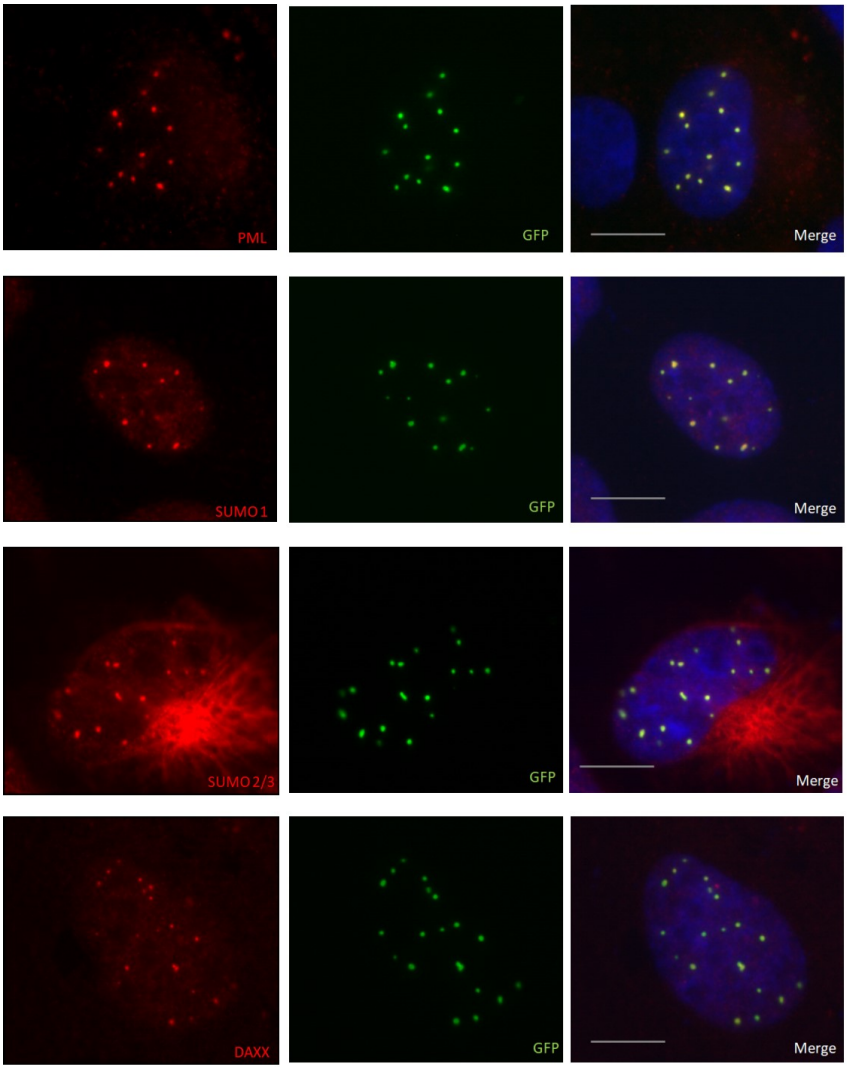

Figure 20: PML NBs formed with PML-BioID-GFP contained SUMO-1, SUMO-2/3 and DAXX. *RPE1 PML KO cells expressing PML-BioID-GFP (green) were stained with anti-PML, anti-SUMO-1, anti-SUMO-2/3 and anti-DAXX antibodies (all red). The nuclei were stained with DAPI (blue). Scale bar, 10 µm.*

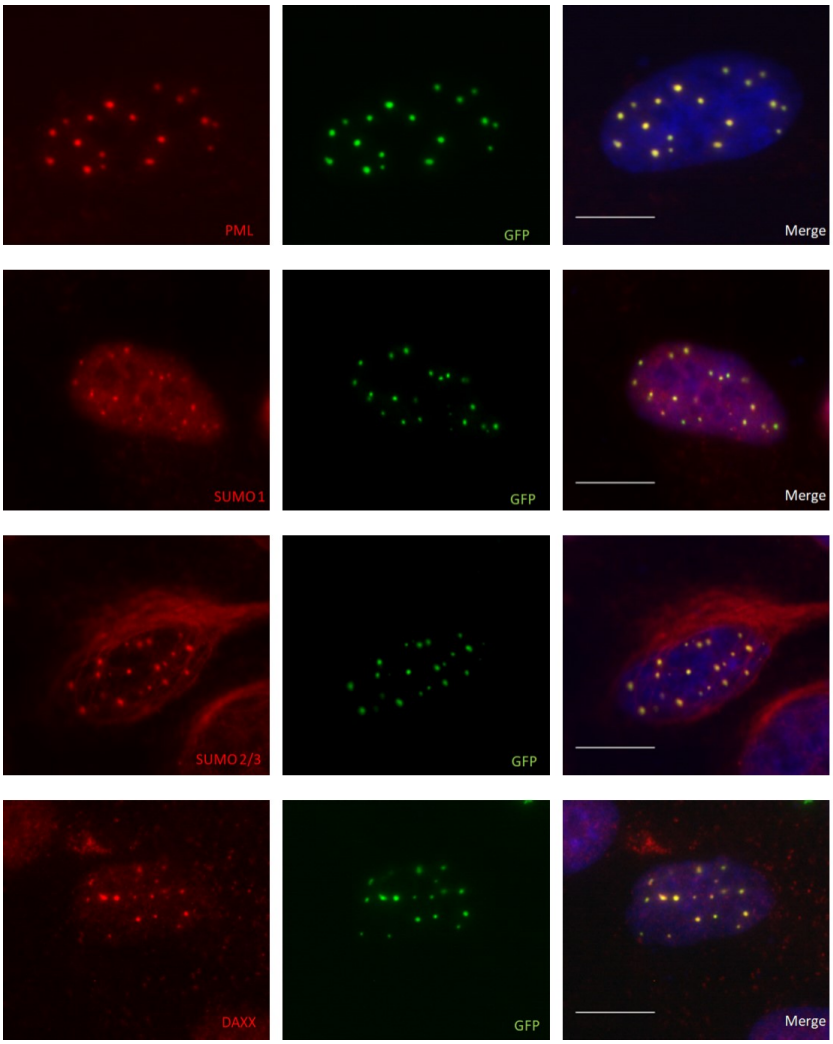

Figure 21: PML NBs formed with PML MUT-BioID-GFP contained SUMO-1, SUMO-2/3 and DAXX. *RPE1 PML KO cells expressing PML MUT-BioID-GFP (green) were stained with anti-PML, anti-SUMO-1, anti-SUMO-2/3 and anti-DAXX antibodies (all red). The nuclei were stained with DAPI (blue). Scale bar, 10 µm.*

All these results indicate that fusion of wild type PML and its truncated form PML MUT to BioID2-GFP did not significantly change the quality of these fusion proteins. Both are able to form PML NBs that are positive for SUMO-1, SUMO-2/3 and DAXX, however, only the wild type PML-BioID-GFP fusion associates with nucleolus after doxorubicin treatment. Importantly, this ability was not affected by the incubation with biotin. Additionally, I detected significant difference in biotinylation signal of PML NBs formed by cells cultivated with/without addition of biotin.

5.3. Preparing RPE1 PML KO cell line stably expressing either PML-BioID-GFP or PML MUT-BioID-GFP

Despite the positive results provided by the experiments described above, the overall characterization of transiently transfected hTERT RPE1 PML KO cells showed that expression of either PML-BioID-GFP or PML MUT-BioID-GFP is accompanied with high heterogeneity in PML expression and rather low transfection efficiency (see Figure 22 and 23). Such heterogeneous population was not suitable for planned experiments involving nuclear fractionation followed by isolation of biotinylated proteins using streptavidin magnetic beads and final mass spectrometry analysis.

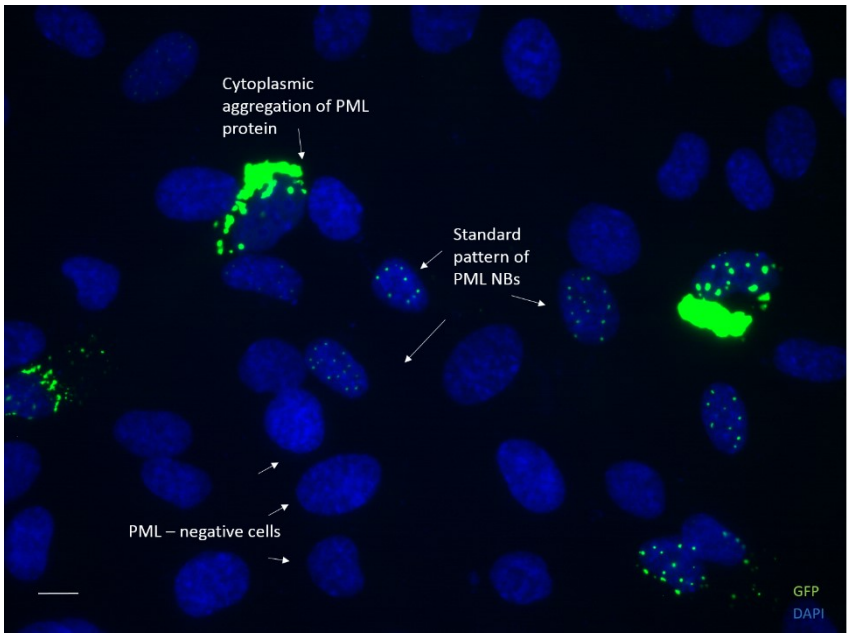

Figure 22: The PML-BioID-GFP revealed heterogeneous pattern after transient transfection. *After transfection of RPE1 PML KO cells with vector expressing PML-BioID-GFP (green) several populations of cells were presented. The lines with arrow point to cells with standard pattern of PML NBs, cells with aggregates of PML fusion protein and untransfected cells. The nuclei were stained with DAPI (blue). Scale bar, 10 µm.*

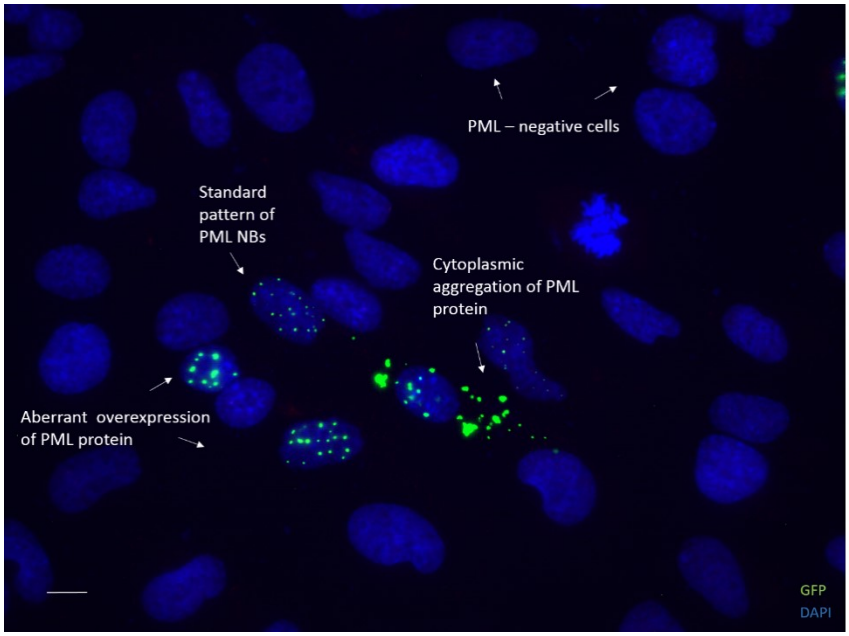

Figure 23: The PML MUT-BioID-GFP revealed heterogeneous pattern after transient transfection. *After transfection of hTERT RPE1 PML KO cells with vector expressing PML MUT-BioID-GFP (green) several populations of cells were presented. The lines with arrow point to cells with standard pattern of PML NBs, cells with aggregates of PML fusion protein and un-transfected cells. The nuclei were stained with DAPI (blue). Scale bar, 10 µm.*

Therefore, I decided to generate a stable cell line expressing either PML-BioID-GFP or PML MUT-BioID-GFP. As it was mentioned previously (Chapter 5.1), comparison of biotinylated proteins between these two samples might allow us to identify proteins in proximity of PML associating with nucleolus. Fusion of PML to GFP enabled us immediately sort for cells with level and pattern of PML comparable with endogenous expression of PML. Note, this procedure was successfully used for generation of hTERT RPE1 cells stably expressing EGFP-PML IV and of hTERT RPE1 PML KO cells stably expressing GFP-PML I. In preparation I tested expression of both fusion proteins from lenti-PML-BioID-GFP and lenti-PML MUT-BioID-GFP in RPE1 PML KO cells after transient transfection. Such cells were analysed by wide field fluorescent microscopy that confirmed undisturbed forming of PML NBs (Figure 24). Consequently, I proceeded to transduction of hTERT RPE1 PML KO cells with these vectors.

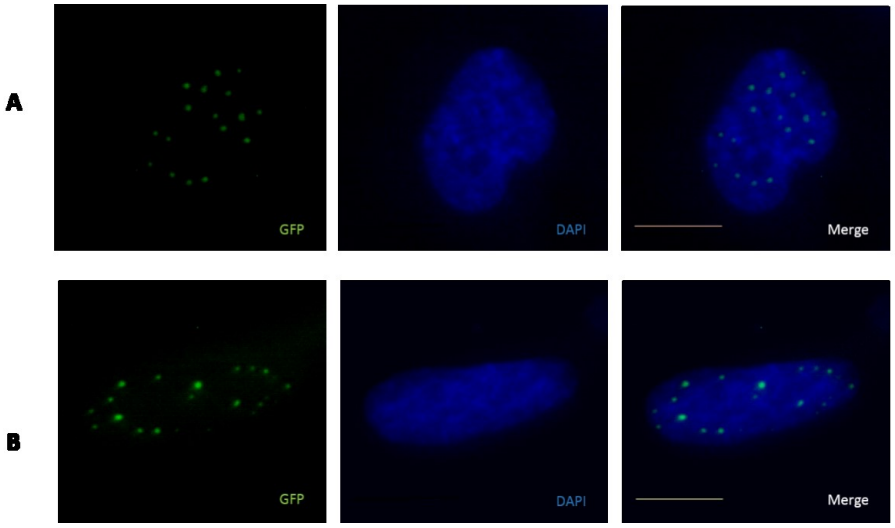

Figure 24: PML-BioID-GFP and PML MUT-BioID-GFP expressed from lentiviral vectors were able to form PML NBs. *hTERT RPE-1 PML KO cells were transiently transfected with lenti-PML-BioID-GFP (A) or lenti-PML MUT-BioID2-GFP (B). The nuclei were stained with DAPI (blue). Scale bar, 10 µm.*

5.3.1. Transduction of hTERT RPE1 PML KO cells with lentiviral vectors coding fusion proteins PML-BioID-GFP or PML MUT-BioID-GFP

Transduction of RPE1 PML KO cells was performed twice, because results of the first one were not satisfactory and there were some technical difficulties during passages of cells for selection. We detected extensive diffusion of GFP signal and overall low number of cells with characteristic pattern of PML NBs (data not shown). Considering this observation, we decided to do transduction with lenti-PML-BioID-GFP and lenti-PML MUT-BioID-GFP again and all following experiments were conducted on cells successfully transduced in 2nd transduction.

According to microscopic documentation of transducted cells three days after transduction, majority of cells were GFP-positive. The intensity of GFP signal was variable, but population of cells with canonical pattern of PML NBs was present (Figures 25 and 26). In addition, cells with diffused GFP signal were not detected. Cells were passaged 5 times in presence of 1.12 mM G418 that was used for selection of successfully transduced cells. However, during this selection period, we observed alterations in pattern of GFP signal, including complete loss of PML NBs and occurrence of diffused GFP signal. Overall, the

population of cells with canonical PML NBs pattern significantly decreased in both cells populations (PML-BioID-GFP / PML MUT-BioID-GFP (Figures 27 and 28).

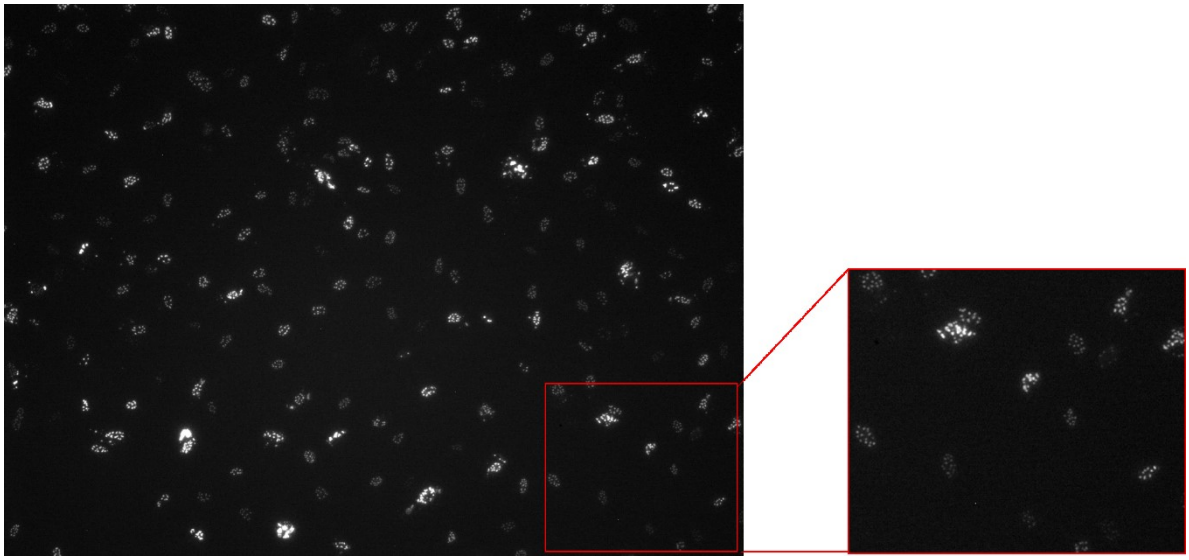

Figure 25: Three days after transduction with "lenti-PML-BioID-GFP" the majority of hTERT RPE1 PML KO cells was GFP positive. *Live cell imaging before 1st passage was done using fluorescent microscope. The left image shows enlarged cells with PML NBs. Scale bar, 200 px.*

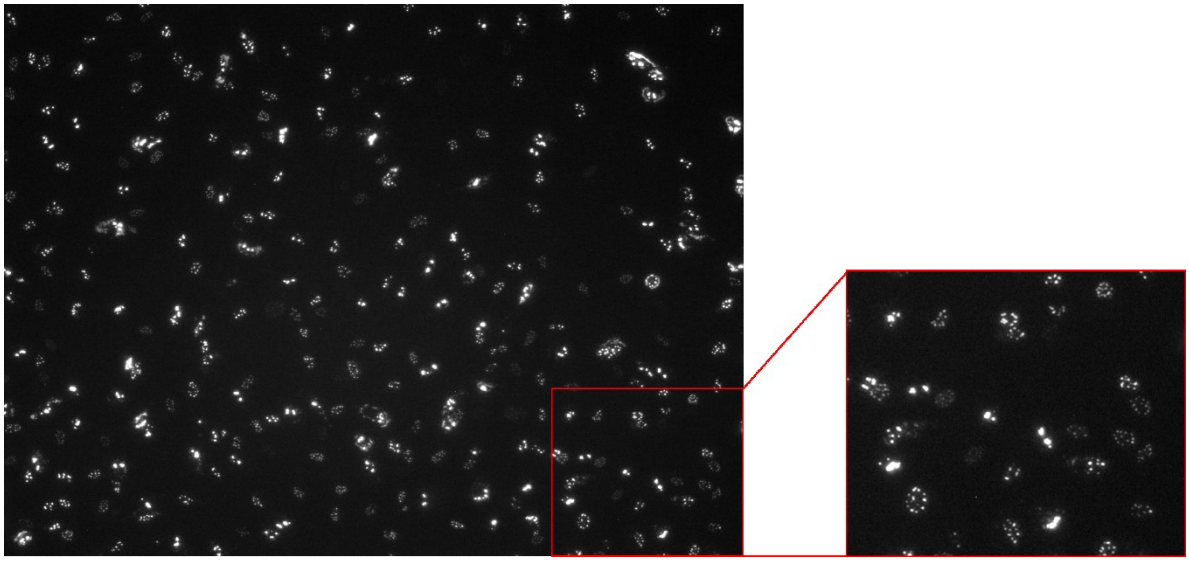

Figure 26: Three days after transduction with "lenti-PML MUT-BioID-GFP" the majority of hTERT RPE1 PML KO cells was GFP-positive. *Live cell imaging before 1st passage was done using fluorescent microscope. The left image shows enlarged cells with PML NBs. Scale bar, 200 px.*

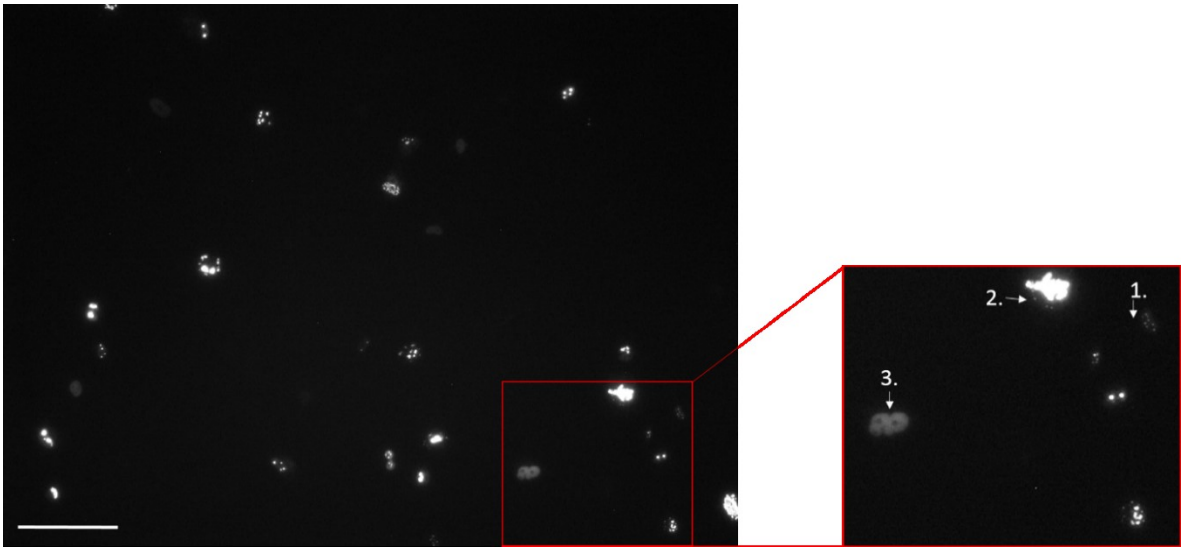

Figure 27: hTERT RPE1 PML KO cell lines expressing PML-BioID-GFP were losing canonical PML NB pattern during passaging. *Live cell imaging before 5th passage was done using fluorescent microscope. The left image shows enlarged cells. The cells with different GFP pattern are shown. 1) Canonical PML NBs, 2) aggregates and 3) diffused GFP. Scale bar, 200 px.*

Figure 28: hTERT RPE1 PML KO cell lines expressing PML MUT-BioID-GFP were losing canonical PML NB pattern during passaging. *Live cell imaging before 5thpassage was done using inverted fluorescent microscope. The left image shows enlarged cells. The cells with different GFP pattern are shown. 1) Canonical PML NBs, 2) aggregates and 3) diffused GFP. Scale bar, 200 px.*

5.3.2.Selection for stable cell line with canonical PML NBs pattern

After 5th passage after transduction, the selected cells were sorted not only into populations according intensity of GFP signal, but into single cells as well. Unfortunately, I was not able to use the cell sorted into populations according the intensity of GFP signal for further experiments, as all obtained populations contained cells with diffuse GFP signal and the population of cells with canonical PML NB pattern was very small. Thus, I concentrated on analysis of colonies obtained from single-cell sorting. I obtained three 96-well plates where single cells expressing PML-BioID-GFP were seeded and two 96 well plates with seeded PML MUT-BioID-GFP. Using fluorescent microscopy, I inspected the pattern of PML NBs and the ability of cells to form the colonies.

Although I focused on colonies that showed homogenous characteristic PML NBs pattern, the majority of promising clones were gradually losing this pattern. After approximately two weeks, I chose four clones expressing PML-BioID-GFP and two clones expressing PML MUT-BioID-GFP for further extension and analysis, despite the pattern of PML NBs not being optimal (Figure 29 and Table 31).

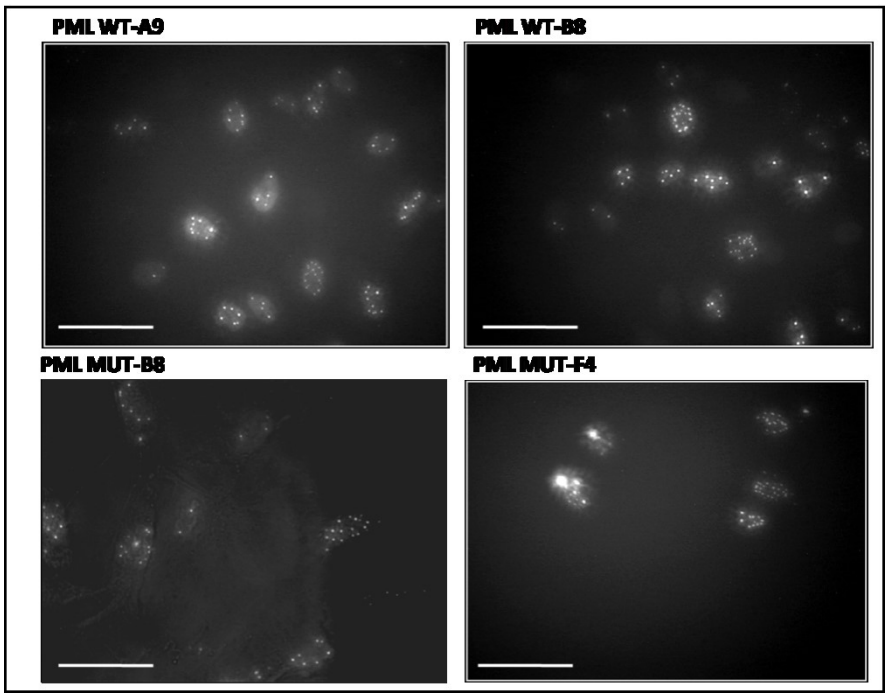

Figure 29: The GFP signal detected in cell lines derived from single cell. *Live cell imaging of stable cell lines captured in 5th passage was performed using inverted fluorescent microscope. Two cell lines expressing PML-BioID-GFP (WT-A9 and WT-B8) and two cell lines expressing PML MUT-BioID-GFP (MUT-B8 and MUT-F4) are shown. Scale bar, 200 px.*

Table 31: Selected cell lines derived from single cell and their names used in following text.

PML-BioID-GFP, clone B8	WT-B8
PML-BioID-GFP, clone F3	WT-F3
PML-BioID-GFP, clone F9	WT-F8
PML MUT-BioID-GFP, clone B8	MUT-B8
PML MUT-BioID-GFP, clone F4	MUT-F4

I tested pattern of these selected cell lines derived from single cell in 10th passage after just before first run of experiments in which the quality of PML NBs was analysed using wide field microscopy. I counted the number of cells with aberrant expression and I found that only approximately 50% of cells contained PML NBs (Figure 30 and Graph 2).

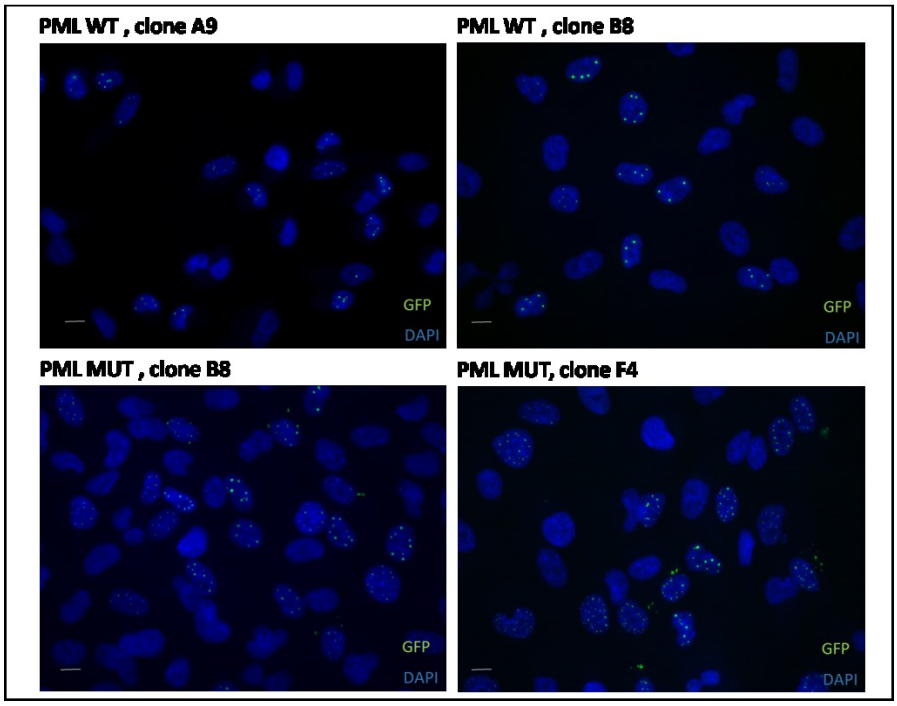

Figure 30: At 10th, the selected cell lines contained PMLNBs only in subpopulation of cells. *Cell lines stably expressing PML-BioID-GFP (WT-A9 and WT-B8) or PML MUT-BioID-GFP (MUT-B8 and MUT-F4) were analyzed by wide field microscopy. The nuclei were stained with DAPI (blue). Scale bar, 10 µm.*

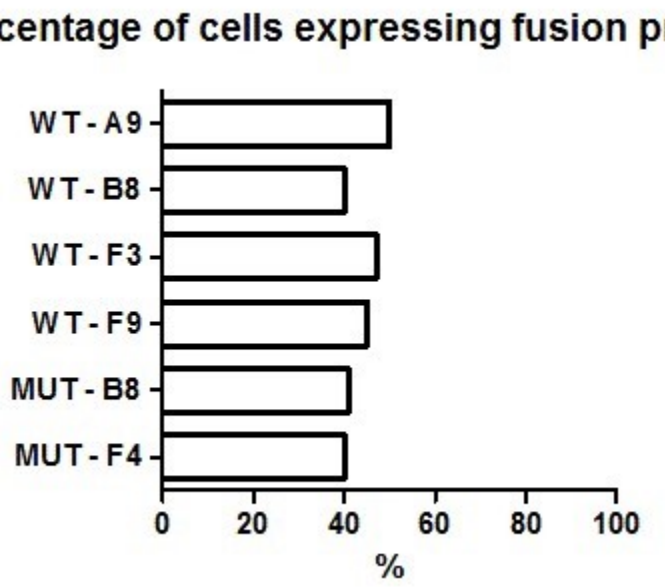

. **Graph 2: Only a subpopulation of cells in chosen transduced cell line revealed standard pattern of PML NBs.** *Untreated cells from each chosen transduced cell line were analyzed by wide field microscopy. The number of cells with standard PML NBs in each population was counted as well as overall number of cells captured during microscopic analyses. Percentage of cells with standard PML NBs in each chosen transduced cell line is plotted in the graph above. Over 60 cells from each chosen transduced cell line were counted*

Despite the fact, that expression pattern of both fusion proteins were not homogeneous, in analysed cell lines I used these selected cell lines stably expressing the transgenes for further analysis. The aim of these experiments was to characterize the clones before deciding how to proceed with the experiment.

5.4. Analysis of selected cell lines derived from single cell

To further characterize the selected cell lines I verified the size of expressed PML fusion proteins. Using wide field microscopy I characterized the PML NBs that were assembled in selected cell lines. Furthermore, I focused on cellular response to doxorubicin treatment and efficiency of biotinylation by BioID2.

5.4.1. Verification of the size of the fusion proteins stably expressed in selected cell lines

To verify the size of expressed fusion proteins, the transduced cells were harvested and the size of expressed fusion proteins was analysed by Western blotting. For detection of fusion proteins the antibody against PML and GFP was used. The size of PML-BioID-GFP and PML MUT-BioID-GFP is 125 and 117 kDa, respectively, but the fact that both PML-fusion proteins contain three lysines that can be sumoylated must be considered.

As is shown in Figure 31, the "PML pattern" uncovered by both used antibodies indicates that cell lines expressing the same fusion protein also possess the same detected pattern. PML antibody unfortunately recognized some unspecific proteins, as is visible in form of positive signal in line in which the proteins from hTERT RPE1 PML KO, but also from hTERT RPE1 PML WT cells, are analysed. Importantly, hTERT RPE1 cells used for this experiment were not treated so the level of PML is low and can serve as negative control. Nevertheless, using the GFP antibody enabled recognition of specific pattern of fusion proteins. The results from Western blotting also indicate that both PML fusions are modified, and as the PML can and often is sumoylated, the addition of SUMO can be assumed. After further examination it could be stated that clone WT-F9 have lower amount of PML fusion proteins than the rest of studied transduced cell lines. In contrast to this, cell lines Mut-B8 and Mut-F4 have higher amount of fusion protein than clones expressing wild type PML-BioID-GFP.

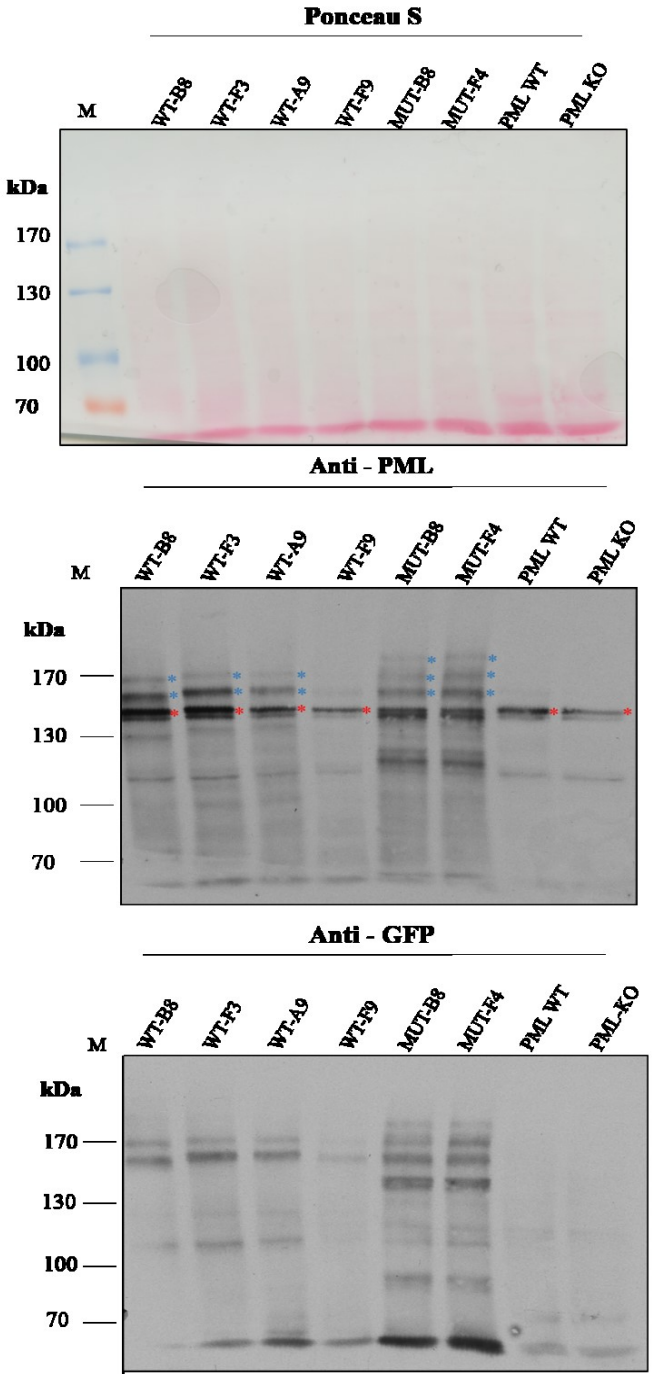

Figure 31: Verification of the size of the fusion proteins stably expressed in selected cell lines. *Proteins isolated from all selected cell lines were analyzed by SDS-PAGE and Western blotting. The amount of proteins was visualized by Ponceau S staining (A), the immuno-detection of fusion proteins using anti-PML antibody (B) and anti-GFP antibody (C) is shown. Modified form of PML fusion proteins marked by blue, non-specific bends that are recognized also in negative controls are marked with red. PML WT – proteins isolated from RPE1 PML WT cells and PML KO – proteins isolated from RPE PML KO cells.*

5.4.2. Microscopic analysis of selected cell lines expressing either PML-BioID-GFP or PML MUT-BioID-GFP in untreated cells, after doxorubicin treatment and after addition of biotin.

To characterize the localization of fusion proteins in all obtained clones, I used wide field microscopy and analysed GFP fluorescence. Based on the fluorescence images it could be stated that cells expressing either PML-BioID-GFP or PML MUT-BioID-GFP form PML nuclear bodies (Figures 32 – 34).

Subsequently chosen clones were subjected to biotin treatment aimed to characterize efficiency of protein biotinylation during proliferation and after addition of doxorubicin. As is shown in Figures 32 – 34, there was practically no biotinylation of PML NBs detected in cells cultivated without addition of biotin while significant increase of biotinylation of PML NBs occurred in cells cultivated with biotin added for 6 hours.

I examined cellular response to doxorubicin treatment as well. Even though I was able to detect nucleolar associations of transiently expressed PML-BioID-GFP, these associations were not observed in cell lines stably expressing the same fusion protein at all.

Lastly I focused on cellular response to combination of both treatments. According to the results, combined treatment by doxorubicin followed by addition of biotin did not show any pronounced changes.

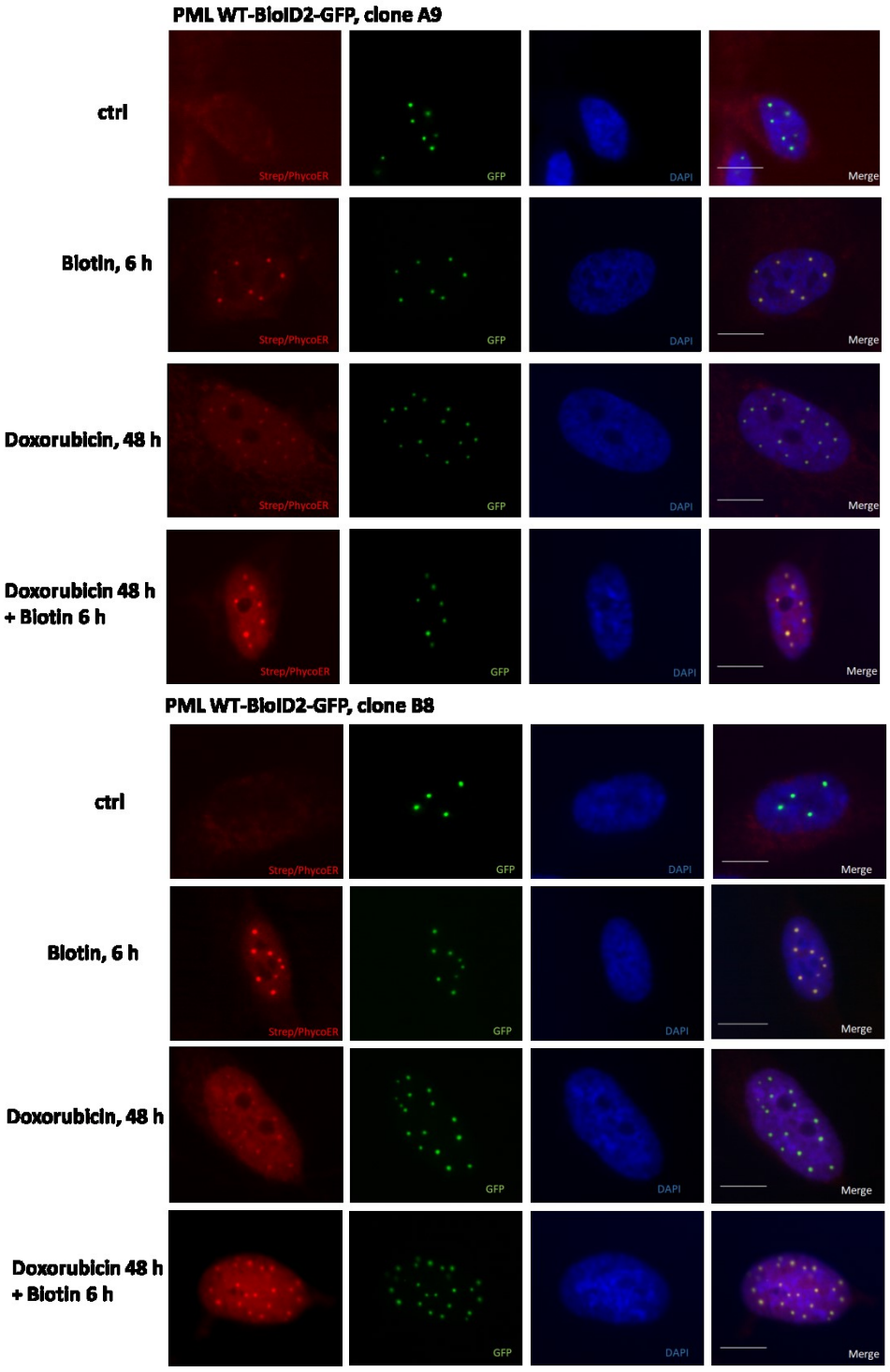

Figure 32: Identification of expression pattern of PML-BioID-GFP and level of biotinylation in cell lines derived from single cell subjected to different treatments. *Stable cell lines WT-A9 and WT-B8 expressing PML-BioID-GFP (green) were cultivated without addition of biotin, or 6 hours in the presence of 50 µM biotin, or were treated with 0.75 µM doxorubicin for 48 hours, or the combined treatment with 0.75 µM doxorubicin (48 hours) and 50 µM biotin (6 hours) was performed. These cells were stained with streptavidin-phycoerythrin (red) to visualized biotinylated proteins and observed using wide field fluorescent microscopy. The nuclei were stained with DAPI (blue). Scale bar, 10 µm.*

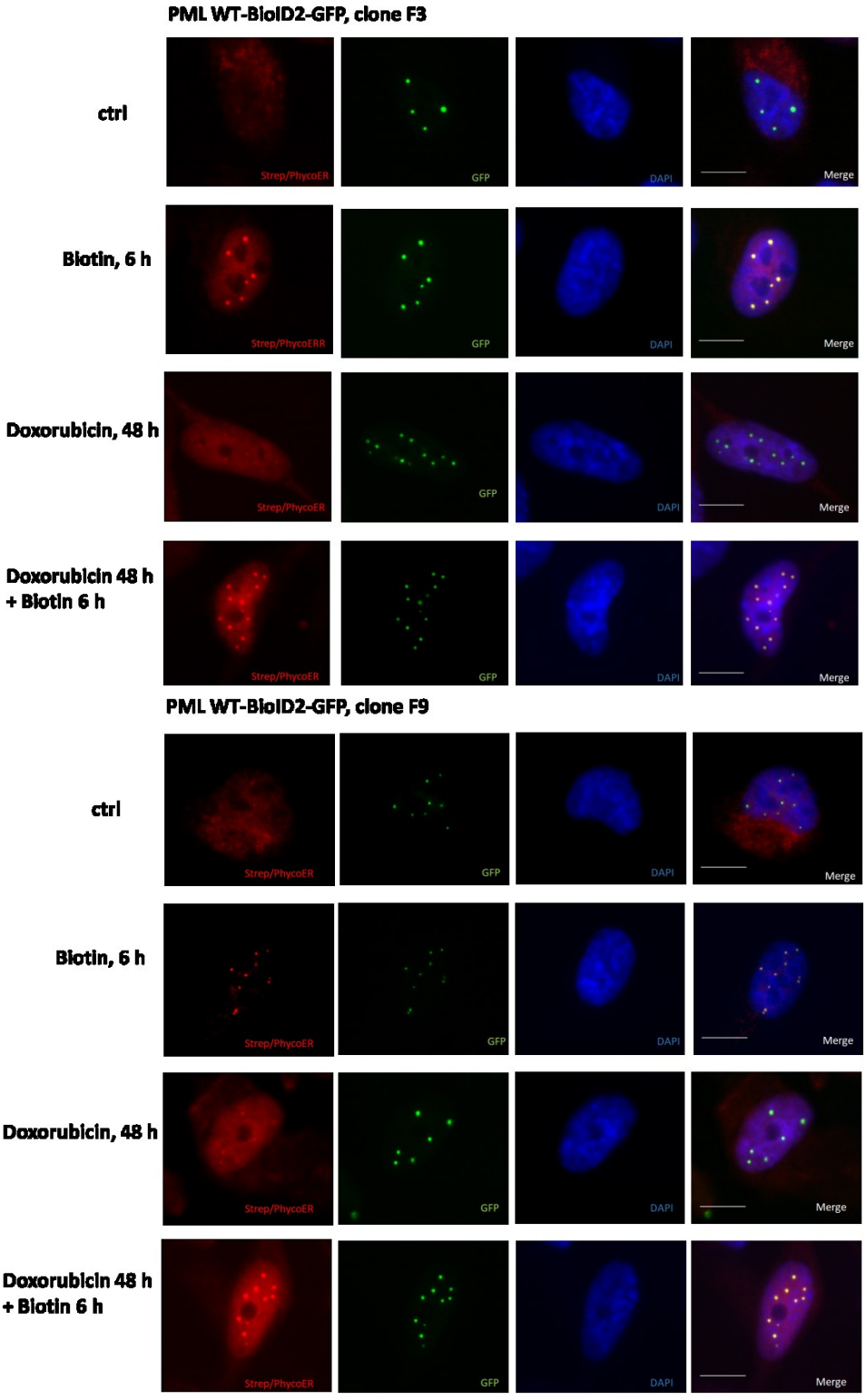

Figure 33: Identification of expression pattern of PML-BioID-GFP and level of biotinylation in cell lines derived from single cell subjected to different treatments. *Stable cell lines WT-F3 and WT-F9 expressing PML-BioID-GFP (green) were cultivated without addition biotin, or 6 hours in the presence of 50 µM biotin, or were treated with 0.75 µM doxorubicin for 48 hours, or the combined treatment with 0.75 µM doxorubicin (48 hours) and 50 µM biotin (6 hours) was performed. These cells were stained with streptavidin-phycoerythrin (red) to visualized biotinylated proteins and observed using wide field fluorescent microscopy. The nuclei were stained with DAPI (blue). Scale bar, 10 µm.*

.

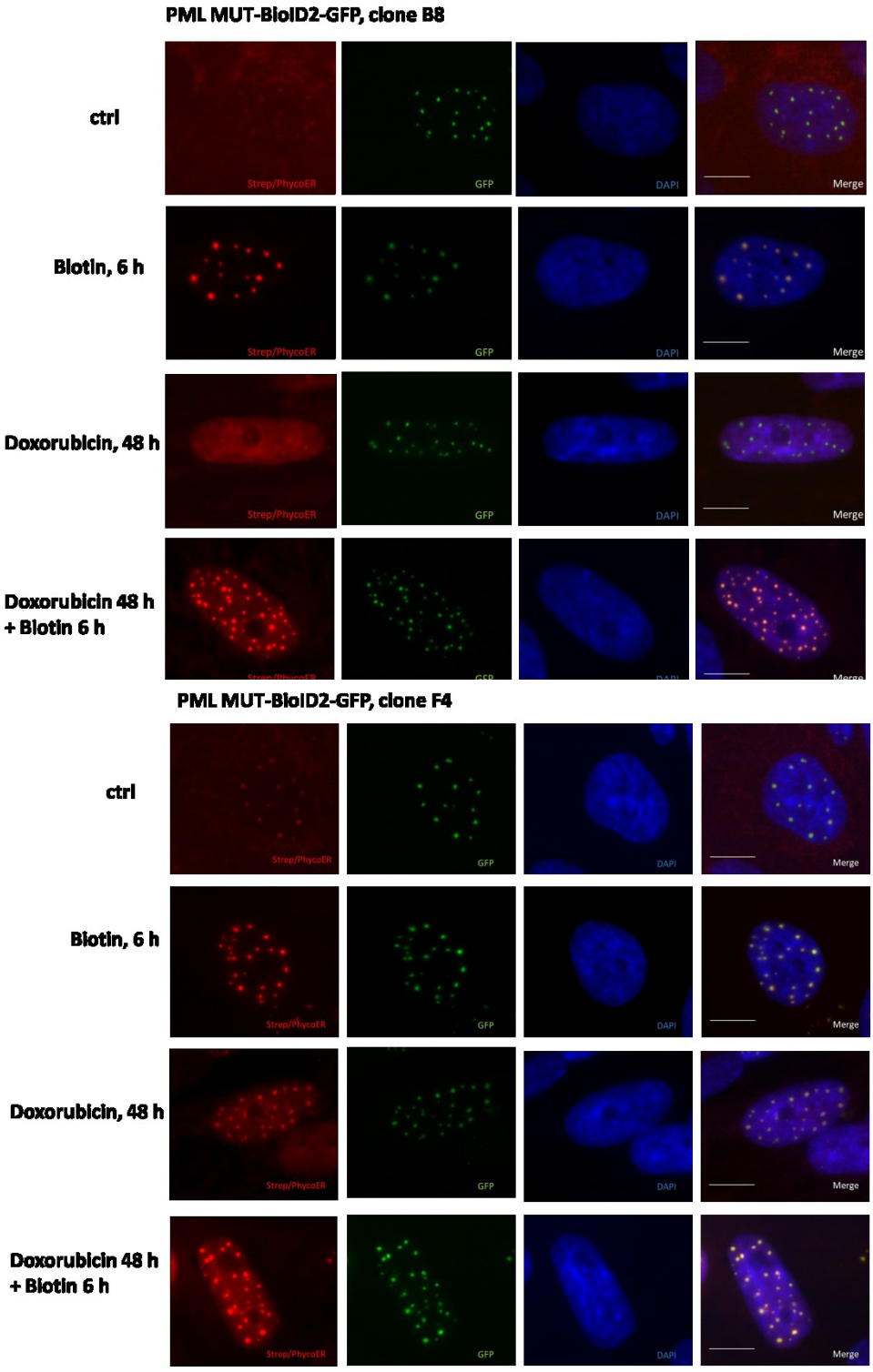

Figure 34: Identification of expression pattern of PML MUT-BioID-GFP and level of biotinylation in cell lines derived from single cell subjected to different treatments. *Stable cell lines MUT-B8 and MUT-F4 expressing PML MUT-BioID-GFP (green) were cultivated without addition biotin, or 6 hours in the presence of 50 µM biotin, or were treated with 0.75 µM doxorubicin for 48 hours, or the combined treatment with 0.75 µM doxorubicin (48 hours) and 50 µM biotin (6 hours) was performed. These cells were stained with streptavidin-phycoerythrin (red) to visualized biotinylated proteins and observed using wide field fluorescent microscopy. The nuclei were stained with DAPI (blue). Scale bar, 10 µm.*

5.4.3.Quantification of PML NBs

To find whether the cell lines that express constructed transgenes generate comparable number of PML NBs during proliferation and after addition of biotin and doxorubicin, I decided to quantify the number of PML NBs under these mentioned conditions. As is shown in Table 32 and Graph 3 cells expressing wild type PML contained fewer PML NBs than mutant form of PML. In addition, the number of PML NBs formed after doxorubicin treatment increased in all cell lines stably expressing wild type form of PML transgene. The change in number of PML NBs in cell lines expressing truncated form of PML was not so prominent. We also quantified the number of PML NBs after addition of biotin but changes that we observed were only mild.

Table 32: The number of PML NBs is expressed as mean value counted at least in 12 cells. The number of PML NBs presented in all selected cell lines derived from single cell under different conditions.

Stable cell lines	**Number of PML NBs [mean value]**		
	No treatment	**Biotin (6 hours)**	**Doxorubicin (48 hours)**
WT-A9	4.7	5.4	7.7
WT-B8	4.6	5.7	9.8
WT-F3	3.9	3.8	7.9
WT-F9	3.4	4.5	7.6
MUT-B8	12.1	14.4	20.6
MUT-F4	17.6	17.1	13.3

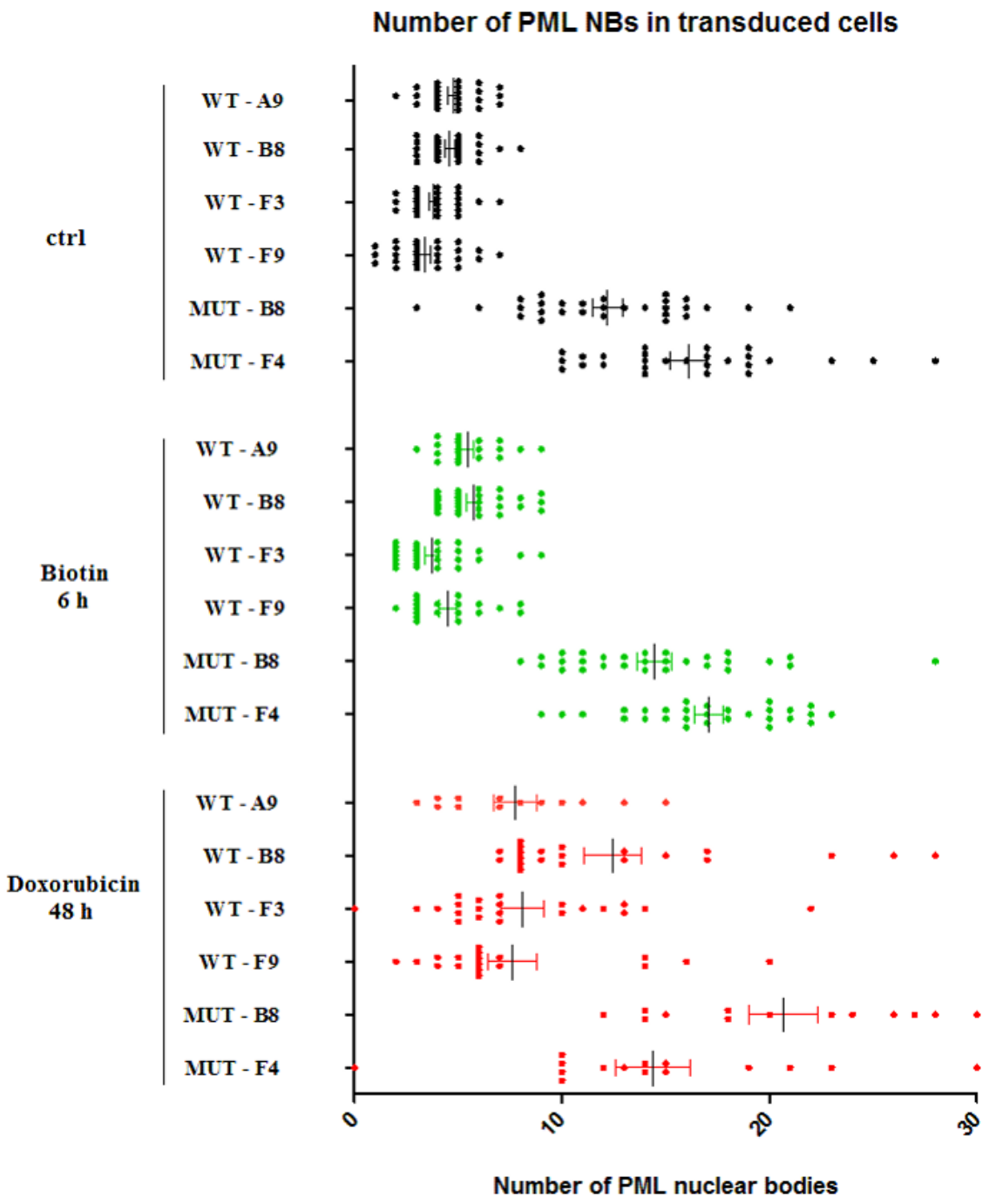

Graph 3: The number of PML NBs in individual cells after different treatments were plotted. *The cell lines derived from single cell were analyzed by wide field microscopy. The number of PML NBs was counted in each individual cell in untreated populations (black dots), after incubation with biotin (6 hours) (green dots) and after treatment with 0.75 µM doxorubicin for 48 hours (red dots). The PML NBs at least in 12 cells were counted. The cells with aggregates, with diffuse signal and no GFP signal were not considered.*

I also analysed the number of PML NBs in hTERT RPE1 PML KO cells after transient transfection with PML-BioID-GFP and PML MUT-BioID-GFP. As is shown in Table 33 and Graph 4 and the number of PML NBs presented in cells transiently expressing PML-BioID-GFP was considerably higher (mean value for PML-BioID-GFP = 18.5) when compared with number of PML NBs detected in selected cell lines expressing same protein (mean values for WT-A9 = 4.7; for WT-B8 = 4.6; for WT-F3 = 3.9, for WT-F9 = 3.4). On the other hand, the difference between number of PML NBs formed by PML MUT-BioID-GFP transiently or stably expressed in hTERT RPE1 PML KO cells was not such prominent as obtained mean values of numbers of PML NBs were comparable (PML MUT-BioID-GFP transiently expressed = 15.5, MUT-B8 = 12.1 and MUT-F4 = 17.6 PML NBs). I also counted number of PML NBs after addition of biotin or doxorubicin. This analysis revealed that neither biotin nor doxorubicin affected the number of PML NBs formed in hTERT RPE1 PML KO cells after transient transfection with wild type or mutated form of PML-BioID-GFP.

These quantifications led me to conclusion that dynamics of PML NBs formation is different between wild type and mutated form of PML when stably expressed in hTERT RPE1 PML KO cells. Notably, this analysis also revealed that reduction of number of PML NBs formed by PML-BioID-GFP occur only in stable cell line as after transient transfection this number was markedly higher and comparable with PML MUT-BioID-GFP.

Table 33: The average number of PML NBs in hTERT RPE1 PML KO cells after transiently transfected with either PML-BioID-GFP or PML MUT-BioID-GFP. *The number of PML NBs was counted in each individual cell in untreated population (ctrl), after incubation with biotin (24 hours) and after treatment with 0.75 μM doxorubicin (48 hours). The PML NBs at least in 20 cells were counted. The cells with aggregates, with diffuse signal and no GFP signal were not considered.*

	PML-BioID-GFP	PML MUT-BioID-GFP
Control	18.5	15.6
Biotin, 24 h	17.2	16.4
Doxorubicin, 48 h	17.9	23.8

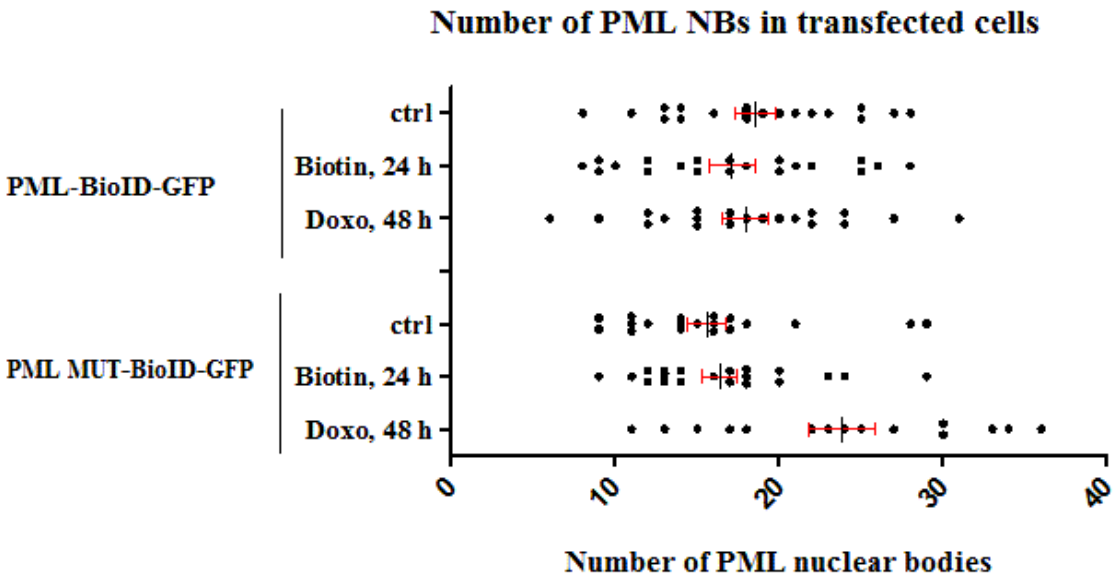

Graph 4: The number of PML NBs in hTERT RPE1 PML KO cells when transiently transfcted with either pPML-BioID-GFP or pPML MUT. *The cell transfected with either one of the DNA constructs were analysed by wide field microscopy. The number of PML NBs was counted in each individual cell in untreated population (ctrl), after incubation with biotin (24 hours) and after treatment with 0.75 µM doxorubicin (48 hours). The PML NBs at least in 20 cells were counted. The cells with aggregates, with diffuse signal and no GFP signal were not considered.*

5.4.4.Analysis of presence of resident proteins such SUMO1, SUMO2/3 and DAXX in PML NBs formed by both fusion proteins

I also examined whether typical resident proteins are still present in PML NBs formed in selected cell lines. The same set of antibodies (anti-PML, anti-DAXX, anti-SUMO1, anti-SUMO2/3) was used as in case of transiently transfected cells.

All PML NBs were recognized by PML, SUMO1 and SUMO2/3 antibodies (Figure 35 and Figure 36). Note, PML NBs formed after transient transfection of RPE1 PML KO cells with plasmids coding both fusion proteins (see Figure 20 and 21) and PML NBs detected in hTERT RPE1 cells that are formed by endogenous PML (Figure 37) were also positive for SUMO1 and SUMO2/3 signal, indicating that there is no distinct change in sumoylation of PML NB assembled in selected cell lines. Interestingly, the staining with DAXX antibody revealed that all four cell lines stably expressing PML-BioID-GFP did not accumulated DAXX signal in the PML NBs (Figure 35) contrary to PML NBs that were formed after ectopic expression of the same transgene (see Figure 21) and contrary to "endogenous" PML NBs that were formed in confluent hTERT RPE1 cells (Figure 37). On the other hand, the

PML NBs assembled in cell lines expressing truncated form of PML (PML MUT-BioID-GFP) Vwere DAXX-positive (Figure 35).

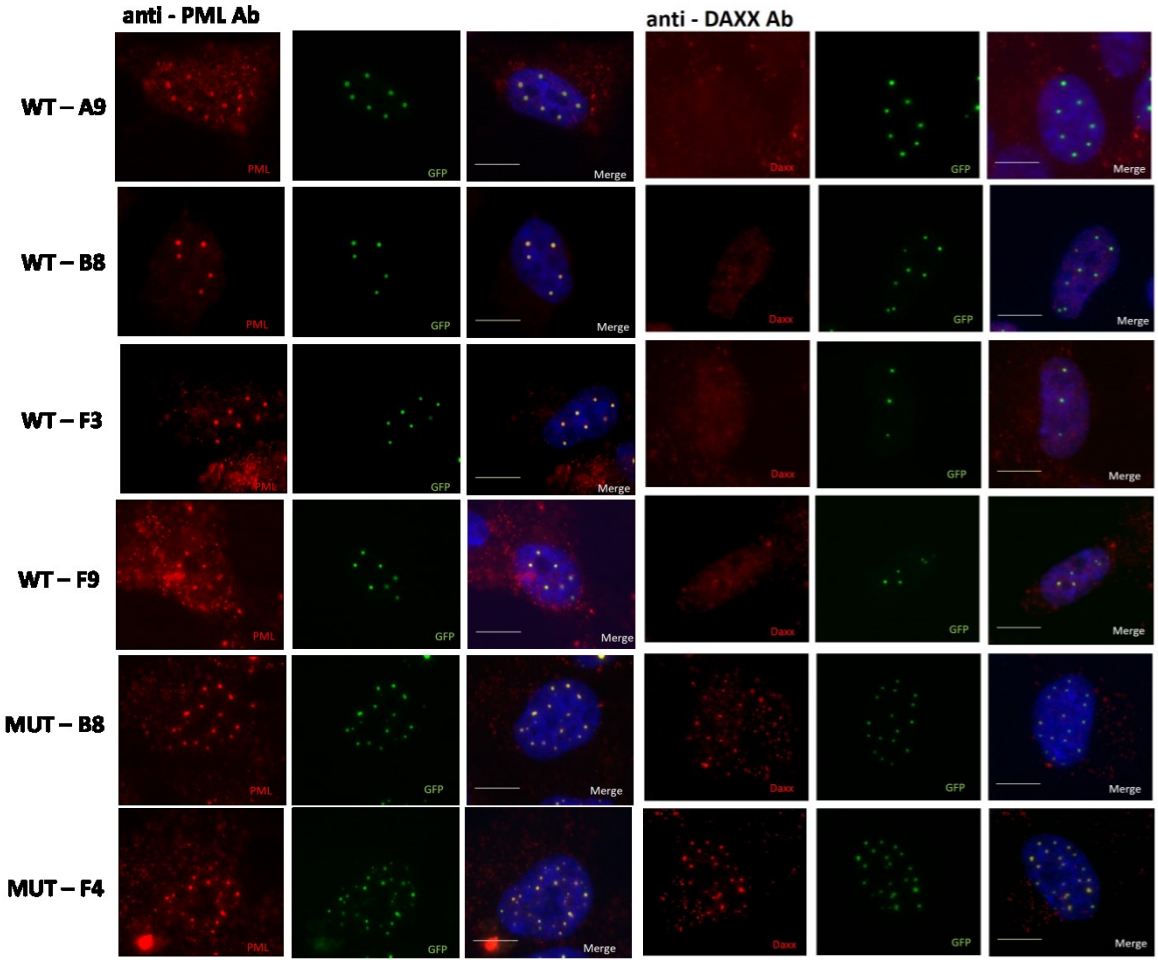

Figure 35: Detection of PML and DAXX in stable cell lines derived from single cells. *The cell lines expressing either PML-BioID-GFP or PML MUT-BioID-GFP (both green) were stained with anti-PML and anti-DAXX antibodies (both red) and analyzed by wide field microscopy. The nuclei were stained with DAPI (blue). Scale bar, 10 µm.*

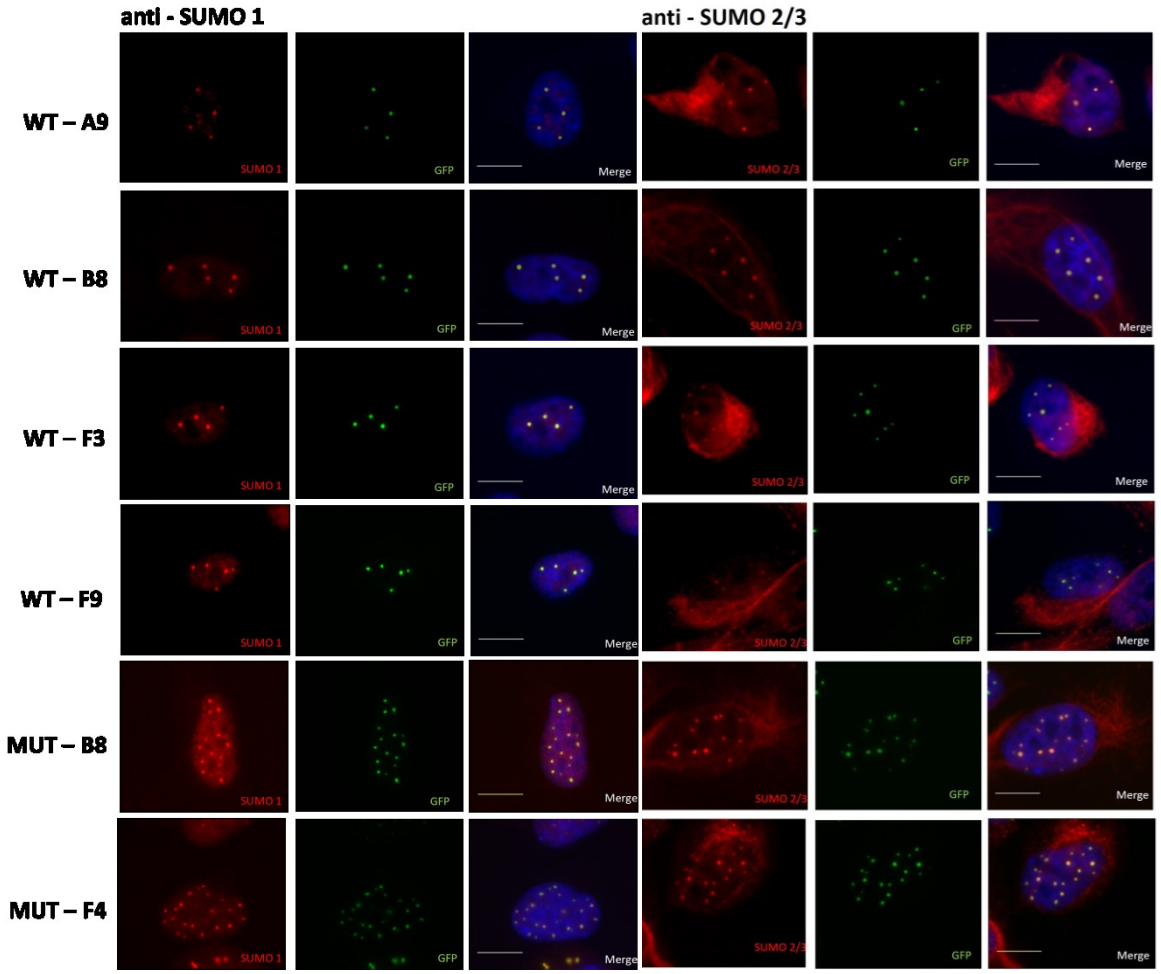

Figure 36: Detection of SUMO1 and SUMO2/3 in stable cell lines derived from single cells. *The cell lines expressing either PML-BioID-GFP or PML MUT-BioID-GFP (both green) were stained with anti-SUMO1 and anti-SUMO2/3 antibodies (both red) and analyzed by wide field microscopy. The nuclei were stained with DAPI (blue). Scale bar, 10 µm.*

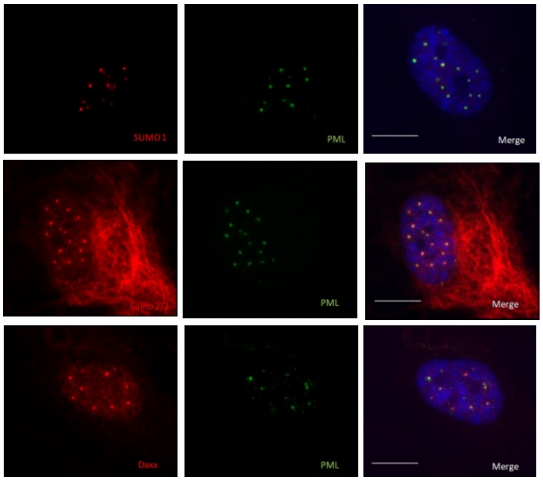

Figure 37: Detection of protein PML, SUMO1, SUMO2/3 and DAXX in hTERT RPE1 *The cells were stained with anti-PML (green) and anti-DAXX, anti-SUMO1 and anti-SUMO2/3 antibodies (all red) and analysed by wide field microscopy. The nuclei were stained by DAPI (blue). Scale bar, 10 µm.*

In conclusion, all tested stable cell lines expressing same transgene revealed similar size of expressed protein and equivalent quality of PML NBs. On the other hand, presented analysis revealed that PML NBs formed by wild type PML-BioID-GFP considerably differ in composition and number from PML NBs formed in cells expressing its truncated form.

5.5. Analysis of biotinylated proteins

Microscopic analysis of obtained cell lines revealed that RPE1 PML KO cells stably expressing PML and its truncated form PML MUT both fused to BioID2-GFP even after single cell cloning still formed heterogeneous population in which only subpopulation of cell contained PML NBs. In addition, PML-BioID-GFP fusion stably expressed in hTERT RPE1 PML KO cells did not associate with nucleolus after doxorubicin treatment. Therefore, the original concept of the experiment based on utilization of these cells for identification of proteins interacting with PML during formation of PNAs was not possible to carry out. On the other hand, after addition of biotin the biotinylated protein accumulated mainly in PML NBs, therefore, I can use these cells as a model for isolation of biotinylated proteins from these membrane-less structures.

5.5.1. Detection of biotinylated proteins using Western blotting

To detect the extent of biotinylation and the size of biotinylated proteins I cultured cell lines with 50 μM biotin for 4 or 6 hours. The total proteins were separated using SDS PAGE and after Western blotting the biotinylated proteins were detected by streptavidin IRDye using Odyssey detection system. The obtained pattern of biotinylated proteins revealed that the biotinylated proteins were presented even without incubation with biotin. Nevertheless, four hours-long cultivation with biotin considerably increased the amount of biotinylated proteins. The prolongation of incubation with biotin for another 2 hours did not have strong effect on amount of biotinylated proteins (Figure 38). This analysis also revealed that the cell lines stably expressing truncated form of PML contained higher amount of biotinylated proteins.

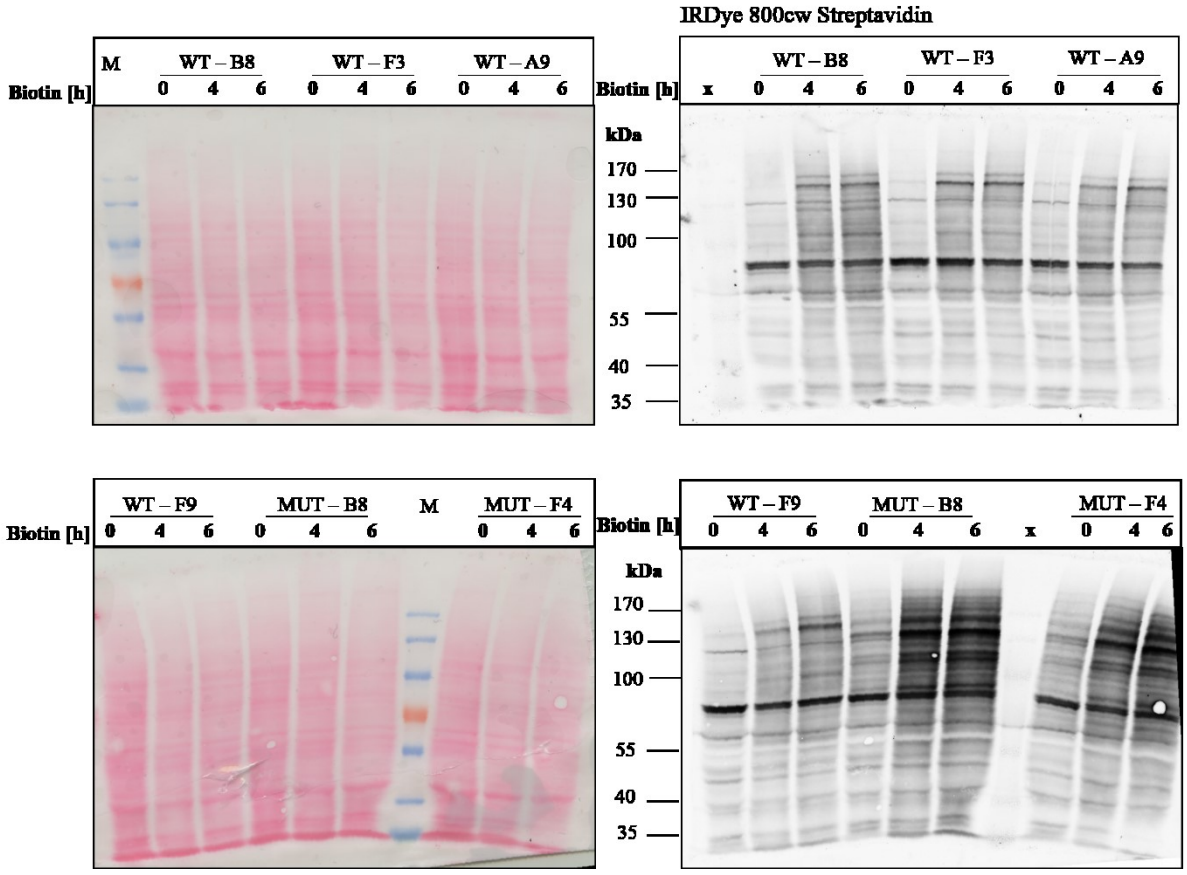

Figure 38: Biotinylation pattern of proteins expressed in selected cell lines: *Stable cell lines were incubated with biotin and protein extracts were analyzed using SDS-PAGE and Western blotting. Biotinylated proteins were detected by IRDye 800cw streptavidin. In the left column the total proteins stained with Ponceau S are shown, in the right column the biotinylated proteins are presented.*

5.6. Isolation of biotinylated protein

5.6.1.Nucleolar fractionation

As the PML is mainly nuclear protein, I performed nuclear isolation followed by extraction of nuclear proteins using buffers with added detergents. Note, the PML is hardly soluble in common buffers used for pull-downs and co-immunoprecipitation. It can also be assumed that some portion of biotinylated proteins may stay insoluble under these conditions. Thus I tested a solubility of biotinylated proteins in buffers that contained NP-40 (1%) and two different concentrations of SDS (0.4 and 1%). According to the literature *(Cheah et al., 2017)* these detergents are compatible with isolation of biotinylated proteins by magnetic beads coated with streptavidin and it is possible to remove them from the sample that is used for mass spectrometry analysis.

In this experiment I tested all selected stable cell lines. First, the cells were cultivated with addition of 50 μM biotin for 4 hours. Subsequently nuclei were isolated and nuclear proteins were extracted into buffer with 1% NP-40 and either 0.4% SDS or 1% SDS. The distribution of biotinylated proteins between cytoplasmic fraction (S1), soluble nuclear fraction (S2) and insoluble fraction (P) was tested using dot blot analysis. The biotinylated proteins were detected with streptavidin IRDye.

As is shown in Figure 40, the biotinylated proteins were mainly present in soluble nuclear fractions S2. Considering the concentration of SDS, the results were not unequivocal. As for following experiments I intended to use only PML-BioID-GFP, I chose the two cell lines expressing this fusion protein and showing the highest level of biotinylation (WT-A9, WT-B8) for further analysis. First I reanalysed already obtained protein fractions by SDS PAGE and Western blotting to better distinguish the possible difference in solubility of biotinylated proteins in buffers with different concentration of SDS. Apart from solubility of biotinylated proteins I also tested behaviour of PML in these buffers. I could confirm that majority of biotinylated proteins was in nuclear soluble fraction (S2-A, S2-B). Considering the results I report no significant difference between efficiency of fractionation dependent on whether used buffer contained 0.4 or 1% SDS, as is presented by fraction S2-A containing nuclear soluble proteins extracted into buffer with 1% NP-40 and 0.4% SDS and fraction S2-B containing nuclear soluble proteins extracted into buffer with 1% NP-40 and 1% SDS (Figure 40).

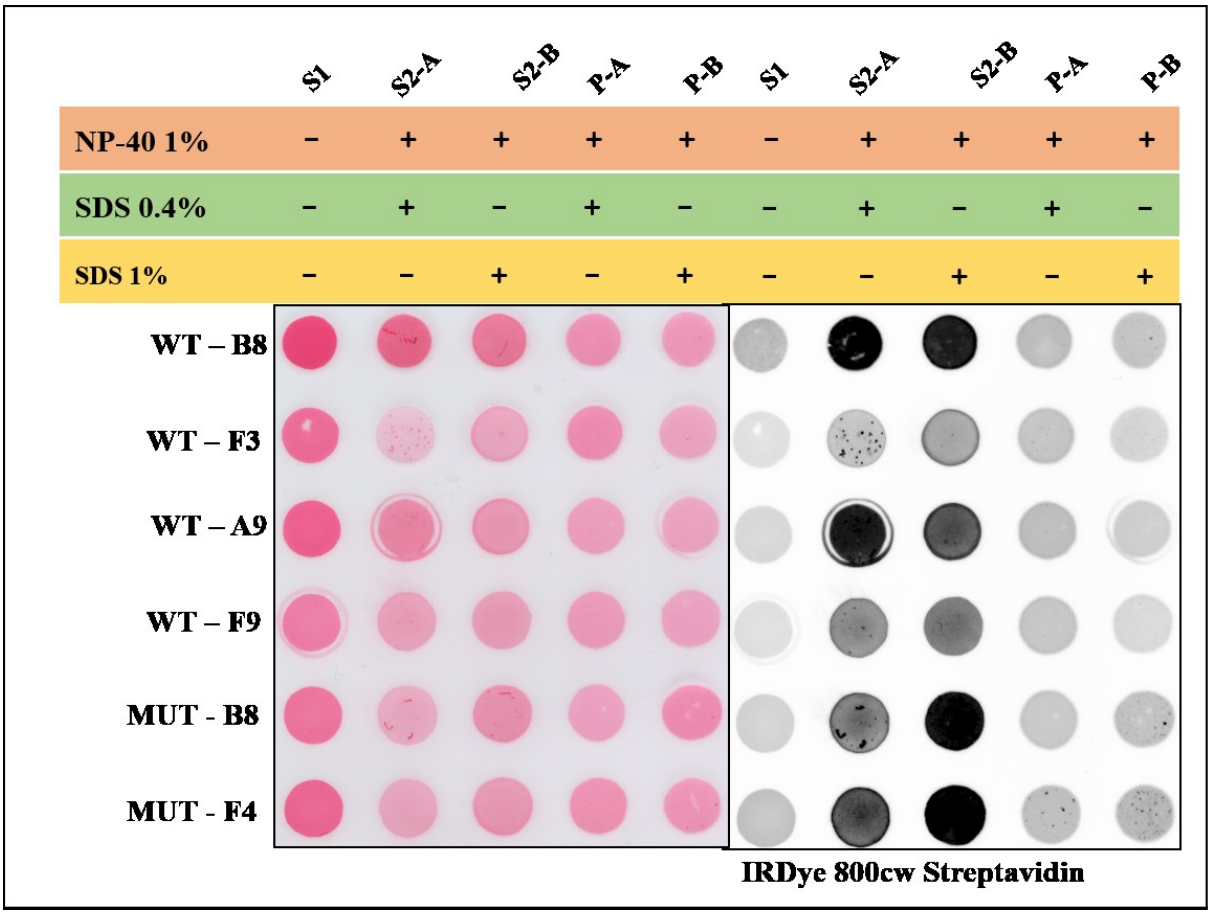

Figure 39: The distribution of biotinylated proteins between cytoplasmic, soluble nuclear and insoluble fraction is shown. *All stable cell lines were incubated with biotin (4 hours) and then the proteins were fractioned. The isolation of nucleolar proteins from all tested cell lines was done using buffer with two concentration of SDS (0.4 and 1 %). The distribution of biotinylated proteins was analyzed using dot blot. The amount of total proteins in individual fractions is visualized by Ponceau S staining. The biotinylated proteins were visualized by IRDye 800cw streptavidin. Cytosolic fraction (S1), nuclear soluble fraction extracted into buffer containing 1% NP-40 and 0.4% SDS (S2-A), nuclear soluble fraction extracted into buffer containing 1% NP-40 and 1% SDS (S2-B), nuclear insoluble fraction extracted into buffer containing 1% NP-40 and 0.4% SDS (P-A) nuclear insoluble fraction extracted into buffer containing 1% NP-40 and 0.4% SDS (P-B) are shown.*

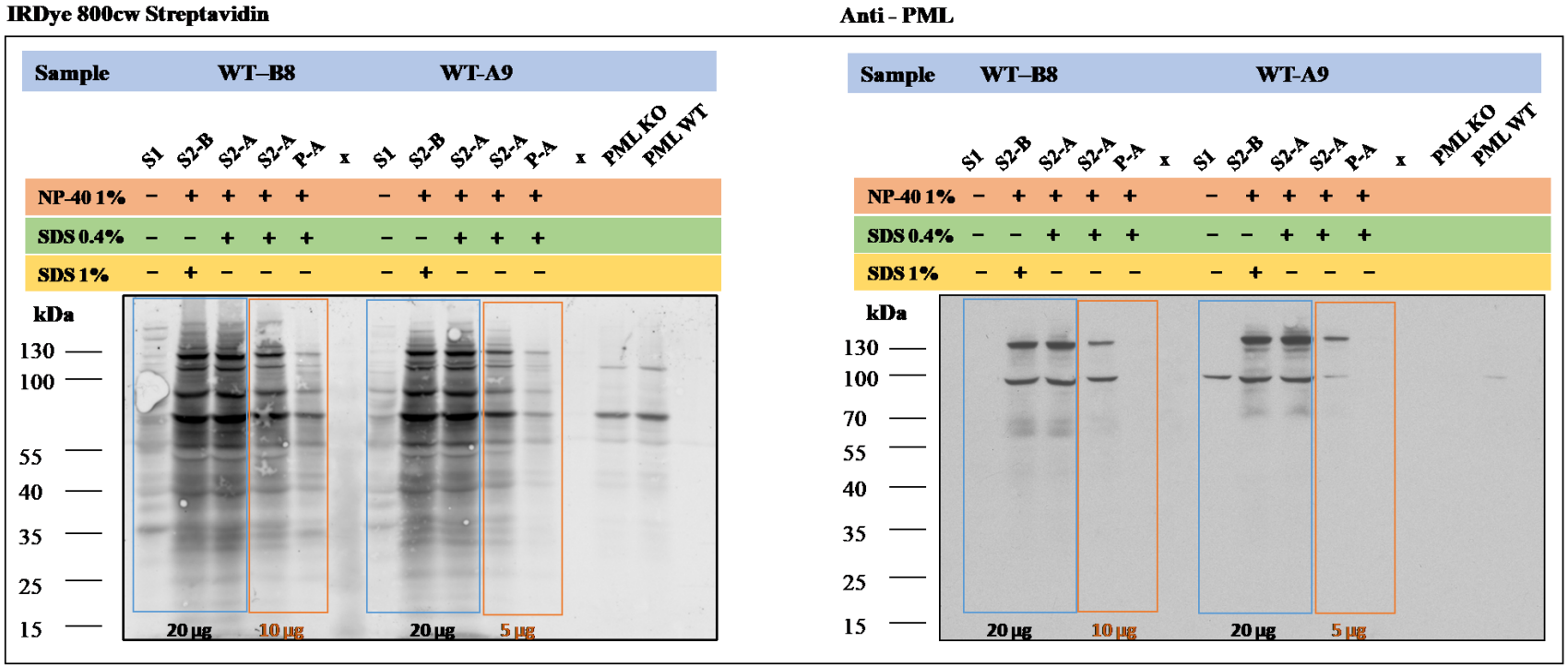

Figure 40: Distribution of biotinylated proteins and PML protein in two stable cell lines expressing PML-BioID-GFP (WT-B8 and WT-A9) between cytosolic (S1), nuclear soluble (S2) and nuclear insoluble fraction is shown. *Two stable cell lines expressing PML-BioID-GFP were incubated with biotin (4 hours) and then the proteins were fractioned. The isolation of nucleolar proteins from all tested cell lines was done using buffer with two concentration of SDS (0.4 and 1 %). The distribution of biotinylated proteins was analyzed using SDS PAGE and Western blotting. The biotinylated proteins were visualized by IRDye 800cw streptavidin and PML with anti-PML antibody. Fraction of cytosolic proteins(S1), nuclear soluble fraction extracted into buffer containing 1% NP-40 and 0.4% SDS (S2-A), nuclear soluble fraction extracted into buffer containing 1% NP-40 and 1% SDS (S2-B), nuclear insoluble fraction extracted into buffer containing 1% NP-40 and 0.4% SDS (P-A) are shown. PML KO line documents amount of biotinylated proteins and PML protein in whole cell protein lysates from hTERT RPE1 PML KO cell, thus representing negative control. PML WT line documents amount of biotinylated proteins and PML protein in non-confluent hTERT RPE1 cells, thus also representing negative control. Same amount of fraction S1, S2-A and S2-B was loaded on 10% SDS-PAGE gel to compare amount of biotinylated proteins and PML protein itself in each fraction. Change of SDS concentration does not have a visible effect of efficiency of isolation. Same amount of soluble (S2-A) and insoluble (P-A) nuclear fraction was loaded on SDS-PAGE gel to evaluate the difference in the amount of biotinylated proteins and PML protein in these two fractions.*

5.6.2.Isolation of biotinylated proteins by Dynabeads™ MyOne™ Streptavidin C1

To test the efficiency of isolation of biotinylated proteins in buffer where 1% NP-40 and 0.4% SDS are present I used cell lines WT-A9 and WT-B8 stably expressing PML-BioID-GFP. I treated these cells with biotin for 4 hours, after that the nuclei were isolated, the nuclear proteins were extracted using buffers with detergents, and soluble nuclear fraction was incubated with Dynabeads™ MyOne™ Streptavidin C1. After that all obtained fractions were analysed using SDS-PAGE and Western blotting and biotinylated proteins were detected using streptavidin IRDye.

As is shown in Figure 41, I detected no obvious loss of biotinylated proteins during any of the three final washes of magnetic beads with the exception of second wash of sample WT-B8 where moderate streptavidin signal informed about moderate loss of biotinylated proteins. Strong streptavidin signal was detected in the final IP sample signifying successful isolation of biotinylated proteins indicating that the buffer with both detergents might be used for isolation.

In conclusion, isolation of biotinylated proteins using Dynabeads™ MyOne™ Streptavidin C1 proved to be effective. According to the SDS-PAGE analysis of all fractions collected during the isolation, I did not detect any significant loss of biotinylated proteins during the three washes and strong streptavidin signal in line analysing the final IP sample signifies that biotinylated proteins were successfully isolated.

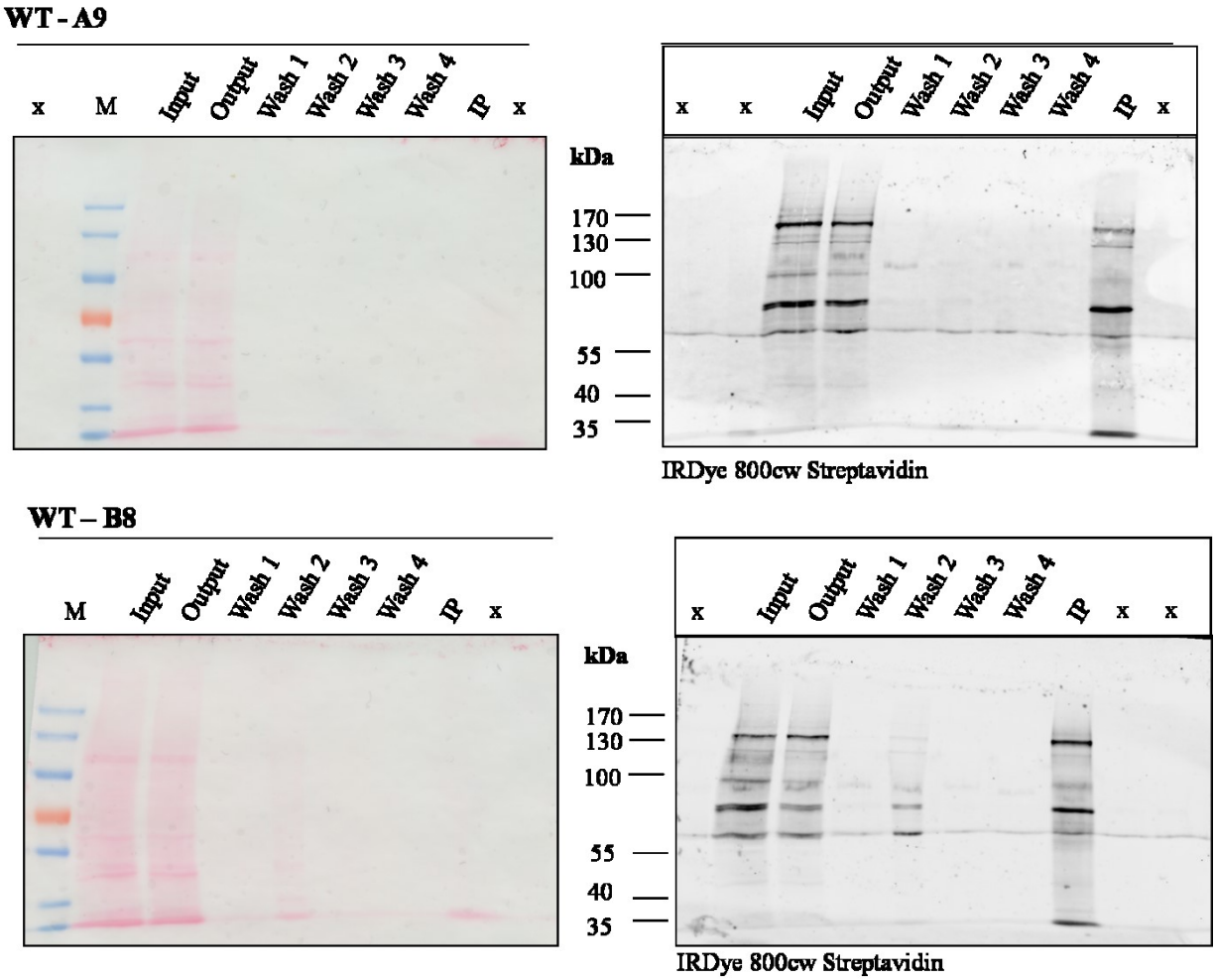

Figure 41: The efficiency of isolation of biotinylated proteins presented in cell lines stably expressing PML-BioID-GFP using magnetic Dynabeads™ MyOne™ Streptavidin C1. *Two stable cell lines expressing PML-BioID-GFP were incubated with biotin (4 hours) and then the proteins were fractioned. The soluble fraction of nuclear protein was incubated with magnetic Dynabeads™ MyOne™ Streptavidin C1. The distribution of biotinylated proteins between individual fractions generated during isolation was analyzed using SDS PAGE and Western blotting. The amount of total proteins in individual fractions was visualized by Ponceau S staining. The biotinylated proteins were detected by IRDye 800cw streptavidin. Input fraction represents original S2-A sample (nuclear soluble fraction), output fraction is the original sample subjected to isolation after incubation with magnetic Dynabeads™ MyOne™ Streptavidin C1. Three washes were performed during the isolation process and no major loss of biotinylated proteins occurred during any of the washes. IP sample, containing biotinylated proteins is a final product of the isolation.*

6. Discussion

In noncancerous cells the PML protein associates with the nucleolus under specific conditions. However, the function of these associations is unclear. One of the approaches that could help to solve this question is the identification of interaction partners of PML specific for its nucleolar association as the description of the protein composition of this structure may help to clarify its function. However, the serious obstacle that should be overcome is the stability of PML complexes preventing the employment of methods commonly used to identify interacting partners such as co-immunoprecipitation.

Therefore, the main goal of my work was to explore relatively novel alternative approach with potential to defeat this issue – proximity biotin labelling *(Kim et al., 2016)*. The specific aims were to prepare vectors expressing wild type and mutant form of PML fused to biotin ligase and to test the suitability of this approach for identification of proteins in the proximity of PML on the boundary of nucleolus.

During my work I found that fusion of PML with biotin ligase indeed enabled biotinylation of PML NBs and, under conditions of transient transfection, was also able to form and biotinylate PNAs. In contrast to transient transfection, my work revealed that hTERT RPE1 PML KO cells stably expressing PML-BioID2-GFP 1) formed heterogeneous population of cells either with PML NBs, with diffuse GFP signal and with no GFP signal at all, 2) generated PML NBs that were sumoylated but contrary to PML NBs appearing in transient transfectants they did not accumulated DAXX and 3) stably expressed PML-BioID-GFP did not associate with nucleolus after doxorubicin addition. Notably, hTERT RPE1 PML KO cells stably expressing truncated form of PML MUT-BioID2-GFP that originally had serve as negative control for MS analysis were also losing the cells with PML NBs during cell culture propagation. Nevertheless, these PML NBs were not only sumoylated but the accumulation of protein DAXX was observed. Finally, regardless all problems with strains stably expressing wild and mutated PML fused to BioID2-GFP, I found that after addition of biotin, the PML NBs in these cells were biotinylated and I was able to isolate these proteins using streptavidin magnetic beads.

Results obtained from characterization of PML-BioID-GFP transiently expressed in hTERT RPE1 PML KO cells were consistent with our expectations. Firstly, this PML fusion was able to form PML NBs and also to associate with nucleolus after doxorubicin treatment. Pattern of PML NBs and frequency of PNAs was comparable with positive

control represented by PML-GFP. Secondly, the fusion protein PML MUT-BioID-GFP, meant to serve as a negative control for MS analysis, also proved to be able to form PML NBs when transiently expressed in hTERT RPE1 PML KO cells. According to expectations, I did not detect any PNAs in cells expressing PML MUT-BioID-GFP after doxorubicin treatment. Another aspect I wanted to evaluate was the maturity of PML NBs that can be characterized by their chemical composition, post-translational modifications. One typical post-translational modification of mature PML NBs is the sumoylation *(Hecker, 2006, Shen 2006)*. As the PML contains SUMO interacting motif (SIM), the SIM-SUMO interaction is involved in homomultimerisation of the PML and formation of PML NBs *(Shen 2006)*. Even more, it is known that PML NBs seem to be hub for proteins that are sumoylated or contain SIM *(Zhong et al., 2000)*. It was described that SIM within DAXX is responsible for localization of this well-known transcription corepressor into the PML NBs (Ding-Yen Lin 2006 Molecular Cell). Importantly, I found that PML NBs formed by both tested fusion proteins indeed contained SUMO1, SUMO2/3 and DAXX. All these analyses confirmed that fusion of PML with BioID2 and EGFP did not affect the formation of PML NBs and PNAs. Moreover, such PML NBs were sumoylated and were able to accumulate the DAXX.

Lastly, I was interested to estimate the biotinylation capability and substrate specifity of fusion proteins. Significantly, biotin ligase proved to be functional in the context of this tripartite fusion protein as I detected an obvious difference in the intensity of biotinylation signal after biotin addition in cells expressing either the DNA constructs compared to control cells with no biotin exposure. As anticipated, the biotinylated proteins accumulated indeed in PML NBs and PNAs as shown by indirect fluorescence microscopy indicating that most of the biotinylated proteins were concentrated in the vicinity of PML and might be the component of PML NBs or PNAs. It should be emphasized that even control cells cultured in the absence of biotin still exhibited weak biotinylation signal accumulated in PML indicating that BioID2 is able to biotinylate even using the endogenous biotin sources. Importantly, in cells expressing PML-GFP (i.e. without biotin ligase) no streptavidin signal in PML NBs was detected confirming the specificity of the signal.

All this analysis confirmed that fusion of the PML with BioID2 and EGFP did not affect the formation of PML NBs and PNAs. Even more, such PML NBs were sumoylated and able to accumulate the regular component of PML NBs, DAXX. As after incubation of biotin mainly the PML NBs and PNAs were biotinylated, this approach proved to be

suitable for identification of proteins in vicinity of PML by proximity-dependent biotin identification. However, it should be stressed that all these favourable observations were present using transient transfectants unsuitable for further biochemical analyses due to population heterogeneity.

During generation of stable RPE1 PML KO cell lines with the goal to reach homogeneous expression of PML IV isoform and its mutant fused to BioID-GFP for subsequent biochemical analyses I encountered the loss of cells with canonical PML NBs pattern. During propagation of stable cell lines, gradual changes involving the increase of aberrant diffused PML-GFP signal in nucleoplasm together with decreased number of cells with regular PML NBs were detected. Considering the heterogeneity of subcellular distribution of PML fusion proteins and primarily the failure to generate stable cell lines with similar intensity of GFP signal by FACSorting, I focused on preparation of cell lines generated from single cells. Nevertheless, even this approach ended in heterogeneous population, where only 50% of cells contained 'normal' PML NBs and the rest revealed diffuse or no GFP signal.

Even though single cell-derived populations contained only 50% of cells with typical PML NBs I decided to characterize them further. Four and two single cell clonal lines expressing wild type and mutant PML fusion proteins, respectively, were subjected to the similar analyses as performed for transient transfectants. Unfortunately, though some analysed features were found as expected (e.g., sumoylation and biotinylation), others showed significant discrepancies. The most relevant one important to reach the goal of the study was the inability of the PML in cells stably expressing the PML-BioID-GFP to associate with nucleolus after doxorubicin treatment. In addition, selected clonal cell lines expressing PML-BioID-GFP (WT-A9, WT-B8, WT-F3, WT-F9) formed lower number of PML NBs together with the absence of DAXX compared to the transient transfectants. On the contrary, the cells carrying the mutant form of PML behaved as expected – the number of PML NBs was normal and they contained DAXX.

These results indicate that the expression of the wild type PML fusion proteins and subsequent formation of PML NBs caused proliferative disadvantage to hTERT RPE1 PML KO cells accounting for the appearance of the cells without or with diffused GFP signal. These results were unexpected as the hTERT RPE1 PML KO stably expressing GFP-PML I and hTERT RPE1 stably expressing GFP-PML IV have been successfully generated previously in the laboratory. The possible explanations are that either the

exclusively expressed PML IV isoform in cell with PML gene knock-out or the fusion of PML with biotin ligase BioID2 can affect cell metabolism.

The possibility that exclusively expressed PML IV is rather unfavourable for the cell can be well explained. Firstly, the PML IV plays an important role in recruitment of p53 and its activation through promoting its acetylation or phosphorylation. This was demonstrated in the study published by Bischof and colleagues performed in MEFs (mouse embryonic fibroblasts) overexpressing PML IV isoform. Western blotting analysis showed increased acetylation and phosphorylation of p53 in these cells. This PML IV-dependent p53 activation and stabilization is part of the process defined in this study as PML-induced premature senescence *(Bischof et al., 2002)*. Secondly, the PML IV is involved in growth regulation as was demonstrated in HEK293T cells transfected with different PML isoforms. Although several of them interacted with PML, only cell transfected with PML IV isoform showed the decrease in level of endogenous c-Myc, suggesting its destabilization in a PML IV-dependent manner *(Buschbeck et al., 2007)*. Despite these facts, I cannot exclude that even low, but permanent biotinylation of PML and its interaction partners affects their function.

As mentioned above, the PML NBs formed by all analysed transductants were biotinylated upon addition of biotin, the indication that biotin ligase is functional in context of both fusion proteins even when they are stably expressed in the hTERT RPE1 PML KO cells. Using wide field microscopy I detected a weak biotinylation of PML NBs even without addition of biotin. This was confirmed by Western blotting analysis indicating that low level of endogenous biotin is sufficient for biotin ligase to biotinylate proteins in its proximity. This can be accounted for the BioID2 being a promiscuous biotin ligase designed by Kim and colleaques *(Kim et al., 2012)* as a modification of original BioID *(Roux et al., 2012).* It is smaller and reportedly provides more selective targeting of fusion proteins. It also requires less biotin supplementation than original BioID. While the efficiency of BioID biotinylation was reduced once concentration of biotin decreased below 50 μM, BioID2 maintained high efficiency of biotinylation even while supplemented only with 3.2 μM biotin. This, although it could be a major advantage, can also constitute disadvantage, for example, by ability to utilize even low concentration of endogenous biotin for biotinylation as was also shown in my study. This presents another problem for the primary goal as it could affect the cellular protein function in general and to obscure clear discrimination of the proteins biotinylated before and after specific treatment (doxorubicin).

Despite this issue, when analysing the biotinylated proteins, the level of biotinylation was higher compared to samples obtained without cultivation with addition of biotin. Therefore, I proceeded to the isolation of biotinylated proteins. Preparation involved the isolation of nuclei and extraction of soluble nuclear proteins. As mentioned, the PML complexes are hardly soluble in common buffers used for pull-downs or co-immunoprecipitation, therefore I tested the solubility of biotinylated proteins in buffer containing detergents such as NP-40 and SDS for its reported compatibility with isolation of biotinylated proteins *(Cheah et al., 2017)*. The isolation of biotinylated proteins was based on the biotin-streptavidin bond, which is one of the strongest noncovalent biological interactions. This strong interaction allowed me to use conditions described above to solubilize the biotinylated proteins. Subsequent isolation of biotinylated proteins using streptavidin magnetic beads also was successful.

7. Conclusion

To identify partners interacting with PML at nucleolar border, I explored the suitability of recently newly designed approach for studying protein-protein interaction based on biotin proximity labelling. For this purpose, I created DNA construct coding either wild type or mutated form of PML IV isoform fused to biotin ligase BioID2 and analysed its impact on formation of both regular PML NBs and doxorubicin-induced PML nucleolar associations, and their capability to biotinylate proximal neighbourhood of PML in two experimental settings of transient and stable expression of fusion proteins.

Analysis of these fusion proteins transiently expressed in hTERT RPE1 PML KO cell showed expected behaviour. PML-biotin ligase fusion proteins formed PML NBs of regular characteristics of endogenous PML and ectopically expressed PML-GFP. The formation of PML nucleolar associations induced by doxorubicin was also preserved altogether indicating the fusion protein retains proper localization both under unperturbed and experimental conditions. Importantly, biotin ligase BioID2 also proved to be functional in the fusion protein.

On the contrary, stable transfectants of fusion proteins showed some drawbacks limiting the primary intention of the method. Most importantly, I did not detect any doxorubicin-induced PML-nucleolar associations. In addition, the expression of wild form of PML IV was incompatible with cell growth resulting in selection of cell clones with less numerous and aberrant PML NBs not accumulating regular component of PML NBs, DAXX.

Despite these restrictions, I utilised the model of stably expressed PML IV isoform fused to biotin ligase BioID2 to test and optimize the process of isolation of biotinylated proteins using magnetic beads coated with streptavidin to prove that biotinylated proteins can be successfully solubilised and isolated using buffers containing strong detergents NP-40 and SDS.

Considering these emerging problems further elaboration and modification of biotin proximity labelling approach to detect PML interacting partners is needed. For example, to overcome the selection of cell clones loosing regular pattern of PML NBs found in PML KO cells we suggest to use PML WT cells for stable expression of PML IV-BioID-GFP in which the EGFP-PML IV fusion protein was previously successfully expressed and this fusion protein colocalized with nucleolus after addition of doxorubicin. The main disadvantage of this model is that it disables the comparison of biotinylated proteins arising in cells

expressing either wild type PML-BioID or mutated PML-BioID fusion as in this setup both proteins are able to associate with nucleolus after doxorubicin treatment by the interaction with endogenous PML. Another solution of above described problems might be to use the inducible expression of both fusion proteins in RPE1 PML KO cells as this approach could better mimic the transient expression and prevent the long-term expression of PML IV that is not compatible with the proliferation and is probably the main reason for observed instability of ectopic stable PML IV expression.

In conclusion, I believe that after some modifications the biotin proximity labelling approach will be suitable to study PML interacting partners.

8. Citations

1 Ahmad, Y., Boisvert, F.-M., Gregor,P., Cobley, A., Lamond, A.I.; 2009: NOPdb nucleolar proteime database-2008 update. Nucleic Acids Res., 37, 181-184.

2 Andersen, J.S. et al.; 2005: Nucleolar proteome dynamics. Nature 433, 77–83.

3 Ayadin, F., Dasso, M., 2004: Distinct In Vivo Dynamics of Vertebrate SUMO. Mol. Cell. Biol., 15, 5208-5218.

4 Bernardi, R. & Pandolfi, P. P.; 2007: Structure, dynamics and functions of promyelocytic leukaemia nuclear bodies. Nat. Rev. Mol. Cell Biol., 8, 1006–1016.

5 Bernardi, R., .Scaglioni, P.P., Stephan Bergmann, Horn, H.F., Vousden, K.H., Pandolfi, P.P.; 2004: PML regulates p53 stability by sequestering Mdm2 to the nucleolus. Nat. Cell Biol. 6, 665–672.

6 Berscheminski, J., Groitl, P., Dobner, T., Wimmer, P. & Schreiner, S.; 2013: The Adenoviral Oncogene E1A-13S Interacts with a Specific Isoform of the Tumor Suppressor PML To Enhance Viral Transcription. J. Virol., 87, 965–977.

7 Bischof, O. et al.; 2002: Deconstructing PML-induced premature senescence. EMBO J., 21, 3358–3369.

8 Boichuk, S., Hu, L., Makielski, K., Pandolfi, P. P. & Gjoerup, O. V.; 2011: Functional connection between Rad51 and PML in homology-directed repair. PLoS One, 6, doi:10.1371/journal.pone.0025814.

9 Bonven, B.J., Grocke, E., Westergaard, O., 1985: A high affinity topoisomerases I binding sequences is clustered at DNAse I hypersensitive sites in Tetrahymena R-chromatin. Cell, 41, 541-551

10 Borden, K. L. et al.; 1995: The solution structure of the RING finger domain from the acute promyelocytic leukaemia proto-oncoprotein PML. EMBO J., 14, 1532–1541.

11 Boutell, C, Orr, A., Everett, R., 2003: PML residue lysine 160 is required for the degradation of PML induced by herpes simplex virus type 1 regulatory protein ICP0. J. Virol., 77. 8686-8694.

12 Boutell, C. et al.; 2011: A viral ubiquitin ligase has substrate preferential sumo targeted ubiquitin ligase activity that counteracts intrinsic antiviral defence. PLoS Pathog. 7, doi:10.1371/journal.ppat.1002245.

13 Brand, P., Lenser, T. & Hemmerich, P.; 2010: Assembly dynamics of PML nuclear bodies in living cells. PMC Biophys., 3:3.

14 Buschbeck, M. et al.; 2007: PML4 induces differentiation by Myc destabilization. Oncogene, 26, 3415–3422.

15 Campagna, M., Herranz, D., Garcia, M.A., Marcos-Villar, L., Gonzalez-Santamaria,J., Gallego,P.;2011: Sirt1 stabilizes PMLpromoting sumoylation. Cell Death Differ, 18, 72-79.

16 Chapman-Smith, A., Cronan, J.E. Jr.; 1999: In vivo enzymatic protein biotinylation. Biomol. Eng., 16, 119-25.

17 Chen, Y., Wright, J., Meong, X., Leppard, K.N., 2015: Promyelocytic Leukmia Protein Isoform II Promotes Transcripption FactorRecruitment to Active Interferon Beta and Interferon-responsive Gene Expression. Mol. Cell. Biol, 35, 1610-1672.

18 Choi-Rhee, E., Schilman, H., Cronan, J.E., 2004: Promiscuous protein biotinylation by Escherichia coli biotin protein ligase. Protein Sci., 13, 3043-50.

19 Carmo-Fonseca, M., Mendes-Soares, L. & Campos, I. ; 2000: To be or not to be in the nucleolus. Nat. Cell Biol., 2, E107–E112.

20 Cmarko, D. et al; 2000: Ultrastructural analysis of nucleolar transcription in cells microinjected with 5-bromo-UTP. Histochem. Cell Biol., 113, 181–187.

21 Condemine, W. et al.; 2006: Characterization of endogenous human promyelocytic leukemia isoforms. Cancer Res., 66, 6192–6198.

22 Condemine, W., Takahashi, Y., Le Bras, M. & de The, H.; 2007: A nucleolar targeting signal in PML-I addresses PML to nucleolar caps in stressed or senescent cells. J. Cell Sci., 120, 3219–3227.

23 Cronan, J.E., 2005: Targeted and proximity-dependent promiscuous protein biotinylation by a mutant Escherichia coli biotin protein ligase. J. Nutr. Biochem., 166, 416-8.

24 D'Amours, D., Stegmeier, F. & Amon, A.; 2004: Cdc14 and condensin control the dissolution of cohesin-independent chromosome linkages at repeated DNA. Cell, 117, 455–469.

25 de Thé, H. et al.; 1991: The PML-RARα fusion mRNA generated by the t(15;17) translocation in acute promyelocytic leukemia encodes a functionally altered RAR. Cell, 66, 675–684.

26 Dellaire, G. & Bazett-Jones; 2004: D. P. PML nuclear bodies: Dynamic sensors of DNA damage and cellular stress. BioEssays, 26, 963–977.

27 Dellaire, G. et al.; 2006: Promyelocytic leukemia nuclear bodies behave as DNA damage sensors whose response to DNA double-strand breaks is regulated by NBS1 and the kinases ATM, Chk2, and ATR. J. Cell Biol., 175, 55–66.

28 Ditlev, J. A., Case, L. B. & Rosen, M. K.; 2018: Who's In and Who's Out—Compositional Control of Biomolecular Condensates. J. Mol. Biol., 430, 4666–4684.

29 Donati, G., Montanaro, L. & Derenzini, M.; 2012: Ribosome biogenesis and control of cell proliferation: p53 is not alone. Cancer Res., 72, 1602–1607.

30 Duprez, E. et al.; 1999: SUMO-1 modification of the acute promyelocytic leukaemia protein PML: implications for nuclear localisation. J. Cell Sci., 112, 381–393.

31 Fogal, V. et al; 2000: Regulation of p53 activity in nuclear bodies by a specific PML isoform. EMBO J., 19, 6185–6195.

32 Froelich-Ammon, S., Osheroff, N., 1995: Topoisomerases poisons: harmessing the dark side of enzyme mechanism. J.Biol. Chem., 270, 21429-21432.

33 Fromont-Racine, M., Senger, B., Saveanu, C. & Fasiolo, F.; 2003: Ribosome assembly in eukaryotes. Gene, 313, 17–42.

34 Fumagalli, S., Ivanenkov, V. V., Teng, T. & Thomas, G.; 2012: Suprainduction of p53 by disruption of 40S and 60S ribosome biogenesis leads to the activation of a novel G2/M checkpoint. Genes Dev., 26, 1028–1040.

35 Gautier, T. et al.; 1997: Nuclear KKE/D Repeat Proteins Nop56p, and Nop58p Interact vith Nop1p and Are Required for Ribosome Biogenesis, Mol. Cell. Biol., 17, 7088–7098.

36 Geng, Y. et al.; 2012: Contribution of the C-terminal regions of promyelocytic leukemia protein (PML) isoforms II and V to PML nuclear body formation. J. Biol. Chem., 287, 30729–30742.

37 Gheitratmand, L., Coyaud, E., Gupta, G.D., Laurent, E.M.N., Hasegan, M., Prosser, S.L., Goncalves, J., Raught, B., 2019" Spatial and proteomic profiling reveals centrosome-independent features of centriolar satellites. EMBO J., 38, e101109, doi"10.15252/embj.201801109.

38 Gillingham, A.K., Bertram, J., Begum, F., Munro, S., 2019: In vivo identification of GTPase interactors by mitochondrial relocalozation and proximity biotinylation. eLife, doi:10.7554/eLife.45916.

39 Gu, B, Lambert, J.-P., Cockburn, K., Gingras, A.-C., Rossant, J.; 2017" AIRE is a critical spindle-associated protein in embryonic stem cells. eLife, doi:107554/Elife.28131.

40 Gurrieri, C.; 2004, Loss if the tumour suppressor PML in human cancers of multiple histologic origins. J. Natl. Cancer. Inst., 96, 269-2799.

41 Hayakawa, F., Abe, A., Kitabayashi, I., Pandolfi, P.P., Naoe, T.; 2008: Acetylation of PML isinvolved in histone deacetylase inhibitor-mediated apoptosis. J. Biol. Chem., 283, 24420-5.

42 Hecker, C.M., Rabiller, M., Haglunf, K., Bayer, P., Dikic, I., 2006: Specification of SUMO1- and SUMO2-interaction motifs. J. Biol. Chem., 281, 16117-27.

43 Hickey, C. M., Wilson, N. R. & Hochstrasser, M.; 2012: Function and regulation of SUMO proteases. Nat. Rev. Mol. Cell Biol., 13, 755–766.

44 Hozák, P., Schöfer, C., Mosgöller, W., Wachtler, F. & Cook, P. R.; 1994: Site of transcription of ribosomal RNA and intranucleolar structure in HeLa cells. J. Cell Sci., 107, 639–648.

45 Huang., X., LeDuc, R.D., Fornelli, L., Schutner, A.J., Bennet, R.L., kelleher, N.L., Licht, J.D., 2019"Defining the NSD2 interactome: PARP1 PARylation reduses NSD2 histone methytransferase activity and impedes chromatin binding. J.Biol. Chem., doi:10.1074/jbc.RA118.006159.

46 Hubackova, S. et al.; 2010: Regulation of the PML tumor suppressor in drug-induced senescence of human normal and cancer cells by JAK/STAT-mediated signaling. Cell Cycle, 9, 3085–3099.

47 Ishov, A. et al.; 2002: Pml Is Critical for Nd10 Formation and Recruits the Pml-Interacting Protein Daxx to This Nuclear Structure When Modified by Sumo-1. J. Cell Biol., 147, 221–234.

48 Ivanschitz, L. et al.; 2015: PML IV/ARF interaction enhances p53 SUMO-1 conjugation, activation, and senescence. Proc. Natl. Acad. Sci. U. S. A., 112, 14278–83.

49 Jackson, S. P. & Bartek, J.; 2009: The DNA-damage response in human biology and disease. Nature, 461, 1071–1078.

50 James, A., Wang, Y., Raje, H., Rosby, R. & DiMario, P.; 2014: Nucleolar stress with and without p53. Nucleus, 5, 402–426.

51 Janderová-Rossmeislová, L. et al.; 2007: PML protein association with specific nucleolar structures differs in normal, tumor and senescent human cells. J. Struct. Biol., 159, 56–70.

52 Javanbakht, H., 2006: Characterization of TRIM5α trimerization and its contribution to human immunodeficiency virus capsid binding. Virology, 353, 234-246

53 Jensen, K., Shiels, C. & Freemont, P. S.; 2001: PML protein isoforms and the RBCC/TRIM motif. Oncogene, 20, 7223–7233.

54 Junéra, H. R., Masson, C., Géraud, G. & Hernandez-Verdun, D.; 1995: The three-dimensional organization of ribosomal genes and the architecture of the nucleoli vary with G1, S and G2 phases. J. Cell Sci., 108 (Pt 1, 3427–41.

55 Kamitani, T. et al.; 1998: CELL BIOLOGY AND METABOLISM : Identification of Three Major Sentrinization Sites in PML Identification of Three Major Sentrinization Sites in PML . J. Biol. Chem., 273, 26675–26682 (1998).

56 Kießlich, A., Von Mikecz, A. & Hemmerich, P.; 2002: Cell cycle-dependent association of PML bodies with sites of active transcription in nuclei of mammalian cells. J. Struct. Biol., 140, 167–179.

57 Kim, D.I., Jensen, S.C., Noble, K.A., Birenda, K.C., Roux, K.H., Motamedchaboki, K., Roux, K.J.; 2016: An improved smaller biotin ligase for BioID proximity labeling. Mol. Cell Biol., 1188-1196.

58 Kim, D.I., Jensen, S.C., Roux, K.J.; 2016: Identifying Protein-Protein Associations as the Nuclear Envelope with BioID. Methods Mol. Biol., 2016, 1411, 133-146.

59 Leppard, K. N., Emmott, E., Cortese, M. S. & Rich, T.; 2009: Adenovirus type 5 E4 Orf3 protein targets promyelocytic leukaemia (PML) protein nuclear domains for disruption via a sequence in PML isoform II that is predicted as a protein interaction site by bioinformatic analysis. J. Gen. Virol.,90, 95–104.

60 Li, C., Peng, Q., Wan, X., Sun, H. & Tang, J.; 2017: C-terminal motifs in promyelocytic leukemia protein isoforms critically regulate PML nuclear body formation. J. Cell Sci., 130, 3496–3506.

61 Li, H., Leo,C., Zhu, J., Wu, X., O`Neil, J., Park, E.J., Chen, J.D., 2000: Sequestration and inhibition of DAXX-mediated transcriptional repression by PML. Mol. Cell Biol., 20, 1784-1796.

62 Lin, H-K., Bergmann, S., Pandolfi, P.P. et al.; 2004: Cytoplasmic PML function in TGF-b signalling. Nature, 431, 205–211.

63 Maroui, M. A. et al.; 2012: Requirement of PML SUMO Interacting Motif for RNF4- or Arsenic Trioxide-Induced Degradation of Nuclear PML Isoforms. PLoS One, 7doi:10.1371/journal.pone.0044949.

64 Maroui, M. A., Pampin, M. & Chelbi-Alix, M. K.; 2011: Promyelocytic Leukemia Isoform IV Confers Resistance to Encephalomyocarditis Virus via the Sequestration of 3D Polymerase in Nuclear Bodies. J. Virol., 85, 13164–13173.

65 Mattsson, K., Pokrovskaja, K., Kiss, C., Klein, G. & Szekely, L.; 2012: Proteins associated with the promyelocytic leukemia gene product (PML)-containing nuclear body move to the nucleolus upon inhibition of proteasome-dependent protein degradation. Proc. Natl. Acad. Sci., 98, 1012–1017.

66 McClintock B., 1934: The relation of a particular chromosomal element to the development of the nucleoli in Zea mays. Microsk. Anat., 21, 294-328.

67 Mehus,A.A., Anderson, R.H., Roux, K.J.; 2016: BioID Identification of Lamin-Associated Proteins. Methods Enzymol., 569, 3-22.

68 Meroni, G. & Diez-Roux, G.; 2005: TRIM/RBCC, a novel class of ‘single protein RING finger’ E3 ubiquitin ligases. BioEssays, 27, 1147–1157.

69 Meyer, K. N. et al.; 1997: Cell cycle-coupled relocation of types I and II topoisomerases and modulation of catalytic enzyme activities. J. Cell Biol., 136, 775–788.

70 Milovic-Holm, K., Krieghoff, E., Jensen, K., Will, H. & Hofmann, T. G.; 2007: FLASH links the CD95 signaling pathway to the cell nucleus and nuclear bodies. EMBO J., 26, 391–401.

71 Montanaro, L., Treré, D. & Derenzini, M.; 2008: Nucleolus, ribosomes, and cancer. Am. J. Pathol.,173, 301–310.

72 Mu, Z.-M., Liu, J.-H., Chang, K.-S., Chin, K.-V. & Lozano, G.; 1994: PML, a growth suppressor disrupted in acute promyelocytic leukemia. Mol. Cell. Biol., 14, 6858–6867.

73 Müller, S., Miller, W.H. Jr, Dejean, A., 1998: Trivalent antimonials induce degradation of the PML-RARα oncoprotein and reorganization of the promyelocytic leukemia NB4 cells. Blood, 92, 4309-4316.

74 Nguyen, N.A. et al.; 2005: Physical and functional link of the leukemia-associated factors AML1 and PML. Blood, 105, 292–300.

75 Nisole, S., Maroui, M. A., Mascle, X. H., Aubry, M. & Chelbi-Alix, M. K.; 2013: Differential Roles of PML Isoforms. Front. Oncol, 3, 1–17.

76 Olausson, K., Nistér, M. & Lindström, M.; 2012: p53 -Dependent and -Independent Nucleolar Stress Responses. Cells 1, 774–798.

77 Osheroff, N., 1985: Biochemical basis for the interactions of type I and type II topoisomerases with DNA. Pharmacol. Ther., 41, 223-241

78 Pederson, T.; 1998: The plurifunctional nucleolus. Nucleic Acids Res., 26, 3871–3876.

79 Peche, L.Y., Scolz, M., Ladelfa, M.F., Monte, M., Schneider, C.; 2012: MageA2 restrains cellular senescence by targeting the function of PML IV/p53 axis at the PML NBs. Cell Death Differ., 19, 926-936.

80 Quignon, F. et al.; 1998: PML induces a novel caspase-independent death. Process. Nat. Genet, 20, 259–265.

81 Regad, T., Chelbi, M.K., 2001: Role and fate of PML nuclear bodies in response to interferon and viral infections. Oncogene, 20, 7274-7286.

82 Reymond, A., Meroni, G., Merla, G., Cairo, S., Luzi, L., Riganelli,D., Zanaria, E., Messali, S, Cainarca, S., Guffanti, S., Minucci, S., Pellici, G.P., Ballabio, A.; 2001: The reipartite motif family identifies cell compartments. J. EMBO, 20, 2140-2151.

83 Rossi. F., Labourier, D., Forné, T., Divita, G., Derancourt, J., Riou, J., Antoine, E., Cathala, G., Brunel C., Tazi, J., 1996: Specific phosphorylation of SR proteins by mammalian DNA topoisomerase I., Nature, 381, 80-82.

84 Roux, K. J., Kim, D. I., Raida, M. & Burke, B.; 2012: A promiscuous biotin ligase fusion protein identifies proximal and interacting proteins in mammalian cells. J. Cell Biol., 196, 801–810.

85 Sahin, U., De Thé, H. & Lallemand-Breitenbach, V.; 2014: PML nuclear bodies: Assembly and oxidative stress-sensitive sumoylation. Nucleus, 5, 499–507.

86 Scaglioni, P. P. et al.; 2006: A CK2-Dependent Mechanism for Degradation of the PML Tumor Suppressor. Cell, 126, 269–283.

87 Seeler, J., Dejean, A., 2001: SUMO: of branched proteins and nuclear bodies. Oncogene, 20, 7242-7249.

88 Seeler, J.-S., Marchio, A., Sitterlin, D., Transy, C. & Dejean, A.; 2002: Interaction of SP100 with HP1 proteins: A link between the promyelocytic leukemia-associated nuclear bodies and the chromatin compartment. Proc. Natl. Acad. Sci., 95, 7316–7321.

89 Shen, T. H., Lin, H. K., Scaglioni, P. P., Yung, T. M. & Pandolfi, P. P.; 2006: The Mechanisms of PML-Nuclear Body Formation. Mol. Cell, 24, doi:10.1016/j.molcel.2006.09.013.

90 Scheer, U., Hock, R.; 1999: Structure and function of the nucleolus. Curr. Opin. Cell Biol., 11, 385–390.

91 Sirri, V., Urcuqui-Inchima, S., Roussel, P. & Hernandez-Verdun, D.; 2008: Nucleolus: The fascinating nuclear body. Histochem. Cell Biol., 129, 13–31.

92 Sternsdorf, T., Jensen, K. & Will, H.; 1997: Evidence for covalent modification of the nuclear dot-associated proteins PML and Sp100 by PIC1/SUMO-1. J. Cell Biol.; 139, 1621–1634.

93 Takahashi, Y., Lallemand-Breitenbach, V., Zhu, J. & De Thé, H.; 2004: PML nuclear bodies and apoptosis. Oncogene, 23, 2819–2824.

94 Talluri, S. & Dick, F. A.; 2014: The retinoblastoma protein and PML collaborate to organize heterochromatin and silence E2F-responsive genes during senescence. Cell Cycle, 13, 641–651.

95 Tavalai, N., Stamminger, T.; 2008: New insights into the role of the subnuclear structure ND10 for viral infection. Biochim. Biophys. Acta - Mol. Cell Res., 1783, 2207–2221.

96 Torres-Rossel, J., Machin, F., Jarmuz, A., Aragon, L.; 2004: Nucleolar segregation lacks behind the rest of the genom and requires Cdc14p activation by FEAR network. Cell Cycle, 3, 496-502.

97 Ullman, R., Chien, C.D., Avanaggiati, M.L., Mulller, S., 2012: An acetylation switch regulates SUMO-dependent protein interaction networks. Mol. Cell, 46, 759-770.

98 Urano, T. et al.; 2002: Efp targets 14-3-3δ for proteolysis and promotes breast tumour growth. Nature, 417, 871–876.

99 Uversky, V. N.; 2017: Intrinsically disordered proteins in overcrowded milieu: Membrane-less organelles, phase separation, and intrinsic disorder. Curr. Opin. Struct. Biol., 44, 18–30.

100 Vancurova, M. et al.; 2019: PML nuclear bodies are recruited to persistent DNA damage lesions in an RNF168-53BP1 dependent manner and contribute to DNA repair. DNA Repair (Amst)., 78, 114–127.

101 Wang, Z. G. et al.; 1998: Pml is essential for multiple apoptotic pathways. Nat. Genet., 20, 266–272.

102 Weidtkamp-Peters, S. et al.; 2008: Dynamics of component exchange at PML nuclear bodies. J. Cell Sci., 121, 2731–2743.

103Wheeler, R. J. & Hyman, A. A.; 2018: Controlling compartmentalization by non-membrane-bound organelles. Philos. Trans. R. Soc. B Biol. Sci., 373, http://dx.doi.org/10.1098/rstb.2017.0193.

104 Wu, W.-S. et al.; 2001: The Growth Suppressor PML Represses Transcription by Functionally and Physically Interacting with Histone Deacetylases. Mol. Cell. Biol., 21, 2259–2268.

105 Xu, Z. X., Zou, W. X., Lin, P. & Chang, K. S.; 2005: A role for PML3 in centrosome duplication and genome stability. Mol. Cell, 17, 721–732.

106 Yang, S. et al.; 2006: Promyelocytic leukemia activates Chk2 by mediating Chk2 autophosphorylation. J. Biol. Chem., 281, 26645–26654.

107 Ye, X., et al.; 2007: Definition of pRb and p53-dependent and independent steps of HIRA/ASF1-mediated formation of senescence-associated heterochromatin foci (SAHF). Mol. Cell Biol., 27, 2452-2465.

108 Zhang, R. et al.; 2005: Formation of macroH2A-containing senescence-associated heterochromatin foci and senescence driven by ASF1 a and HIRA. Dev. Cell, 8, 19-30.

109 Zhong, S. et al.; 2000: Role of SUMO-1-modified PML in nuclear body formation. Blood 95, 2748–52.